Manuel Entfellner BSc

Prediction of Displacements and Shotcrete Lining Utilization –

Decision strategy for a timely application of ductile support systems in conventional tunnelling

Master's Thesis

Submitted in fulfilment of the requirements for the degree of

Diplom-Ingenieur

Master's programme Civil Engineering, Geotechnics and Hydraulics

at

Graz University of Technology

Supervisor
O.Univ.-Prof. Dipl.-Ing. Dr.mont. Wulf Schubert
Institute of Rock Mechanics and Tunnelling
Graz University of Technology

Dipl.-Ing. Alexander Kluckner BSc
Institute of Rock Mechanics and Tunnelling
Graz University of Technology

Graz, September 2017

„Vor der Hacke ist es duster.“

(alter Bergmannsspruch, Autor unbekannt)

AFFIDAVIT

I declare that I have authored this thesis independently, that I have not used other than the declared sources/resources, and that I have explicitly marked all material which has been quoted either literally or by content from the used sources. The text document uploaded to TUGRAZonline is identical to the present master‘s thesis.

Date	Signature

Acknowledgements

I want to express my sincerest thanks to my supervisor, Prof. Wulf Schubert for his guidance and suggestions. His deep knowledge in tunnelling and critical questions during hours of joint discussions opened me new food for thoughts and subsequently triggered further progression of my thesis.
I would like to thank Alexander Kluckner for his tireless efforts, discussions and suggestions. His support has significantly contributed to the success of this work.

Site visits, data of current tunnelling projects of the Austrian Federal Railways (ÖBB) and suggestions of Gerold Lenz, Erich Neugebauer, Johann Bauer and Alexander Poisel finally enabled the development of a practical method.

Thanks also to my friends in Graz and my friends at home in Flachau who shared many hours with me behind the life of research work. During extensive ski- and mountain tours with my faithful fellow climbers I found motivation and new inspirations for my studies.

Furthermore, I would like to thank Prof. Qian Liu, Prof. Scott Kieffer, Wolfgang Obermüller, Ass.Prof. Dirk Schlicke, Matthias Ehrhart, Prof. Robert Galler, Franz Wilhelmstötter, Peter Schubert, Wolfgang Aldrian, Roland Mayr and Oliver Kai Wagner for their support.

Finally, I want to express my deepest gratitude to my family – Maria, Josef and Christoph. Without their support in all respects the study would not have been conceivable at all. Thank you!

Graz, August 2017 Manuel Entfellner

Abstract

This master thesis deals with the prediction of displacements and shotcrete lining utilization in conventional tunnelling. 3D-displacement monitoring at specific monitoring sections is currently used for the evaluation and prognosis of the system behaviour as well as for the calculation of the shotcrete lining utilization. As monitoring sections are installed at a certain distance only, information about the displacement development of the opening between the last monitoring section and the current tunnel face does not exist. For selecting an appropriate excavation- and support concept, this information would be most helpful. The method presented in this thesis uses semi-automatic curve-fittings of measured displacements and the identification of trends of fitting parameters, allowing a prediction of the system behaviour ahead of the last monitoring section. Existing monitoring data interpretation approaches are applied, new ones introduced, and the results in combination with geological assessments finally used to increase the accuracy of the short-term prediction. Having the temporal and spatial displacement development predicted, a most probable utilization development of shotcrete linings recently installed or of those to be installed soon, can be calculated. Thus, possible stability problems of the (planned) support may be identified timely and excavation and support adapted if necessary (e.g. switch to ductile support system). The practicability of the method is illustrated by two case studies.

Kurzfassung

Diese Masterarbeit befasst sich mit der Prognose von Verschiebungen und Spritzbetonauslastung beim konventionellen Tunnelvortrieb. Zur Beurteilung und Prognose des Systemverhaltens sowie zur Berechnung der Spritzbetonauslastung werden derzeit 3D-Verschiebungsmessungen an definierten Messquerschnitten herangezogen. Da Messquerschnitte nur in einem definierten Abstand installiert sind, existieren keine Informationen bezüglich der Verschiebungsentwicklung im Bereich zwischen dem letzten Messquerschnitt und der aktuellen Ortsbrust. Für die Festlegung eines geeigneten Ausbruch- und Stützmittelkonzeptes wären diese Informationen jedoch äußerst hilfreich. Die in dieser Arbeit vorgestellte Methode verwendet semi-automatische Ausgleichsrechnungen (Kurvenfittings) von gemessenen Verschiebungen und die Bestimmung von Trendentwicklungen der Fitting-Parameter, um eine Prognose des Systemverhaltens vor dem letzten Messquerschnitt zu ermöglichen. Zur Erhöhung der Kurzzeitprognosesicherheit werden in Kombination mit geologischen Bewertungen, bewährte sowie neu entwickelte Methoden der Messdateninterpretation angewandt. Mit der zeitlich und räumlich prognostizierten Verschiebungsentwicklung kann anschließend die Auslastung von kürzlich hergestellten Spritzbetonschalen, oder von jenen, welche demnächst hergestellt werden, berechnet werden. Somit kann frühzeitig auf mögliche Stabilitätsprobleme des (geplanten) Ausbaus reagiert und dieser gegebenenfalls angepasst werden (z.B. Umstellung auf duktilen Ausbau). Die Praxistauglichkeit der Methode wird anhand von zwei Fallbeispielen aufgezeigt.

Contents

1 Introduction

Tunnelling in weak ground conditions with large displacements is a challenging task. Since for such projects only local geological investigations at the elevation of the tunnel alignment are possible, geotechnical engineers have to deal with big uncertainties regarding the rock mass structure and quality. However, for a technical and economical satisfying design and construction, a proper knowledge of expected displacements is necessary.

Many projects in the past have shown that using a stiff support with a high bearing capacity in weak zones causes severe damage of the lining [1]. This leads to a very dangerous situation for workers and to costly and time-consuming reshaping works in order to fulfil the structural requirements and clearance profile. Hence, in the last decades so-called *Ductile Support Systems* (“Yielding Elements”) were developed [2]. These elements are installed in the shotcrete lining of conventional excavated tunnels with the aim to avoid damages.

Nowadays, the calculation of shotcrete lining utilization is performed up to the last monitoring section, based on measured displacement vectors [3]. Due to lack of information of the displacement development in the excavation area, a timely choice of support measures is difficult. Hence, ductile support systems are often installed too late when damages in the shotcrete lining already occurred and remediation measures are necessary [4].
Prompted by this, a consistent and practical method for predicting displacements and shotcrete lining utilization ahead of the last monitoring section – or, even ahead of the current tunnel face – is developed. Therefore, a hybrid approach of the *Observational Method* [5] during construction is used. By combining existing and new developed monitoring data analyses with extensive geological interpretations, an increasing accuracy of the short-term prediction of the *System Behaviour* is possible. Finally, with the predicted displacement development, mathematical interpolation processes and an extended constitutive material model for shotcrete, a lining utilization is calculated. This information can be used as a decision criterion for a timely selection of support measures.

Furthermore, in combination with a geotechnical safety management, potential problems can be identified beforehand and counter-measures applied immediately. This increases the working safety and reduces economical risks for client and contractor.

2 State of the Art

Tunnelling and mining has a millennia-long tradition and is still a challenging task. Tunnels are an integral part of society and economy and often declared as a so-called C*ritical Infrastructure* with high efforts regarding operational lifetime, structural resistance and resilience [6]. To fulfil these requirements, special technologies to tunnel through difficult ground conditions have been developed in the past. The basic principle of this thesis follows the *Guideline for the Geotechnical Design of Underground Structures with Conventional Excavation* [7] of the Austrian Society for Geomechanics (ÖGG). In order to enable the definition of the thesis' objectives, a brief review of the state-of-the-art is presented below.

2.1 Historical Development of Tunnel Linings

In the past, many different systems have been used to deal with high radial deformations during tunnelling – most of them with limited success. For tunnels it was common to use a timber support and perform re-shaping if the support got destructed [8]. In mining, the idea of using support systems with a high ductility to deal with large deformations was first mentioned by Lenk [9]. During the construction of the Trans-Iranian Railway (1927-1938), Rabcewicz recognized that using a stiff support under weak ground conditions with long-lasting displacements is useless and introduced the so-called *Hilfsgewölbebauweise* with timber elements, which increase the ductility of the lining:

"Even for the temporary support it is futile to face the ground pressure with stiff and heavy support measures since they will inevitably get destroyed. The forces resulting from ground loosening are tremendous and can only be countered with comparable means. Since we do not have such means, we have to leave it up to nature to help us by creating a yielding zone. In order to accomplish this, space and time are necessary" [10].

This idea is still valid today. By allowing the ground to deform in a certain manner, the ground pressure is reduced and less support resistance is necessary. For a successful excavation through weak ground, the excavation- and support concept must comply with the behaviour of the surrounding rock mass, which is the essential bearing structure in all underground works.

In the 1950's and 1960's the *New Austrian Tunnelling Method* (NATM) was developed by Ladislaus von Rabcewicz, Leopold Müller and Franz Pacher [11]. The improvement of the shotcrete technology in combination with bolting significantly reduced the loosening of the surrounding rock mass and facilitated tunnelling in soft ground. Under shallow ground conditions tunnels could successfully be built with a thin shotcrete lining and quick ring closure. It was thought that the low initial stiffness of the young shotcrete provides enough deformation potential for the rock mass and the same system can be used under high overburden [8]. This conclusion changed in the 1970's during the construction of the first tube of the Tauerntunnel in Austria. A high stress state in combination with a geological fault zone led to radial displacements up to 1.2 m (see Fig. 2) and caused severe damages of the shotcrete lining [1].

The tunnel engineers recognized that using a closed shotcrete lining under high overburden and weak ground conditions is technically and economically not purposeful. This was the birth of open *Deformation Gaps* in the shotcrete lining which allow a certain deformation without causing damage [1]. With this method several tunnels in Austria under difficult ground conditions such as the Tauerntunnel, Arlbergtunnel, Karawankentunnel and Inntaltunnel could be built successfully [8].

As a result of the tunnel collapse during the advance in the so-called *Hinterbergstörung* at the Galgenbergtunnel [12], a new support system was developed. The most distinctive step was the application of so-called *Yielding Elements* [8]. Steel tubes with a welded end plate and drillings at the bottom to reduce the high initial buckling stiffness were installed in the shotcrete lining. With this system, hoop forces and a higher utilization could be generated in the shotcrete lining and less deformations occurred.

Basically, there are three *Yielding Principles* to cope with deformations without causing damage of the lining [13, 14]:

- Installation of yielding elements in the shotcrete lining, to allow deformation in tangential direction; used in conventional tunnelling;
- Arranging a compressible layer between the extrados of a stiff lining and the excavation boundary, which is the standard solution for mechanical tunnelling with TBMs;
- Using steel supports with yielding couplings;

Since the topic of this thesis is related to conventional tunnelling, only the first principle will be further discussed. Nowadays, many different types of yielding elements for conventional tunnelling applications are available (Fig. 1). They can generally be divided into porous elements made of concrete and steel or just made of steel. The essential parameters are their load-displacement behaviour, capacity and practical handling on-site [4].

An ideal ductile element would start yielding just before the support pressure reaches it bearing capacity. As the system behaviour is project- and ground specific, systems with various characteristics are available. In Central Europe the most common ductile support systems for conventional tunnelling applications are:

- *Lining Stress Controller* (LSC) by DSI Underground Austria GmbH
- *Wabe* by Bochumer Eisenhütte Heintzmann GmbH & Co. KG
- *hiDCon* by Solexperts AG
- *Welle* by SZ Schacht- und Streckenausbau GmbH

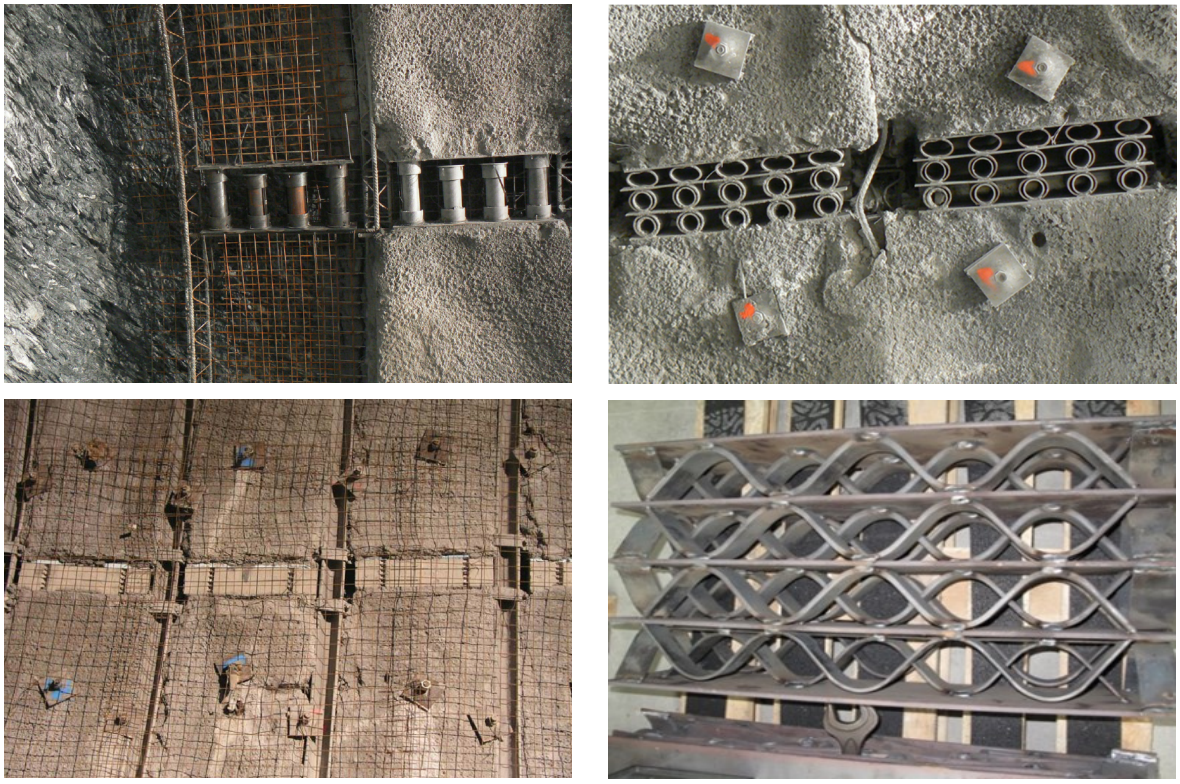

Fig. 1: Different types of yielding elements: LSC (top left), Wabe (top right), hiDCon (bottom left) and Welle (bottom right).

The development of yielding elements has not been completed yet. Recent researches on the LSC system of Sitzwohl [15], Verient [16] and Brunnegger [17] for example focus on adapting the load-displacement behaviour of the system to facilitate higher degrees of utilization of the shotcrete lining, allow an easier adjustment to site-specific conditions, increase the practical handling on-site and reduce production costs.

2.2 Limits of Closed Linings

There are several situations where damages of the shotcrete lining are likely to occur. The most important case is linked with large displacements. A conventional shotcrete lining can sustain tangential strains (compression) of approximately 0.6 % to 0.8 % before cracks occur [4]. In more detail, the utilization of a shotcrete lining highly depends on its deformation characteristic as vividly demonstrated by Lenz et al. [18]. This means, the knowledge of final displacements is not sufficient, but also their timely- and spatial development must be considered.

Critical sections for the load-bearing capacity of a shotcrete lining, caused by large displacements, are typically fault zones in combination with a high stress state. The practical problem is, that displacements are face position- and time-dependent and do not necessarily occur immediately after excavation. At the beginning of a fault zone, the weaker material “appends” on the stiffer one, leading to almost no additional displacements. Divergent stress orientations as described in section 4.5.3 further increase this effect. With advancing face and stress redistribution, displacements suddenly start to increase, causing unexpected loading of the adjacent support [4]. Hence, ductile support systems are often installed too late when damages already occurred [14].

Fig. 2 shows an example of the positive influence of yielding elements on the rock mass - support interaction. During the construction of the first tube of the Tauerntunnel in Austria (1971-1975), crown settlements up to 1.2 m in a fault zone caused severe damages of the support [1]. When the same fault zone was excavated at the second tube (2006-2010), four rows of yielding elements were installed and crown settlements could be reduced to 0.4 m [19].

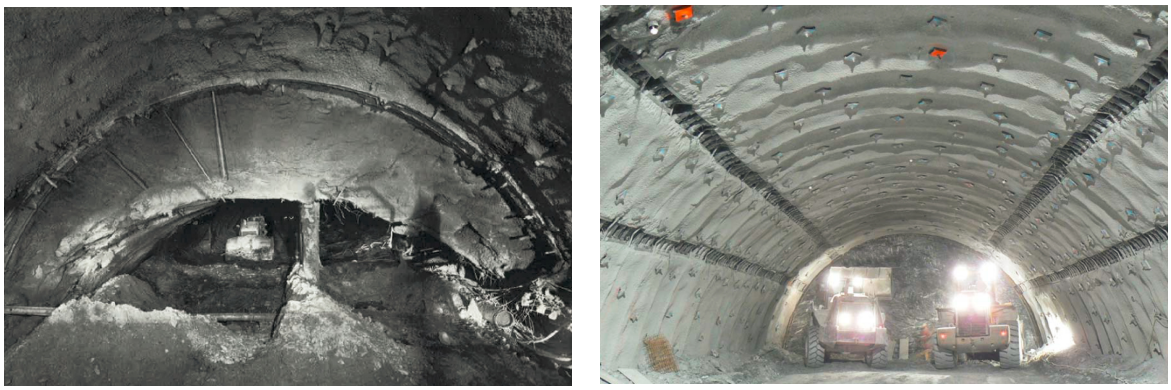

Fig. 2: Crown settlements up to 1.2 m in the first tube (left) and controlled settlements up to 0.4 m in the second tube (right) at the Tauerntunnel [1, 19].

Other typical zones for lining damages are changes of the cross-section (e.g. widening or intersections) or local shearing in foliated rock masses [4].

2.3 Monitoring Data Interpretation

In conventional tunnelling – especially when applying the NATM – observational method as referred in Eurocode 7 [5] is an integral part. With absolute 3D displacement monitoring techniques and monitoring data interpretation, the system behaviour of the tunnel is observed and evaluated. Furthermore, the gained information is used for the geotechnical safety management [18]. The set-up, execution of measurements and data interpretation is described in the handbook *Geotechnical Monitoring in Conventional Tunnelling* [20].

2.3.1 Absolute-, Horizontal- and Vertical Displacements

With geodetic measurements by means of using total stations, absolute displacements in space are monitored. These data are the basis for all further interpretations. By plotting displacements for example in time-displacement, distance-displacement and cross-section graphs, structural influences or failure mechanisms (e.g. local shearing, failure of invert, etc.) can be detected [21].
With state- and trend lines (for details see [20]), the current system behaviour can be evaluated, deviations (e.g. changing ground conditions) can be recognized and predictions regarding the situation ahead of the face can be made [22, 23].
For all these interpretations, a link to the construction sequences is necessary.

2.3.2 Vector Orientation

"The vector orientation L/S is the ratio between longitudinal displacements (L) and settlements (S) and is expressed in terms of an angular deviation of the displacement vector from vertical" [20]. A rotation of the vector orientation against the direction of drive indicates ground conditions with lower stiffness ahead of the face and vice versa, a rotation in the direction of drive indicates ground conditions with higher stiffness ahead of the face [24]. Experiences showed that the vector orientation of the crown point is most suitable for the identification of stiffness distinctions [25]. In contrast to radial displacements, the vector orientation changes earlier when approaching a less stiff zone due to stress redistribution [26].

2.3.3 Additional Monitoring Measures

For further methods to interpret monitored displacement data, it is referred to [20].
Face displacement monitoring can be also a good indicator for changing ground conditions ahead of the face, but due to practical difficulties it is commonly not used [27–29]. Other methods like convergence measurements, anchor load cell-, extensometer-, inclinometer-, tilt- and strain measurements, digital ground mappings with photogrammetry, laser scanning or fibre-optic sensors in a shotcrete lining can also provide useful information regarding the ground- and system behaviour and should be applied as necessary.

2.4 Calculation of Shotcrete Lining Utilization

With monitored 3D displacement data, strains are calculated between adjacent monitoring targets in cross-section, or between adjacent monitoring sections in longitudinal direction. For the interpolation process in cross-section, cubic spline-functions are best suitable; in longitudinal direction quadratic splines should be used [3]. The type of spline and its properties can highly influence the results.
By using sophisticated constitutive models for shotcrete – considering the time-dependent and rheological behaviour (e.g. with *Rate-of-Flow-Method [30, 31]* or *Hybrid-Method* [32]) – stresses in the shotcrete lining are calculated. With this method, an assessment of the lining utilization based on measured displacements is possible [33]. Fig. 3 shows a 3D-view of a shotcrete lining utilization plot, back-calculated from measured displacements.

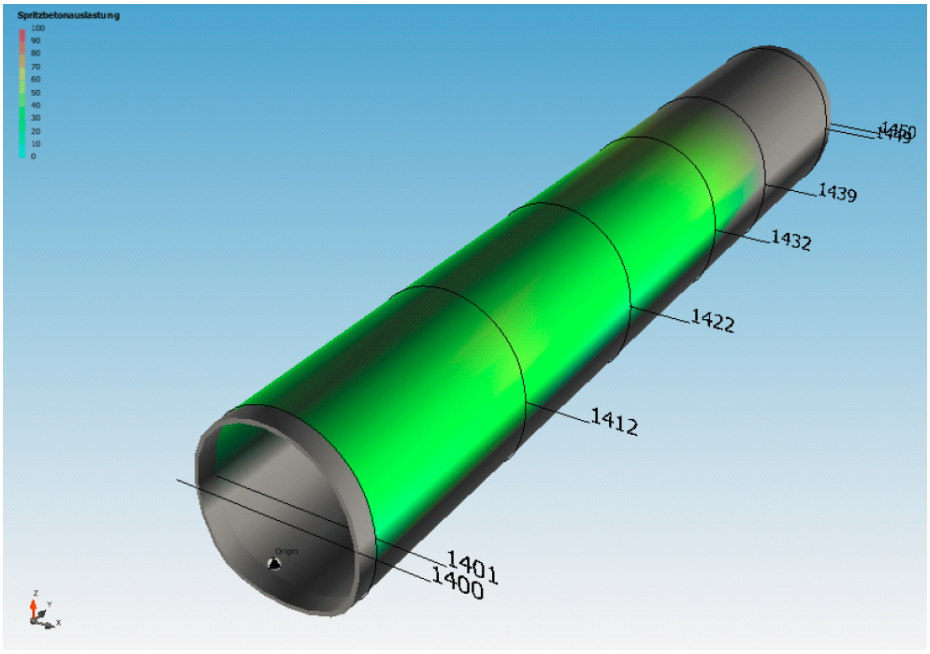

Fig. 3: 3D-view of a shotcrete lining utilization, based on measured displacements at specific monitoring sections (Software: *Tunnel:Suite* [34]).

3 Definition of Objectives

After the literature research and outlining the state-of-the-art, following questions regarding prediction of displacements and shotcrete lining utilization in the excavation area are identified:

- Geological-geotechnical short-term prediction:
  - Which geological-geotechnical parameters indicate changing ground conditions ahead of the tunnel face?
  - How can they be evaluated systematically?

- Short-term prediction of displacements with monitoring data interpretation:
  - Which monitoring data interpretation tools are best suitable for the short-term prediction of displacements?
  - Are there other monitoring data interpretation methods for predicting changing ground conditions ahead of the tunnel face?
  - What influence has the measuring accuracy on the monitoring interpretation?

- Calculation of displacements and shotcrete lining utilization:
  - How is a prediction of displacements in the excavation area feasible?
  - Which approach is necessary to calculate the shotcrete lining utilization ahead of the last monitoring section based on predicted displacements?
  - Which constitutive material model is best suitable for shotcrete?

- Decision criterion for ductile support systems:
  - Is the prediction of shotcrete lining utilization sufficient for a timely application of ductile support systems?

4 Prediction of Displacements and Shotcrete Lining Utilization

Nowadays, the calculation of shotcrete lining utilization is just performed in-between contiguous monitoring sections, based on observed and interpolated displacement vectors [3]. Since these sections typically have a distance of 5 - 20 m [20], information on the displacement development between the last monitoring section and current excavation area is not available. With the presented method, a prediction of displacements and shotcrete lining utilization ahead of the last monitoring section – or, even ahead of the current tunnel face – is possible. Hence, potential problems can be identified beforehand and proper excavation- and support measures selected timely.

4.1 Decision Strategy

The applied approach uses a combination of monitoring data and geological data to increase the accuracy of short-term prediction of displacements and finally of the shotcrete lining utilization. To illustrate the applied procedure, an overview of the method and decision strategy is shown in Fig. 4 and Fig. 5.

The proposed strategy in general follows the recommendations for the evaluation of the system behaviour during construction, outlined in the *Guideline for the Geotechnical Design of Underground Structures with Conventional Excavation* [7].

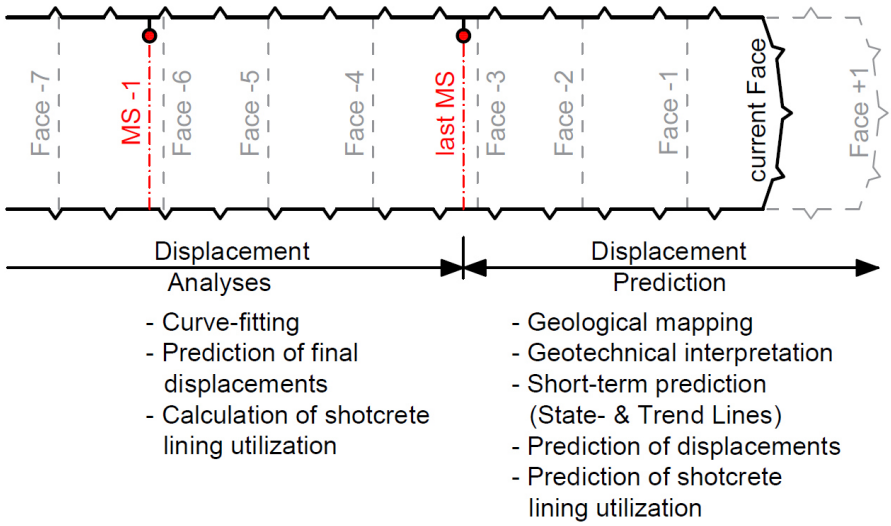

Fig. 4: Overview of the applied procedure for the prediction of displacements and shotcrete lining utilization.

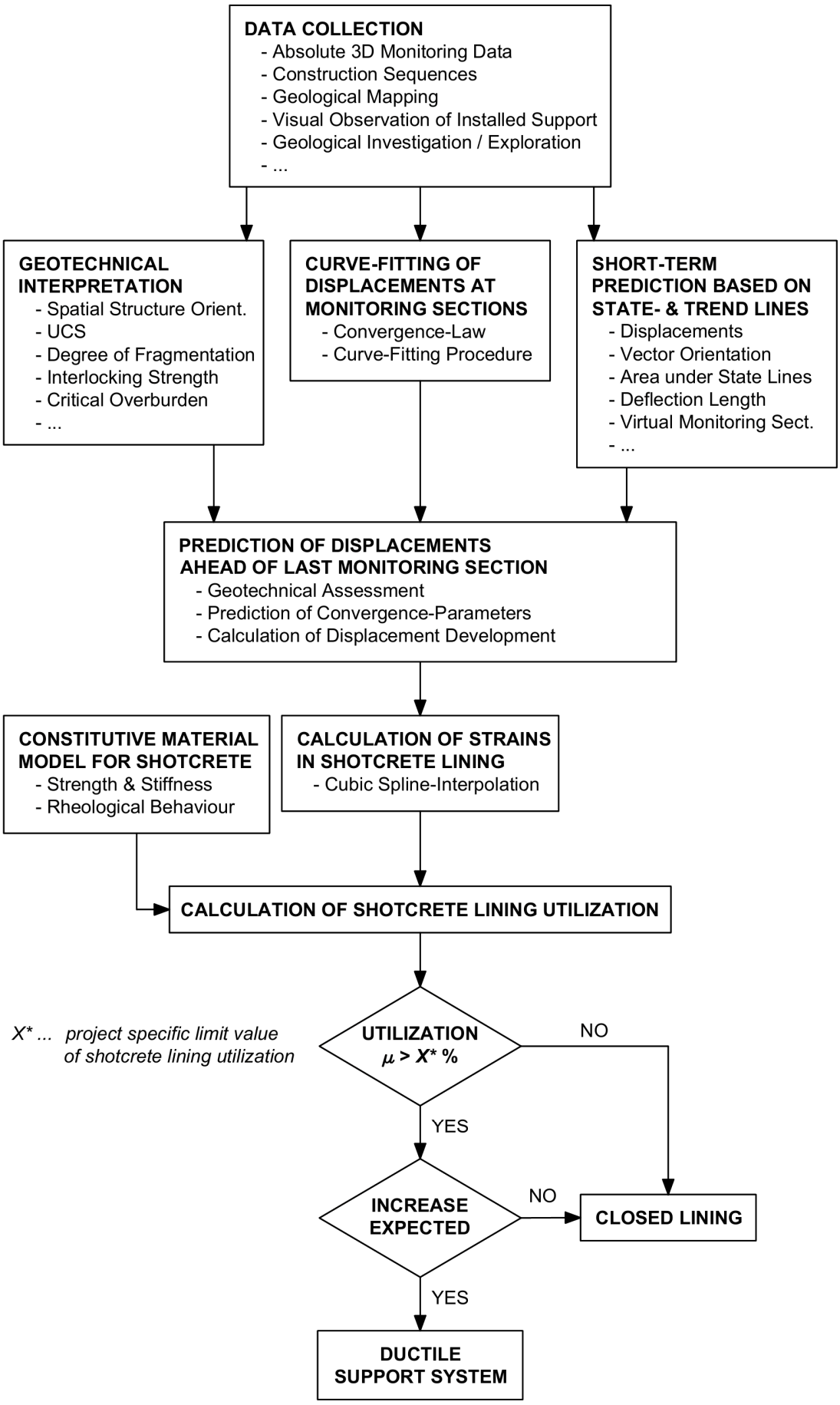

Fig. 5: Decision strategy for the application of ductile support systems.

In a first step, absolute 3D displacement monitoring data, corresponding construction sequence data, information on geological conditions and visually observed information are gathered. After each face mapping, a geological-geotechnical interpretation and short-term prediction ahead of the face is done. Then, the displacements of relevant monitoring sections with ongoing deformations are processed by a curve-fitting procedure according to the *Convergence-Law* of Sulem et al. [35].

Based on the results of the previous analysed monitoring sections and in combination with the updated geological model and various trend lines, a short-term prediction of the expected deformations of the following rounds (ahead of the current face) is performed.

From the predicted deformation of the excavation profile (displacement measurements at five points), strains in the tunnel lining are back-calculated. Subsequently, based on the Rate-of-Flow-Method [30, 31], the shotcrete utilization is calculated. If the utilization exceeds a project specific defined limit and trend developments indicate weaker ground ahead, the installation of a ductile support system is recommended. Otherwise a closed lining is sufficient.

After each face mapping and monitoring epoch, and after additional exploratory measures have been performed, the newly gathered information should be used to update the input parameters for the proposed procedure and to refine the prognosis.

The following sections describe in detail all steps necessary to find an answer to the question “Is a ductile support system in the next rounds required?” in a consistent way.

4.2 Data Collection

The first step is the identification and recording of representative data for the proposed method. Obtained information and technical documents from the design phase (geological sections, ground types, behaviour types, system behaviour, construction concepts, time schedule, sketches, etc.) serve as basis and are updated during construction.

4.2.1 Absolute 3D Monitoring Data

An accurate 3D displacement monitoring is one of the most essential parts for a proper analysis of the system behaviour and the basis for short-term predictions. Details to 3D displacement monitoring and monitoring data interpretation can be found in the handbook *Geotechnical Monitoring in Conventional Tunnelling* [20].

The distance between monitoring sections is project specific and should comply with the current geotechnical situation. For a timely identification of geological features (e.g. fault zones) or for an optimum changeover to a ductile support system, monitoring section distances should be reduced. The monitoring section should be installed as close

as possible behind the face (typical ~0.5-1 m) and the zero reading taken immediately [20]. For a reliable monitoring data interpretation, readings close to excavation activities should be taken at least on a daily basis [20]. Generally, lower distances between monitoring sections and higher reading frequencies increase the accuracy of prognoses.

The coordinate system and numbering of monitoring targets used in the thesis is defined in Fig. 6.

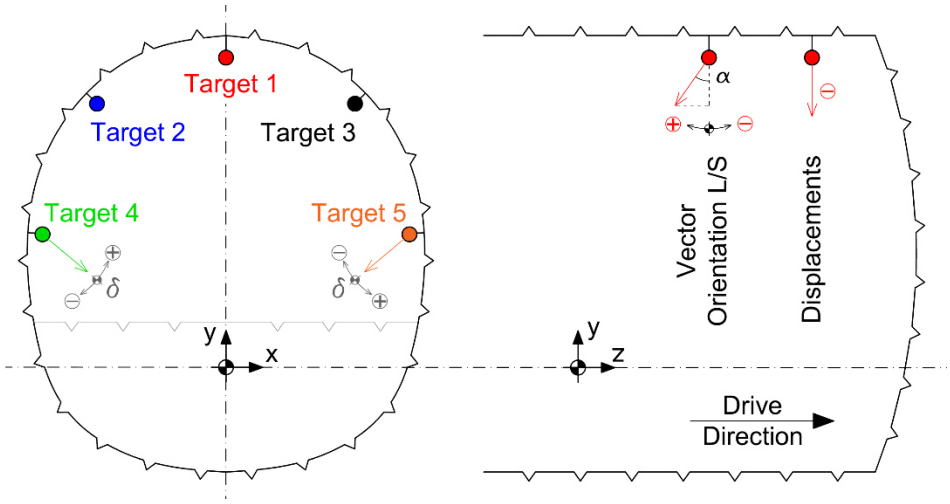

Fig. 6: Cross-section (left) and longitudinal section (right) showing the local coordinate system and numbering of monitoring targets.

For a proper analysis of monitoring data the construction sequence must be considered.

4.2.2 Geological Mapping

For an increasing accuracy of short-term prediction of the system behaviour, geological mapping forms the second fundamental part of the thesis' approach. Since the geology is project specific (hard rock, soft ground, etc.), *Key Parameters* are defined in the design phase (for details see [7, 36]). During construction, these geotechnical relevant parameters are gathered and assessed.

For this thesis, following exemplarily ground specific parameters are considered:

- Spatial structure orientation (dip & dip direction; evaluation based on [37])
- Unconfined Compressive Strength – UCS (acc. to [36])
- Degree of fragmentation (foliation/bedding/discontinuities; acc. to [36])
- Interlocking strength (for details see [38])

4.2.3 Visual Observation of Installed Support

A simple but useful method to identify critical situations is the visual observation of the installed support. Reasons for cracks in the shotcrete lining and deformed or broken anchor heads should continuously be recorded and their cause investigated immediately. With this information, the geotechnical engineer gets a rough overview of the degree of support utilization and of problematic zones. In case of any damage of the support, the geotechnical engineer then can compare the predicted utilization of the support measures with the observed one and fine-tune the procedure for the prognosis if required. This is just an ancillary method and should always be combined with measures described in section 4.2.1 and 4.2.2. Further researches on this topic are actually done by Lengauer [39].

4.2.4 Additional Methods

If additional methods are applied especially in unclear situations or in regions where weak zones are predicted, their information should be considered in the decision-making process. For exploration drillings ahead of the face a changing colour of the flushing water, an increase of fine-grain fractions or a decrease of drilling resistance can be a hint for weak material ahead [40]. Under certain circumstances, geophysics can provide useful information [41, 42]. Other methods like those as mentioned in section 2.3.3, or detailed information from the engineering geological investigation program (core drillings, laboratory tests, etc.) should be used as required and available.

4.3 Geotechnical Interpretation

In combination with the geological interpretation and short-term prediction of the geologists, geotechnical interpretations of the ground- and system behaviour are carried out. By systematically comparing data of each mapped tunnel face, a geotechnical prognosis of the next rounds can be performed. The aim is to use existing and internationally approved approaches for the interpretation. Since geological- and boundary conditions are project specific, the evaluation of other characteristics might be necessary or meaningful (e.g. seepage, etc.). Below an exemplarily selection is given.

4.3.1 Spatial Structure Orientation

The spatial structure orientation relative to the tunnel axis highly influences the ground- and system behaviour [43, 44] and therefore provides useful information for the interpretation of displacement characteristics and shotcrete lining utilization. Francis [37] developed a simple stereonet overlay for describing the favourability of structure orientation as basis for a geomechanical classification. The application of the method is modified here and used as a supplementary tool to estimate the final displacement magnitude and to identify changes in displacement characteristics in combination with the interpretation of initial displacements.

Since the tunnel face and side walls generally show different failure mechanisms in jointed rock masses [43], the influence of spatial structure orientation is evaluated separately for the crown, the left- and right side wall. The poles of observed governing structural features are plotted in a lower hemispherical stereonet (Fig. 7) and rated from 1 (very favourable) to 5 (very unfavourable).

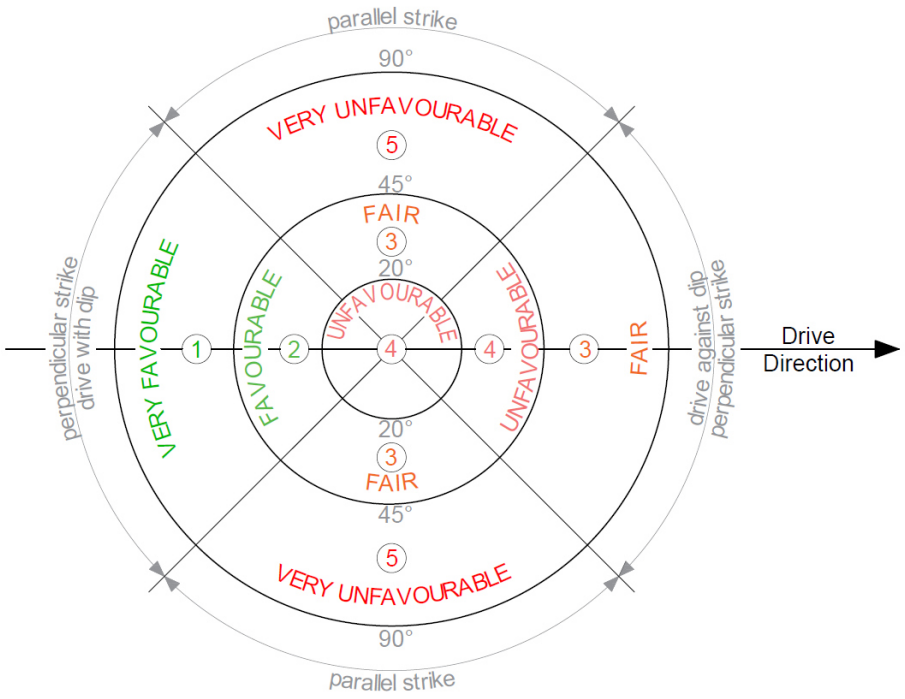

Fig. 7: Favourability of spatial structure orientation on the displacement development behind the face (after [37]).

A foliation striking parallel to the tunnel axis generally leads to higher displacements (increasing $C(x,t)$) and to a larger influence length of the excavation (increasing X) than a foliation striking perpendicular to the tunnel (Fig. 8). The parameters C and X are part of the Convergence-Law of Sulem et al. [35], which is described in section 4.4.1.

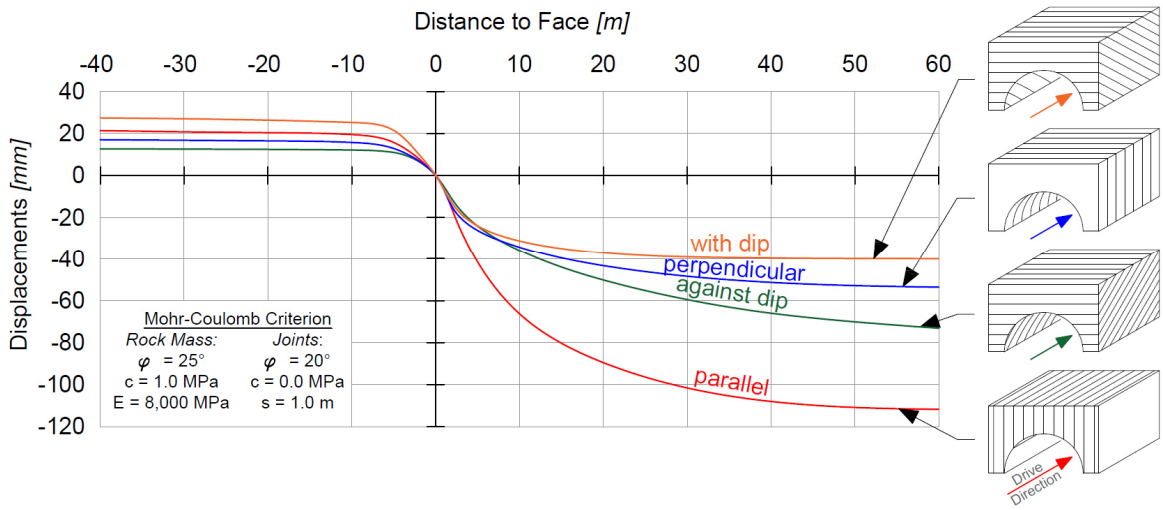

Fig. 8: Influence of spatial structure orientation on the displacement development; the figure shows results of numerical FEM-simulations.

Investigations show that tunnelling against the dip direction of a jointed rock mass is more unfavourable with regard to the displacements developing after passing the face, than tunnelling in the direction of the joint dip [45]. If the tunnel is driven against the dip direction, less than 20 % of the total displacements occur ahead of the face, whereas for a drive in dip direction over 60 % of the displacements already develop ahead of the face as shown in Fig. 8 (note that the ratio between pre- and total-displacements depends on many factors, e.g. dip angle and joint shear-strength; compare with [44]). This circumstance has been considered by Francis [37] developing the stereographic overlay for the classification of the structure orientation. This means, with higher rating values according to the classification shown in Fig. 7, larger displacements $C(x,t)$ and/or greater influence lengths X are expected.

Sometimes governing structures are outside the excavated profile and hence cannot be observed at the tunnel face but highly influence the system behaviour. A very unfavourable case for example is a steeply dipping fault, striking sub-parallel to the tunnel axis. Since stress concentrations cause increasing deformations of the respective side wall, comparing adjacent displacement vectors in cross-section can provide hints to such geological/structural features outside of the excavation profile. A deviation of the displacement vector orientation in cross-section is also often governed by structural features of the rock mass (e.g. foliation) [21].

In combination with the parameters described in the following sections and by comparing hemispherical plots of structural features and spatial structure orientation ratings of rock mass zones lately excavated, the geotechnical engineer may be able to deduce, whether displacement developments in the current excavation area – compared to the last monitoring section – are expected to increase or decrease.

4.3.2 Unconfined Compressive Strength (UCS)

Increasing or decreasing displacements are often correlated with a change of the rock mass strength/stiffness, mainly depending on the intact rock strength, degree of fragmentation and discontinuity properties. For the assessment of the intact rock strength in the field, the classification acc. to ÖNORM EN ISO 14689-1 [36] can be used. With simple methods the geologist can estimate a range of UCS directly at the tunnel face. Results are plotted in a bar graph showing the frequency of UCS classes per tunnel face (Tab. 1). By comparing graphs of adjacent faces as shown in Fig. 9, a trend might be identified [38].

Tab. 1: Estimation of UCS of the intact rock at the tunnel face (based on [36, 46]), including an example of the distribution of UCS classes.

Unconfined Compressive Strength - UCS (ÖNORM EN ISO 14689-1:2004)			
Term	*UCS [MPa]*	*Frequency [%]*	*Field Identification*
Extremely weak	< 1 MPa	4 %	Indented by thumbnail
Very weak	1-5 MPa	49 %	Crumbles under firm blows with point of geological hammer, can be peeled by a pocket knife
Weak	5-25 MPa	25 %	Can be peeled by a pocket knife with difficulty, shallow indentations made by firm blow with point of geological hammer
Medium strong	25-50 MPa	10 %	Cannot be scraped or peeled with a pocket knife, specimen can be fractured with single firm blow of geological hammer
Strong	50-100 MPa	4 %	Specimen requires more than one blow of geological hammer to fracture it
Very strong	100-250 MPa	6 %	Specimen requires many blows of geological hammer to fracture it
Extremely strong	> 250 MPa	2 %	Specimen can only be chipped with geological hammer
	Sum:	*100 %*	

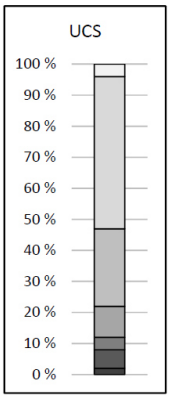

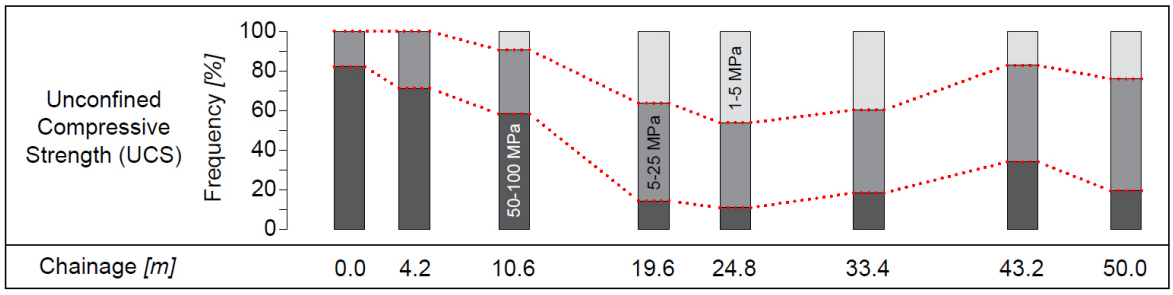

Fig. 9: Example for a trend development of observed UCS distributions.

4.3.3 Degree of Fragmentation

The same kind of evaluation as for the distribution of UCS can be applied to the fragmentation degree of the rock mass (see Tab. 2). The spacing of bedding planes and discontinuities are classified acc. to ÖNORM EN ISO 14689-1 [36]. Decreasing spacing of these features can be an indication for approaching weaker rock masses [38], as exemplarily shown in Fig. 10 for a transition zone in front of a fault zone. Generally, a higher degree of fragmentation is associated with a lower strength/stiffness of the rock mass and hence, larger displacements are expected [47].

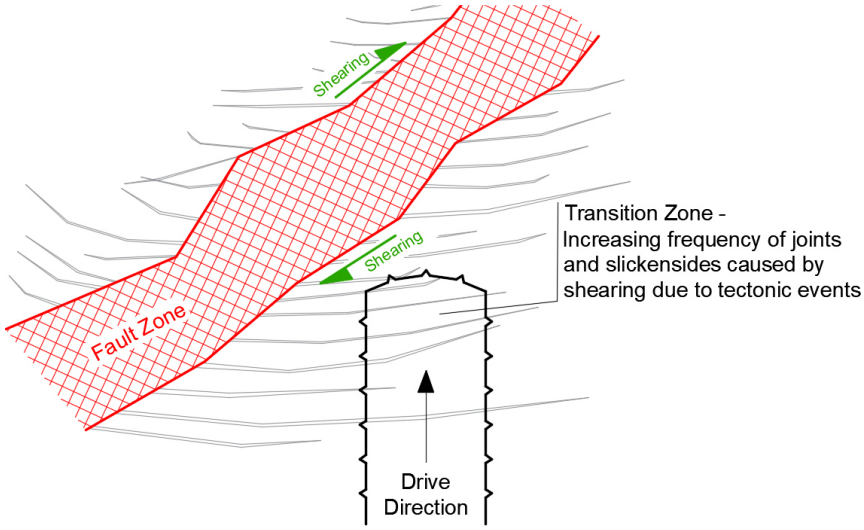

Fig. 10: Schematic sketch to highlight the basic idea of increasing discontinuity frequency and increasing degree of fragmentation of the rock mass, respectively, when approaching a weaker zone.

Tab. 2: Evaluation of bedding plane- and discontinuity spacing to classify the degree of fragmentation of the rock mass (based on [36]).

Degree of Fragmentation		
Bedding Planes (ÖNORM EN ISO 14689-1:2004)		
Term	*Spacing [cm]*	*Frequency [%]*
Very thick	> 200 cm	2 %
Thick	60-200 cm	5 %
Medium	20-60 cm	8 %
Thin	6-20 cm	16 %
Very thin	2-6 cm	15 %
Thickly laminated	0.6-2 cm	39 %
Thinly laminated	< 0.6 cm	15 %
	Sum:	*100 %*

Discontinuities (ÖNORM EN ISO 14689-1:2004)		
Term	*Spacing [cm]*	*Frequency [%]*
Very wide	> 200 cm	4 %
Wide	60-200 cm	3 %
Medium	20-60 cm	9 %
Close	6-20 cm	13 %
Very close	2-6 cm	48 %
Extremely close	< 2 cm	23 %
	Sum:	*100 %*

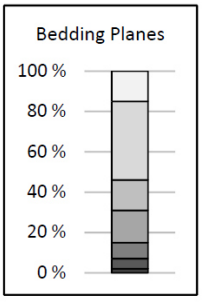

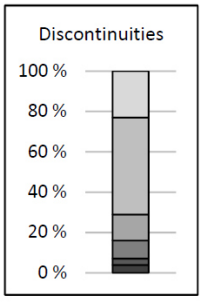

4.3.4 Interlocking Strength

The interlocking strength is a descriptive sum parameter of the degree of fragmentation, the frictional- and persistence properties of discontinuities and the stress conditions near the face [38]. By visual observation of the side walls and face during excavation, the geotechnical engineer can assess the behaviour of the system in the unsupported area and link it to the local interlocking strength. For the assessment, definitions based on Prinz & Strauß [48] and modifications from Lenz et al. [38] are used.

Tab. 3: Descriptive evaluation of interlocking strength at crown, left- and right side wall for one excavation round (acc. to [38]).

Interlocking Strength (Lenz et al., 2017, Prinz & Strauß, 2010)			
Term	*Description*	*Observations at Tunnel Face*	*System Behaviour in Excavation Area*
compact	no visible open discontinuities, good interlocking	cutter and shovel marks clearly visible	stable
moderately disintegrated	poor interlocking within a discontinuity set		small-scale rock fall and over-breaks
disintegrated	several open discontinuity sets with poor interlocking	cutter and shovel marks not clearly visible	repetitive large-scale caving of the face and the walls, potential for large-scale collapse
loose	fractured rock bodies without interlocking, virtually non-cohesive rock material		

Left Side Wall:	compact	**Crown:**	moderately disintegrated	**Right Side Wall:**	disintegrated

4.3.5 Critical Overburden

The *Critical Overburden* (H_{crit}) as defined in Eq. 1 was developed by Radončić [49] to define an application limit of closed linings.

$$H_{crit} = (H_0 + H^* * \tan\varphi) - 75 * \left[1 - \left(\frac{X}{X + \varepsilon - \varepsilon_0}\right)^2\right] \quad \text{Eq. 1}$$

with:
- H_{crit} … critical overburden *[m]*
- H_0, H^* … pre-defined function parameter depending on excavation concept *[m]*
- X, ε_0 … pre-defined function parameter depending on excavation concept *[-]*
- ε … total unsupported radial strain *[-]*
- φ … friction angle of rock mass *[°]*

Note: The parameter *X* in Eq. 1 is not the same as the one in the Convergence-Law of Sulem et al. (Eq. 2).

Depending on the excavation sequence (full-face, top-heading, top-heading with invert), pre-defined function parameters H_0, H^*, X and ε_0 are selected. ε describes the total radial strain for the unsupported case and can either be determined with numerical simulations (FEM/DEM) or with analytical calculations (e.g. Feder & Arwanitakis [50], Carranza-Torres [51], Sulem et al. [52]).

The parameter, which takes the geological conditions into account, is the friction angle of the rock mass φ. Representative values can be taken from preliminary investigations, back-calculated with the Hoek-Brown failure criterion [53] or estimated on-site. Due to assumptions made for the development of the approach, results with friction angles higher than 30° get fuzzy and are not reliable any more [4].

The ratio between the critical overburden H_{crit} and the actual overburden H is used as indication regarding shotcrete lining utilization and considered for the decision-making process in this thesis.

4.4 Curve-Fitting of Displacements at Monitoring Sections

Basis for displacement predictions ahead of the last monitoring section are analyses and interpretations of displacements at previous monitoring sections. Measured displacements are fitted mathematically (section 4.4.2) and their further devolvement and final displacements extrapolated. Function parameters (section 4.4.1) of the curve-fitting procedure – describing the characteristics of the displacement development – are then used as reference values for predicting displacements ahead of the last monitoring section. For the final calculation of shotcrete utilization, absolute displacements of all monitoring targets must be analysed.

4.4.1 Convergence-Law

To predict the displacement development at monitoring sections based on measured data, the Convergence-Law of Sulem et al. [35] is used (see Eq. 2). The equation can be divided in a time-dependent and time-independent part, representing the long-term and short-term behaviour of the ground. Therefore, information about chainage, excavation time of top-heading/bench/invert, distance between monitoring sections and the tunnel face, and timespan between excavation and zero reading are necessary.

$$C(x,t) = C_{x\infty} * \left[1 - \left(\frac{X}{X+x}\right)^2\right] * \left\{1 + m * \left[1 - \left(\frac{T}{T+t}\right)^{0.3}\right]\right\} \qquad \text{Eq. 2}$$

with:
- $C(x,t)$ … face- & time-dependent displacement *[mm]*
- $C_{x\infty}$ … ultimate time-independent displacement *[mm]* (≠ final displacement!)
- X … curve-fitting parameter *[m]* (describes the influence length of time-independent displacements)
- m … ratio of ultimate time-dependent displacements and time-independent displacements *[-]*
- T … curve-fitting parameter *[d]* (describes how fast time-dependent displacements develop)
- x … distance between monitoring section and current excavation face *[m]* (function of advance rate)
- t … elapsed time since excavation of the round where the monitoring section is located *[d]*

An example for a typical deformation development at a constant advance rate is given in Fig. 11.

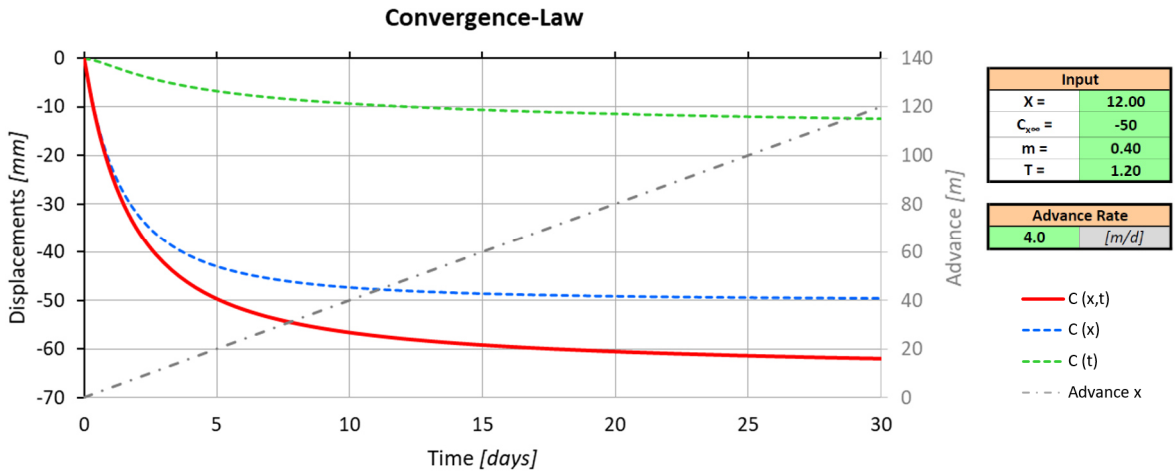

Fig. 11: Typical deformation development of absolute displacements (C(x,t), red solid line) at a constant advance rate, calculated with Sulem's Convergence-Law. Time-dependent (C(t), dashed green line) and time-independent (C(x), dashed blue line) parts are shown separately for illustrative purposes.

Discussion of function parameters:

Analyses of fitted displacement developments show, that all function parameters of the Convergence-Law are within a common range [14]:

- $4 \leq X \leq 30$
- $0.1 \leq m \leq 0.8$
- $0.5 \leq T \leq 2.0$

Parameter X depends on the ground structure and stress/strength ratio of the ground. For example, if the foliation strikes parallel to the tunnel axis, higher values of X are expected than in case of a perpendicular strike (see section 4.3.1). Panet & Guenot [54] propose to use $X = 0.84 * \text{plastic radius}$, which means that highly stressed grounds lead to higher values of X. Since for the critical overburden (section 4.3.5) also the plastic radius for the unsupported case is calculated, this information can be used to estimate X.

Parameters m and T highly depend on the time-dependent characteristics of the ground and the current stress state. Values of m in the upper range are typical for weak ground conditions with a long-lasting deformation behaviour [14].

The graphs in Fig. 12 show the influence of function parameters on the displacement development for a constant advance rate of 4 m/day.

Fig. 12, top left: The ultimate time-independent displacement parameter $C_{x\infty}$ defines the magnitude of time-independent displacements (vertical move of the curve) and is not equal to the final displacements (if $m > 0$).

Fig. 12, top right: The parameter X describes the influence length within the time-independent displacements occur. In a time-displacement graph, X determines how fast these displacements develop.

Fig. 12, bottom left: Parameter m describes the ratio between ultimate time-dependent and time-independent displacements at infinite time and distance:

$$C(x = t = \infty) = C_{x\infty} * [1] * \{1 + [m]\}.$$

For example, m = 0.5 means, that if the tunnel is cut-through at x = ∞, after infinite time (t = ∞) the time-dependent displacements amount to 50 % of the final displacements.

Fig. 12, bottom right: The curve-fitting parameter T has a minor influence on the displacement development only and is used for fine-tuning during the curve-fitting procedure. It describes how fast time-dependent displacements develop. With increasing parameter m, also the influence of parameter T on the displacement development increases and vice versa.

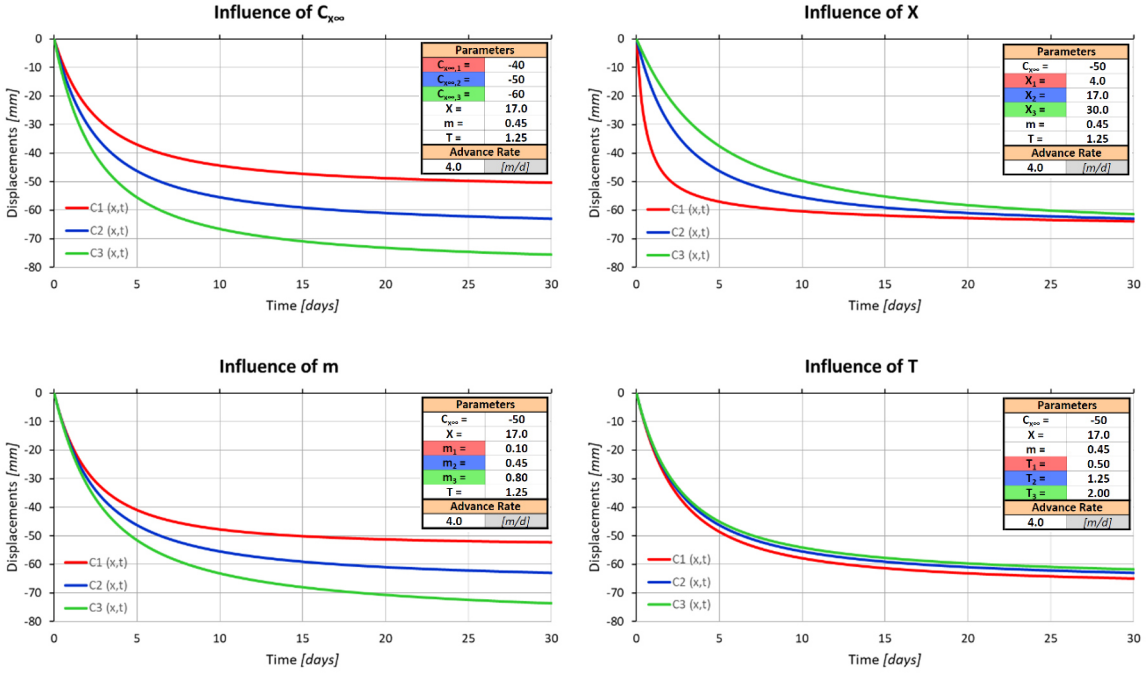

Fig. 12: Influence of the Convergence-Law function parameters $C_{x\infty}$ (top left), X (top right), m (bottom left) and T (bottom right) on the displacement development.

4.4.2 Curve-Fitting Procedure

With the Convergence-Law (Eq. 2) and a mathematical curve-fitting procedure, the function parameters $C_{x\infty}$, X, m and T are back-calculated from measured absolute V-H (vertical-horizontal) displacements. For an easier determination, an automatic fitting-algorithm based on the *Method of Least Squares* is used. To gain reasonable results, at least two follow-up measurements are necessary. All automatic fitted parameters can be adapted manually for fine-tuning. With the determined parameters, the further development of the displacements – after the last reading – is predicted (Fig. 14). Therefore, the advance rate of the following rounds must be estimated.

To consider the displacement vector orientation in cross-section for the prediction, the last measurement point is linearly connected with the zero-measurement point (= target position) and extrapolated (Fig. 13).

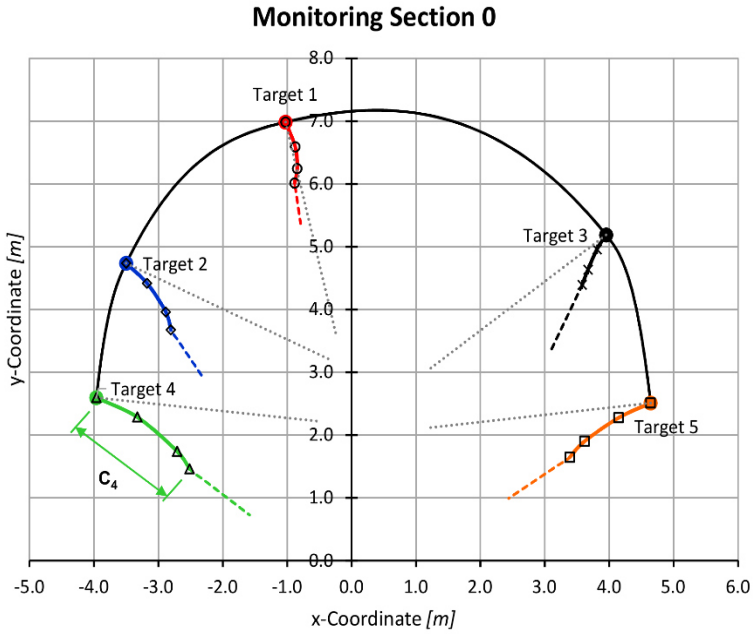

Fig. 13: Monitoring section with five targets: interpolated tunnel lining (black solid line), measured displacements (coloured solid lines with markers) and predicted displacement vector trends (coloured dashed lines). To highlight the deviation of the displacement vectors from a perfectly radial deformation pattern, lines perpendicular to the tunnel boundary are shown (grey-dotted lines). Displacement vectors are scaled-up by a factor of 50 (see also Fig. 14).

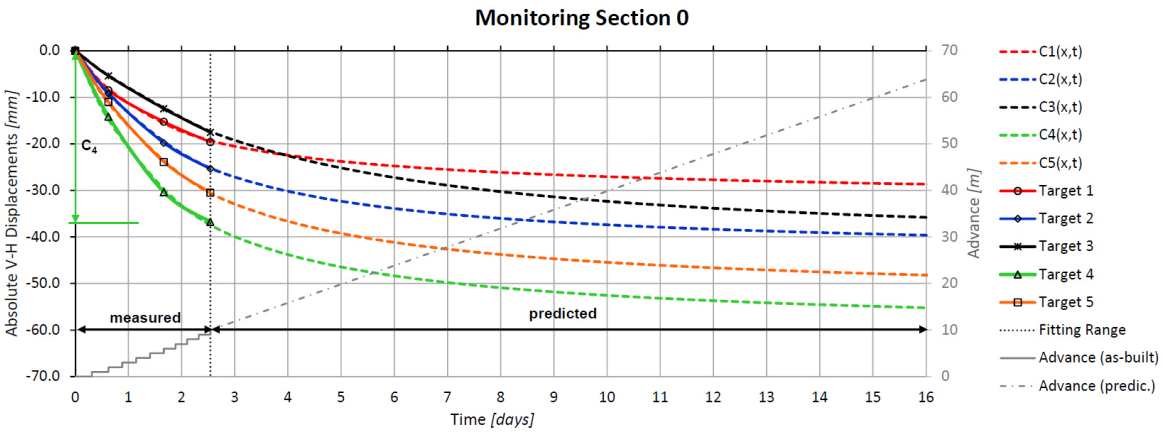

Fig. 14: Time-displacement graph with measured displacements (coloured solid lines with markers) and fitted/adapted displacement development (coloured dashed lines) for five targets.

After each follow-up measurement (usually on a daily basis), all function parameters at monitoring sections of interest are updated. In case of a sequential excavation sequence, it might be necessary to perform two independent curve-fittings – one for the top-heading excavation and another for the bench/invert excavation (see [20]). Further information on the prediction of displacements can be found in the thesis of Sellner [55].

4.5 Short-Term Prediction based on State- and Trend Lines

State lines and trend lines as defined in the monitoring handbook [20] allow a good overview on the displacements over a certain tunnel section and time period. Big advantage of this kind of analyses – compared to common time-displacement graphs – is to get information about the system behaviour ahead of the last monitoring section. The information of various types of state- and trend lines of all installed monitoring targets are used to increase the accuracy of short-term prediction of the displacement development in the excavation area. In this thesis, state- and trend lines of absolute V-H displacements (section 4.5.1) and L/S vector orientations (L-longitudinal displacements / S-settlements, section 4.5.2) are analysed. Further types of state- and trend lines [20] can be used as required. With advanced analyses of state lines (section 4.5.3), new tools are introduced for the geotechnical short-term prediction.

4.5.1 Absolute Displacements

State lines of vertical-/horizontal- or absolute displacements can provide useful information about the system behaviour and stress redistribution. The estimation of pre-displacements which develop between the current face position and monitoring section and timespan between excavation of the monitoring section and the zero-measurement is done by using the prediction model of Sellner [20, 55].

Evaluating several trend lines with different distances behind the face are used to obtain additional information. An increasing distance between those lines is an indication for changing stress redistribution and hence is associated with a larger parameter *X* and vice versa (see Fig. 15).

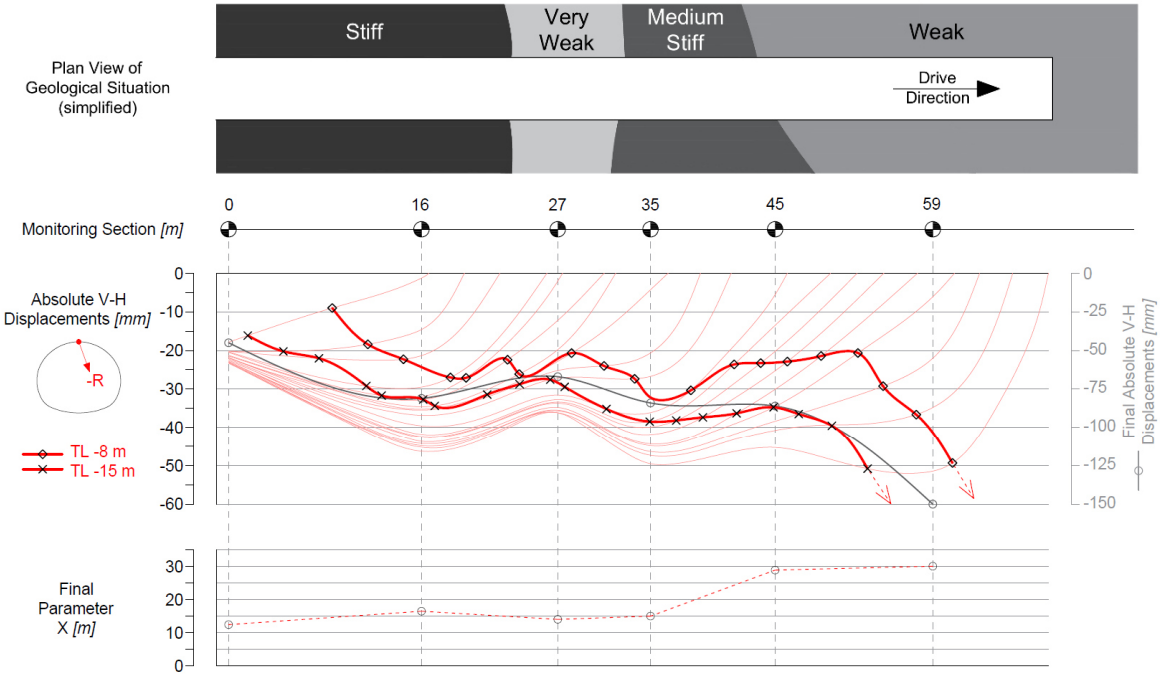

Fig. 15: Distance between trend lines as indication for changing ground conditions: geological plan view (top), trend lines of absolute V-H displacements at the crown (red solid lines with markers, 8 m and 15 m behind the face) with final displacements (grey solid line with markers; note the different scale of the ordinate) and parameter X back-calculated from final displacements (bottom).

For the geotechnical short-term prediction, state- and trend lines of absolute displacements are only conditionally applicable. The main reason is that the total amount of displacements does not develop immediately. Especially when approaching weak zones, the effect of delayed development of displacements increases (see also section 2.2 and 4.5.3). Hence, short-term predictions should not be based just on state- and trend lines of displacements, but in combination with other evaluation methods as described in the following sections.

4.5.2 Vector Orientation

"The L/S trend evaluation is the most appropriate method to identify changes in the ground conditions" [20]. Since an early identification of changing ground conditions ahead of the face is vital for a timely displacement prediction, the vector orientation L/S is often used as a governing indicator. However, recent investigations have shown that in very heterogeneous rock masses with low stiffness contrasts and/or unfavourable structure orientations, the vector orientation may not provide reliable results [38].
In case of a low displacement level, the measuring accuracy may be another issue. Displacements in cross-section can be measured very accurately (based on angle measurement), whereas longitudinal displacements underlie higher inaccuracies (based on distance measurement) [20]. Investigations for this thesis have shown, that at small displacement levels up to few centimetres this issue can totally distort the evaluation of the vector orientation. Here, trend lines often show a fluctuation. Furthermore, the observed longitudinal displacements highly depend on the distance between monitoring section and tunnel face and on the moment of zero-reading [24].

4.5.3 Advanced Analyses of State Lines

During research for this thesis, detailed investigations of state lines are performed. Based on findings of numerical simulations and case studies, following conclusions when approaching a weak zone are made (see Fig. 16):

- Secondary stresses behind the actual excavation area tend to orientate against the direction of drive (stress redistribution);
- This causes an increase of the deflection length, affecting the displacement development in the supported area (see section 4.5.3.2);
- A change of the vector orientation in longitudinal direction as described by Budil [24] and Steindorfer [23] can be observed;
- Stress concentrations ahead of the face cause increasing face displacements/extrusion (see Jeon et al. [27] and Cantieni [29]);
- Divergent stress orientations impede the displacement development at the moment close behind the face (compare with section 4.5.1 and [4]) and can reduce the interlocking strength temporarily;

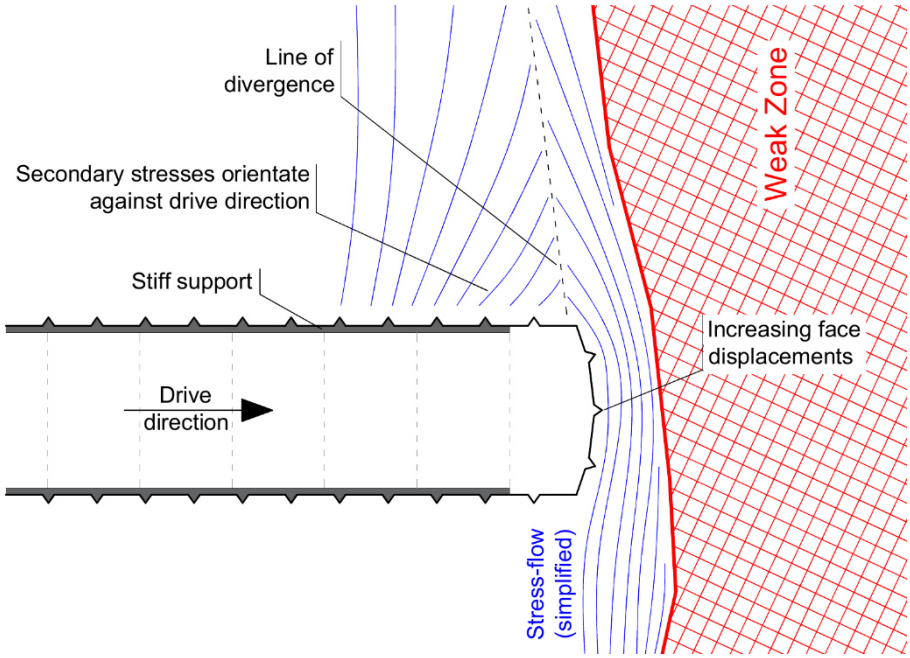

Fig. 16: Illustration of stress flow (simplified) and stress redistribution when approaching a weak zone.

Prompted by this, advanced analyses – focusing on state lines in the vicinity of the actual round – are developed. The methods should be used to increase the accuracy of the geotechnical short-term prediction and may identify weak zones earlier. A combined consideration with state- and trend lines as mentioned in section 4.5.1 and 4.5.2 is recommended.

For all further analyses, state lines of absolute V-H displacements are used. Theoretically, some of the introduced methods can also be applied to other state lines (e.g. horizontal displacements, etc.).

4.5.3.1 Area under State Lines

The *Area under State Lines* is a measure of external energy, released due to failure of the rock mass and the support. Rock mass with higher stiffness, accompanied usually with a higher strength, can store more energy, which leads to less deformation at the same loading level. The same applies to the support given that no failure occurs. This theorem was taken as occasion to investigate normalized areas under state lines.

By comparing areas of sections with similar lengths (e.g. 20 m from the face), a trend of the ground-/system behaviour can be identified (see Fig. 17). Increasing areas indicate weaker ground ahead. To decrease the influence of selected pre-displacements, the use of greater lengths behind the face (~ 1-3 diameter) is recommended.

Fig. 17 shows state lines of absolute V-H displacements at the crown (red solid lines) and the trend line of the area under the state lines (red solid line with markers). The shaded areas start at each face position of the state line and feature a constant pre-defined length L (here: 20 m). Markers of the trend line are linked to the face position. To calculate the area correctly, chainage and displacements must have the same unit and scaling.

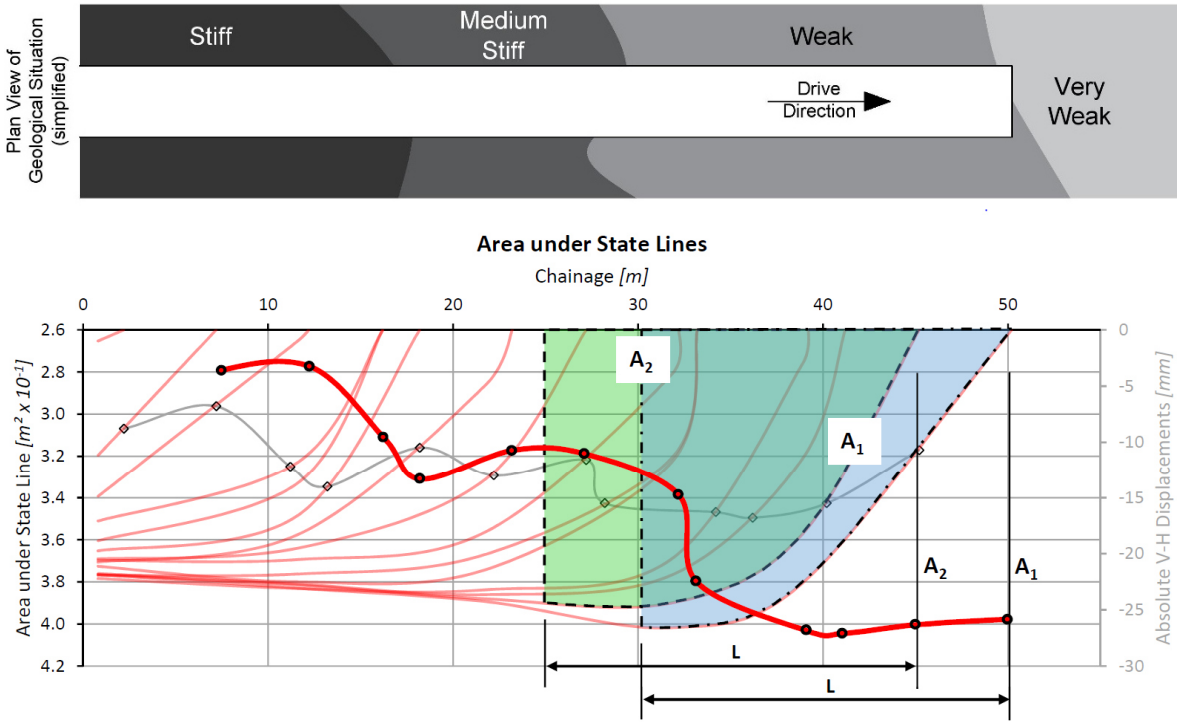

Fig. 17: Geological plan view (top) and area under state lines as measure of external energy to identify changing ground conditions (red solid line with markers); trend line is linked to the face positions; trend line of absolute V-H displacements 5 m behind the face (grey solid line with markers) is shown for comparative purposes.

Analysing the diagram in Fig. 17, an increasing trend of the area under the state lines along the investigated section can be observed. Especially at geological boundaries with different stiffnesses of adjacent rock masses a significant increase occurs. Due to the calculation of an area, a smoothening-effect is achieved and hence influences of local limited features are reduced.

This type of analysis seems to be suitable to obtain information of the trend development of displacements and stress redistributions over a longer section. To verify the general applicability, further investigations are necessary.

4.5.3.2 Deflection Length of State Lines

The *Deflection Length* is defined as the longitudinal distance between the tunnel face and the theoretical point of intersection of two adjacent state lines. This length can be determined mathematically or graphically as shown in Fig. 18. For the definition of the theoretical point of intersection, a tolerance can be introduced (e.g. Δ = 1 mm).

The size of the deflection length is a measure of how far behind the current excavation still additional displacements in the supported area occur. An increase of the deflection lengths can indicate a weaker rock mass ahead of the face as stress redistributions are more likely to happen against the direction of the drive (towards the stiff and supported rock mass sections) than towards the weak zone (limited capacity for stress redistribution).

By plotting the deflection length of each state line, a trend line can be developed. For the evaluation, the spatial structure orientation has to be considered (see section 4.3.1).

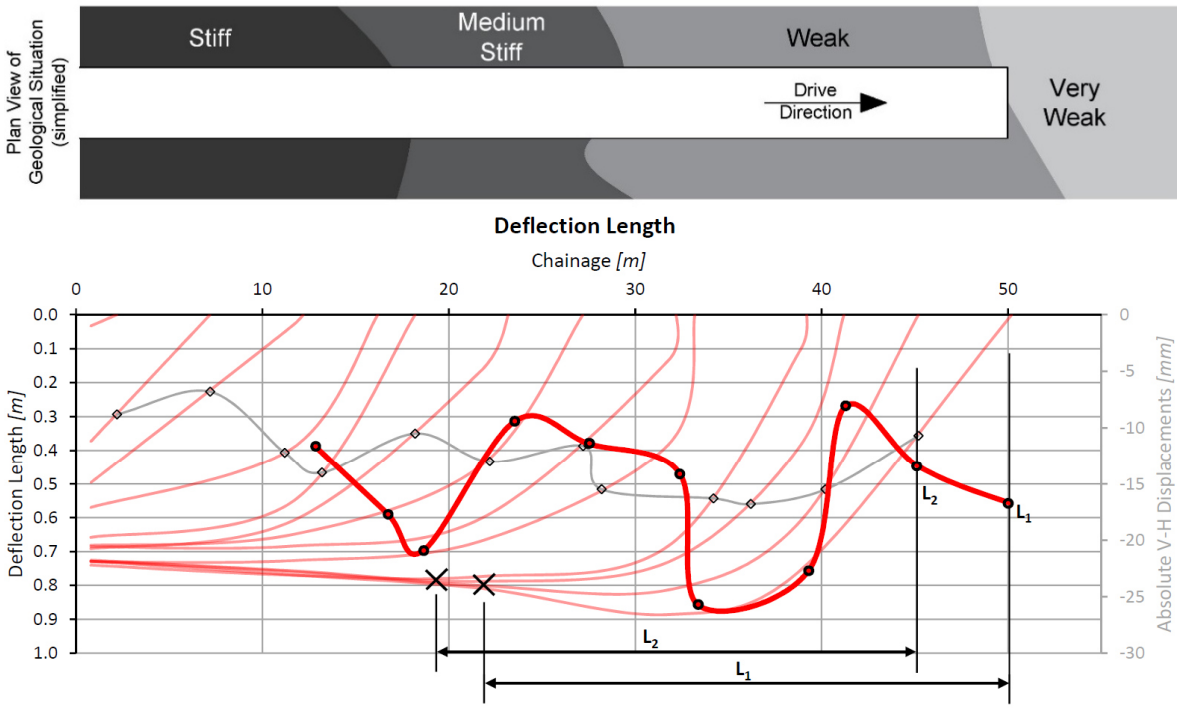

Fig. 18: Geological plan view (top) and definition of the deflection length of absolute V-H displacement state lines at the crown as indication for the stress redistribution (red solid line with markers); trend line is linked to the face position; trend line of absolute V-H displacements 5 m behind the face (grey solid line with markers) is shown for comparative purposes.

The deflection lengths illustrated in Fig. 18 show a strong correlation to changes in rock mass stiffnesses and to stress redistributions. When approaching weaker zones, the deflection length starts to increase and reaches its maximum as soon as the excavation enters the weak zone. Due to a normalization of the stress redistribution, a decrease of the deflection length is observed in the middle of the present zone.
The deflection length as a measure for stress redistributions, seems to be suitable to identify changing ground conditions ahead of the face. Further investigations are necessary to verify the general applicability.

4.5.3.3 Virtual Monitoring Sections

If the last monitoring section is far behind the excavation area or additional information about the displacement development in-between or ahead of monitoring sections are requested, *Virtual Monitoring Sections* can be introduced. At an arbitrary chainage in the distance-displacement graph, a vertical line is plotted and displacements are determined (Fig. 19, middle). An intersection with at least two state lines is recommended and the time of excavation of the chosen chainage should be known exactly.
Since each state line is linked to a specific date, information of the virtual monitoring section can be transferred to a time-displacement graph (Fig. 19, bottom). Here, a curve-fitting procedure and determination of the function parameters of the Convergence-Law as described in section 4.4 is done. For a correct comparison of function parameters of “real” monitoring sections and virtual monitoring sections, the pre-displacements are set to zero.

Note that state lines are interpolated splines and hence cannot describe abrupt changes in the displacement development as may be caused by geology. Therefore, a critical comparison with geological observations is inevitable.

The investigated virtual monitoring sections of Fig. 19 indicate larger displacements ahead of MS 19 since the initial gradients continuously increase and show little converging tendencies (Fig. 19, bottom). The curve-fitting parameters X also tend to increase.
Virtual monitoring sections are suitable to identify trends of the displacement developments and of the parameter X ahead of the last monitoring section and can provide useful information for the short-term prediction of displacements.

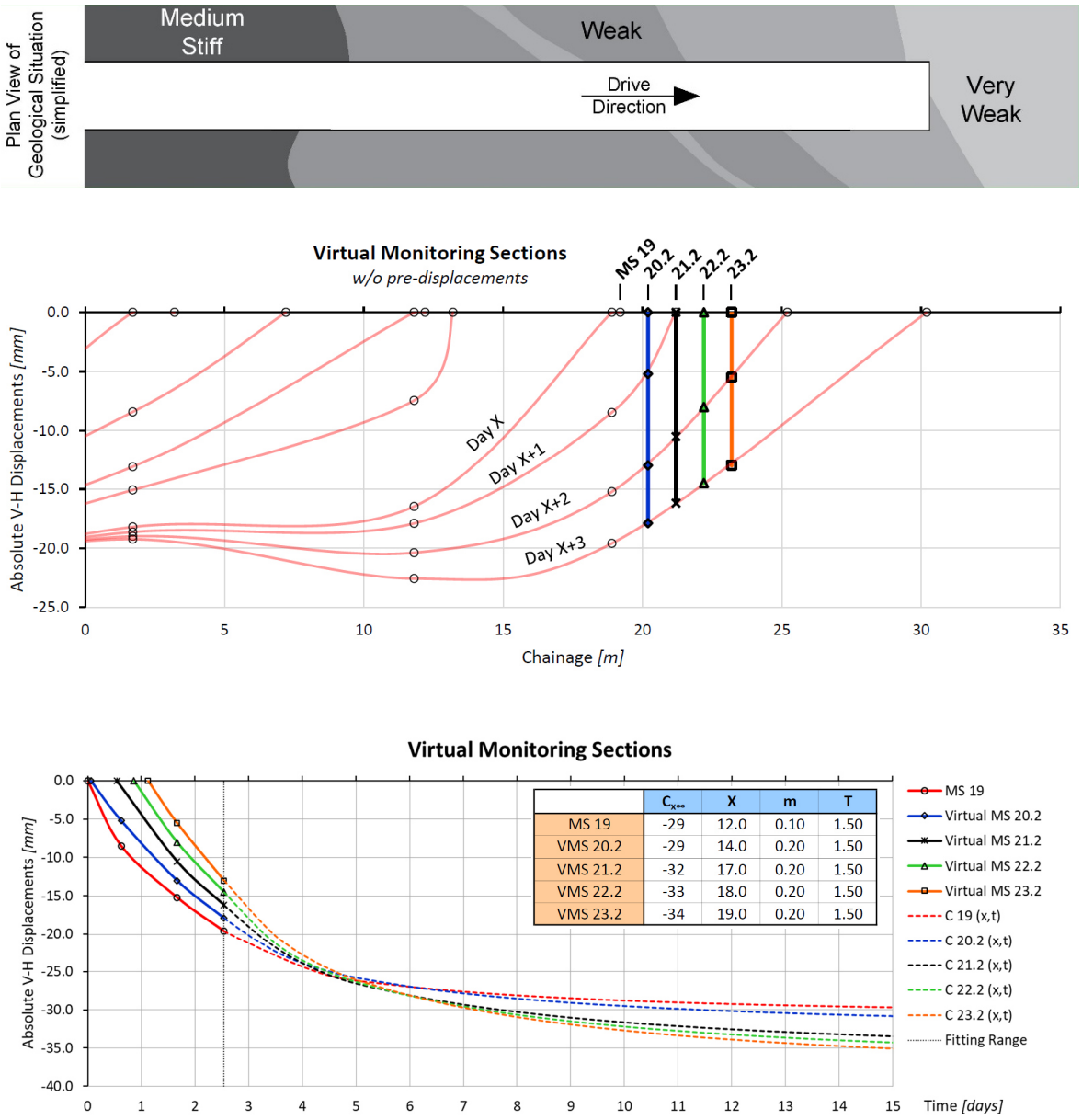

	$C_{x\infty}$	X	m	T
MS 19	-29	12.0	0.10	1.50
VMS 20.2	-29	14.0	0.20	1.50
VMS 21.2	-32	17.0	0.20	1.50
VMS 22.2	-33	18.0	0.20	1.50
VMS 23.2	-34	19.0	0.20	1.50

Fig. 19: Geological plan view (top), state lines of absolute V-H displacements at crown without pre-displacements including virtual monitoring sections (middle) and time-displacement graph for MS 19 and virtual monitoring sections 20.2, 21.2, 22.2 and 23.2 including predicted displacement developments (bottom).

4.6 Prediction of Displacements ahead of last Monitoring Section

This section is the key part for the prediction of shotcrete lining utilization ahead of the last monitoring section. All information gained from sections before (summarized in Fig. 4) is assessed systematically and with that information displacement developments for areas ahead are developed.
The approach is segmented as follows:

- Geotechnical assessment (section 4.6.1)
    - Geotechnical interpretation
    - Short-term prediction of displacements based on state- and trend lines
    - Prognosis of ground behaviour in cross-section
    - Prediction of displacement vector orientation δ in cross-section
- Prediction of Convergence-Parameters (section 4.6.2)
    - Curve-fitting of previous monitoring sections
    - Determination of $C_{x\infty}$, X, m and T for crown, left- and right side wall
- Calculation of expected displacement development (section 4.6.3)

4.6.1 Geotechnical Assessment

The systematic assessment of geotechnical parameters, observations and trend lines is done in a descriptive way by comparing trends of observed features described in section 4.3 and section 4.5. Therefore, a specific chainage/cross-section – between the last monitoring section and current face, or even ahead of the current face – must be chosen. To consider local differences in cross-section, crown (target 1), left side wall (target 4 & 2) and right side wall (target 3 & 5) are assessed separately (see Tab. 5). For the descriptive assessment, the rating system should be adjusted project specific. Ratings of Tab. 4 – referred to the influence on the shotcrete lining utilization – are used in this thesis.

Tab. 4: Rating system for the descriptive assessment of geotechnical parameters, observations and trend lines.

Positive influence on the shotcrete lining utilization	No change / no influence on the shotcrete lining utilization	Negative influence on the shotcrete lining utilization
+ + +		- - -
+ +	o	- -
+		-

For example, minus in context of displacements means that their magnitude increases (e.g. increasing from -50 mm to -60 mm). Minus in context of the vector orientation L/S means that the vector rotates against the direction of drive (e.g. from -5° to +5°, as defined in Fig. 6). It is about the kind of influence, positive (plus) or negative (minus), rather than the sign of the parameter change. It is up to the geotechnical engineer to weigh each parameter/trend accordingly.

Tab. 5: Descriptive rating of geotechnical parameters and trend lines at crown, left- and right side wall ahead of the last monitoring section, exemplarily for one face. The ratings are linked to the behaviour of previous rounds.

Face 10				
	Term	**Left Side Wall** *[Target 4 & 2]*	**Crown** *[Target 1]*	**Right Side Wall** *[Target 3 & 5]*
Geological-Geotechnical Parameters	Spatial Structure Orientation	- -	- - -	- -
	UCS	o	-	o
	Degree of Fragmentation	- -	- -	- -
	Interlocking Strength	o	+	+
	Critical Overburden	- -	- -	- -
	Behaviour of Support	o	o	o
State- & Trend Lines	Absolute Displacements	+	+	+ +
	Horizontal Displacements	+	n/s	+ +
	Vector Orientation L/S	+	+	-
	Area under State Lines	o	o	o
	Deflection Length	- -	- -	- -
	Displacements Virtual MS	- -	- -	-

As the translation and rotation of each point of the liner relative to each other determines the resulting strains and highly influences the shotcrete lining utilization, the vector orientation in cross-section δ must be considered and possible changes for areas ahead of the last monitoring section predicted.

Since the deformation pattern is always governed by structural rock mass features, it is necessary to understand potential failure mechanisms (ground behaviour) in order to properly predict the displacement development. For a better understanding, simple sketches of the expected ground behaviour are drawn. Based on the deformation pattern observed at previous monitoring sections in combination with the evaluation of the current geological conditions, the change in orientation of each displacement vector in cross-section δ is predicted (see Fig. 20)

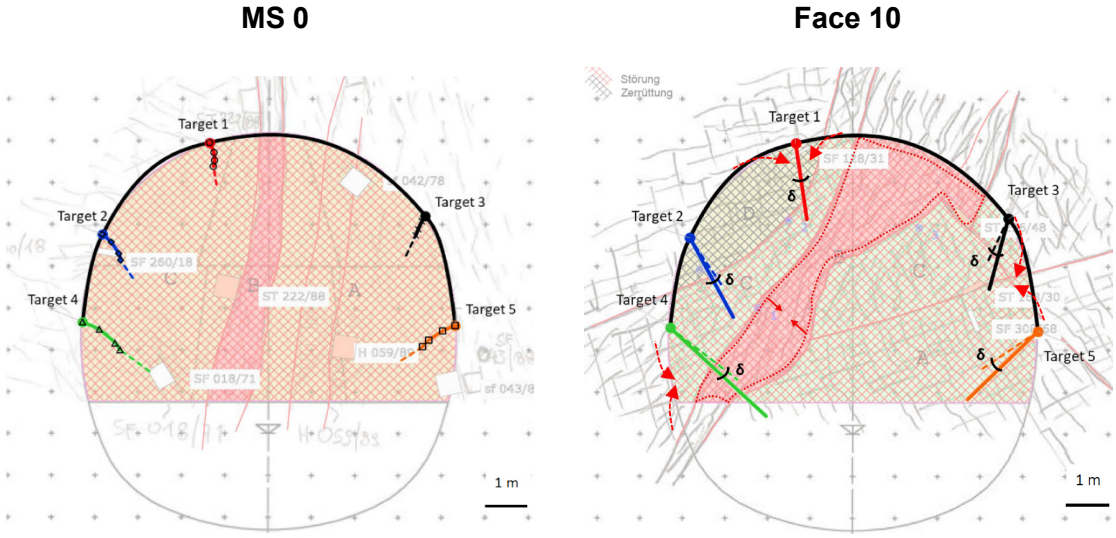

Fig. 20: Measured displacements at last monitoring section (left) and expected displacement vector orientation δ and ground behaviour at current face (right). Displacement vectors are scaled-up by a factor of 30.

4.6.2 Prediction of Convergence-Parameters

Using the fitted function parameters from the last monitoring section (section 4.4) as a starting point and considering assessments and short-term predictions of geological-geotechnical parameters (section 4.3) and of the system behaviour (section 4.5), the function parameters $C_{x\infty}$, X, m and T of the Convergence-Law at the specific cross-section are predicted (see Fig. 4). Common ranges for the parameters are listed in section 4.4.1. Tab. 6 shows the principal input screen of the systematic determination.

With this step, the expected displacement development is assigned to the cross-section chosen for the prediction. As strains are calculated in-between each virtual monitoring target (section 4.7), displacement developments of all targets (1 to 5) must be predicted.

This procedure can be repeated after each excavation step (with updated data) until the next real monitoring section is installed. Here, the geotechnical engineer has the possibility to verify his previous predictions and use monitored displacements and newly obtained Convergence-Parameters as basis for further predictions.

Tab. 6: Systematic determination of Convergence-Parameters and displacement vector orientation δ at a specific chainage ahead of the last monitoring section. Fitted function parameters of the last MS 0 are used as a starting point. The descriptive ratings of the monitoring section are linked to the previous monitoring section; the ratings of the current face are linked to the behaviour of the last few rounds.

Convergence-Parameters at MS 0									
		Trend Left Side Wall	*Target 4*	*Target 2*	*Trend Crown*	*Target 1*	*Trend Right Side Wall*	*Target 3*	*Target 5*
Fitted Parameters	$C_{x\infty}$	o	-54	-37	o	-29	+	-28	-46
	X	-	13	14	-	14	- -	16	15
	m	o	0.1	0.1	o	0.1	o	0.1	0.1
	T	- -	1.3	1.1	o	1.5	- -	1.5	0.7
Prediction at Face 5									
		Trend Left Side Wall	*Target 4*	*Target 2*	*Trend Crown*	*Target 1*	*Trend Right Side Wall*	*Target 3*	*Target 5*
Prediction at previous Face	$C_{x\infty}$	- -	-63	-43	- -	-34	-	-31	-50
	X	o	14	15	o	15	+	14	13
	m	-	0.2	0.2	-	0.2	-	0.2	0.2
	T	o	1.3	1.1	o	1.5	o	1.5	0.7
	δ		±0°	±0°		±0°		+5°	+5°
Prediction at Face 10									
		Trend Left Side Wall	*Target 4*	*Target 2*	*Trend Crown*	*Target 1*	*Trend Right Side Wall*	*Target 3*	*Target 5*
Prediction at current Face	$C_{x\infty}$	- -	-80	-55	- -	-45	- -	-45	-70
	X	-	15	15	-	15	+	12	10
	m	o	0.2	0.2	o	0.2	o	0.2	0.2
	T	o	1.3	1.1	o	1.5	o	1.5	0.7
	δ		-5°	-5°		±0°		+10°	+10°

For the shotcrete lining utilization – which is typically highest in the first few days after installation [56] – $C_{x\infty}$, X and δ are the crucial parameters. At this early stage the time-dependent parameters m and T play a minor role and should just be adapted if ground conditions significantly change.

4.6.3 Calculation of predicted Displacement Development

Based on the previously defined Convergence-Parameters and displacement vector orientations δ (section 4.6.2), the displacement development of all virtual monitoring targets at the chosen cross-section is calculated (Fig. 21 & Fig. 22).

Since these displacement curves are used to calculate the shotcrete lining utilization, just displacements occurring after shotcreting are considered. Therefore, the current advance rate and timespan between excavation and shotcreting must be specified.

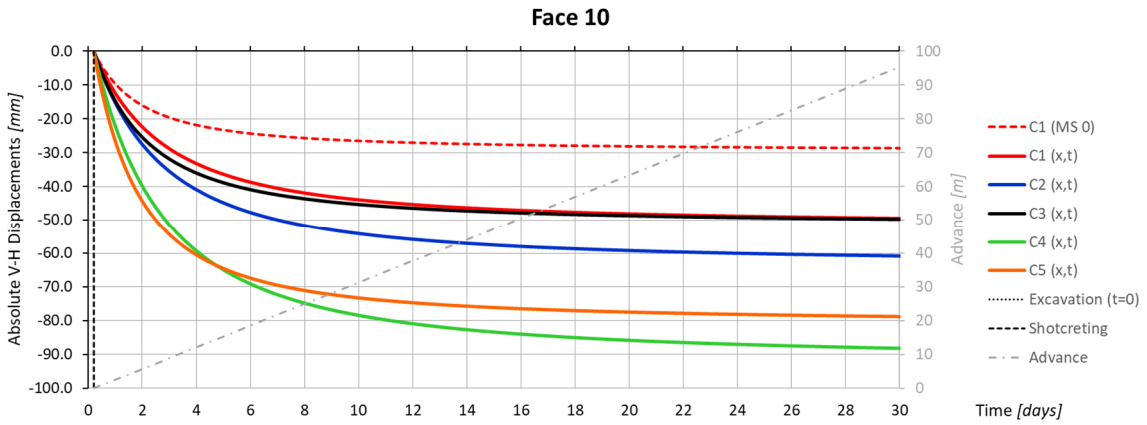

Fig. 21: Predicted displacements after shotcreting at chosen chainage (coloured solid lines, based on Convergence-Parameters of Tab. 6). Fitted displacement curve of target 1 of the previous MS 0 (dashed red line) is shown for comparative purposes.

4.7 Calculation of Strains in Shotcrete Lining

With the determined displacement curves (section 4.6.3), tangential strains are calculated in-between the predicted displacement vectors. Therefore, cubic spline-functions [57] as proposed by Brandtner et al. [3] are used (see section 2.4). Since the predicted displacements are defined with a mathematical continuous function, strains can be calculated at any given time.

The initial length of the spline (black solid line, Fig. 22) is taken from the zero-measurement of the previous monitoring section and used as reference value for the calculation of the strains at the chosen cross-section. A piecewise segmentation of the spline (targets 4-2, 2-1, 1-3, 3-5) enables a local calculation of the strains as shown in Fig. 23.

For example, the segmental calculation of the strains between the virtual target 1 and 3 at any given time is calculated according to Eq. 3:

$$\varepsilon^{1-3} = \frac{{L_0}^{1-3} - {L_i}^{1-3}}{{L_0}^{1-3}} * 10^3 \qquad \text{Eq. 3}$$

with: ε^{1-3} … tangential strain of the segment 1-3 at end of timespan Δt_i *[mm/m]*
(plus {+} = compression; minus {-} = tension)
L_0^{1-3} … initial reference length of the spline 1-3 *[m]*
(taken from zero-measurement of the previous monitoring section)
L_i^{1-3} … current length of the spline 1-3 at end of timespan Δt_i *[m]*

Fig. 22 shows the predicted displacement vectors and the procedure of cubic spline-interpolation between the virtual monitoring targets.

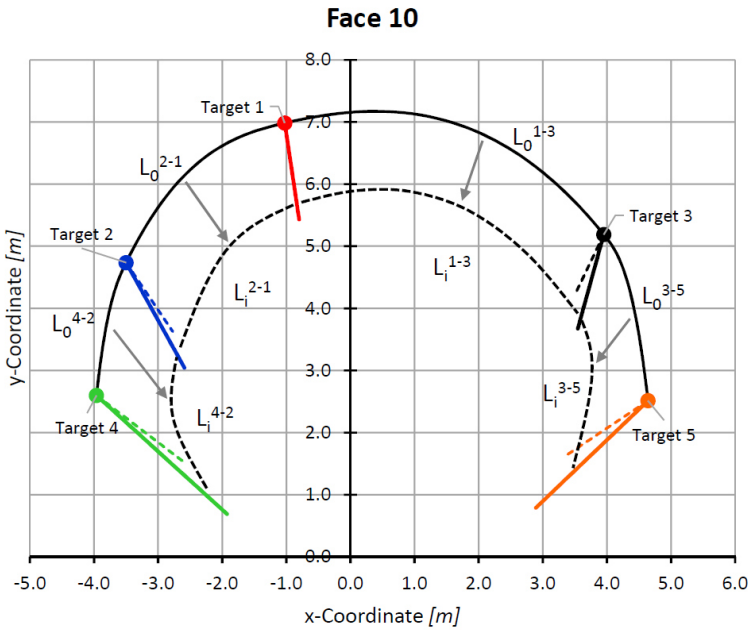

Fig. 22: Virtual monitoring targets for the prediction of the shotcrete lining utilization: continuous cubic spline-interpolation (black solid- and dashed lines) between displacement vectors; predicted displacement vectors at chosen cross-section (coloured solid lines) and fitted displacement vectors of the previous monitoring section (coloured dashed lines). Displacement vectors are scaled-up by a factor of 30.

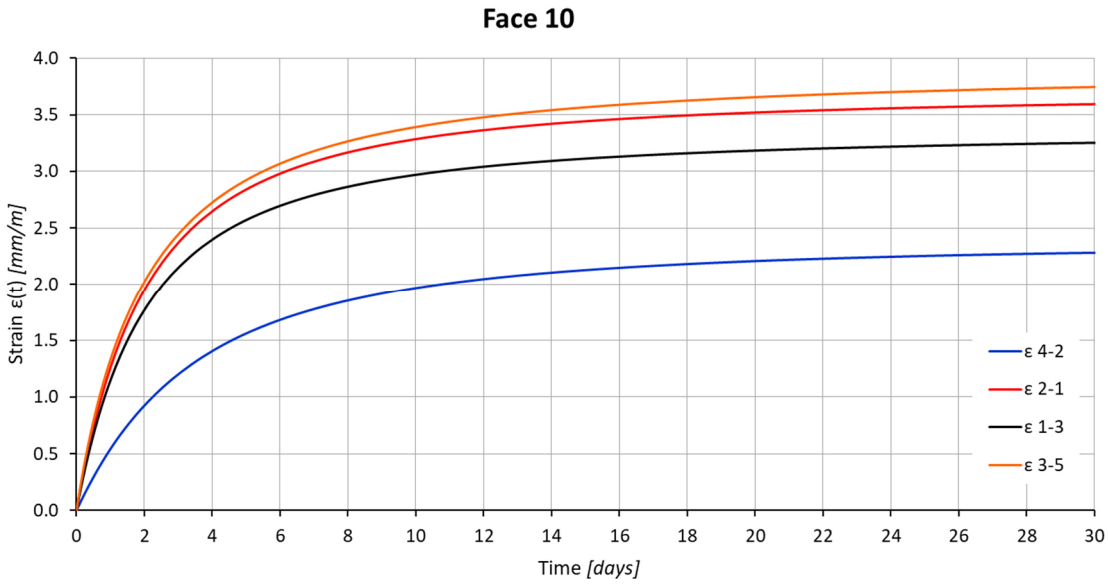

Fig. 23: Predicted strains between the virtual monitoring targets at chainage 10.0 m.

With this method it is possible to analyse strains:

- at real monitoring sections based on measured displacements (section 4.4);
- at real monitoring sections based on predicted displacements (fitting of displacement development with Convergence-Law, section 4.4);
- at virtual monitoring sections ahead of the last real monitoring section or ahead of the current face based on predicted displacements (fitting of displacement development including adjustment according to prognisis of ground-/system behaviour, section 4.6);

In cooperation with the Austrian Federal Railways (ÖBB), fibre-optical sensors are installed in the shotcrete lining at one cross-section of the *Semmering Base Tunnel*, measuring strains with a resolution of 2 cm every minute. Comparisons with the results described in the thesis of Wagner [58] have shown, that a smooth interpolation of strains between each monitoring target and between each displacement vector is suitable for the intended accuracy of this thesis.

4.8 Constitutive Material Model for Shotcrete

To calculate stresses in a shotcrete lining based on pre-determined strains, an appropriate constitutive material model must be applied. In general, shotcrete cannot be described with a common constitutive model for concrete, hence special methods are necessary.

4.8.1 Shotcrete Strength and Stiffness

Depending on the foreseen application (metro tunnel, alpine tunnel, etc.) and national specifications, different types of shotcrete mixtures are used, featuring quite different strength/stiffness development characteristics. To adequately describe these characteristics, equations defined for standard concrete in Eurocode 2 [59] are adapted by the author to shotcrete applications. With these new mathematical relationships (Eq. 4 / Eq. 5 / Eq. 6) an individual adjustment to different kinds of shotcrete is possible.

The temporal development of shotcrete strength $f_{cm}(t)$ is expressed as follows:

$$f_{cm}(t) = \beta_{cc}(t) * f_{cm} \qquad \text{Eq. 4}$$

with

$$\beta_{cc}(t) = \exp\left\{s * \left[1 - \left(\frac{28}{t}\right)^{\alpha 1}\right]\right\} \qquad \text{Eq. 5}$$

with:
- $f_{cm}(t)$ … mean shotcrete compressive strength at an age of t days *[N/mm²]*
- f_{cm} … mean cylinder compressive strength at 28 days *[N/mm²]*
- $\beta_{cc}(t)$ … coefficient, depending on shotcrete age *[-]* (Eq. 5)
- s … cement hardening coefficient *[-]* (modified for shotcrete by author)
- t … age of shotcrete in days *[d]*
- α1 … exponent of shotcrete strength *[-]* (0.5 for standard concrete; substituted for shotcrete by author)

Notes:

- exp{ } has the same meaning as $e^{( )}$ (exponential function)
- compressive strength of shotcrete f_{cm} at 28 days is in Austria usually higher than the values of corresponding strength classes (e.g. SpC 25/30 → $f_{cm,28} \approx$ 40-60 N/mm²)
- coefficients *s* and *α1* should be determined acc. to early strength classes of shotcrete [60] or by considering results of experimental testings (penetration needle- or stud-driving method)

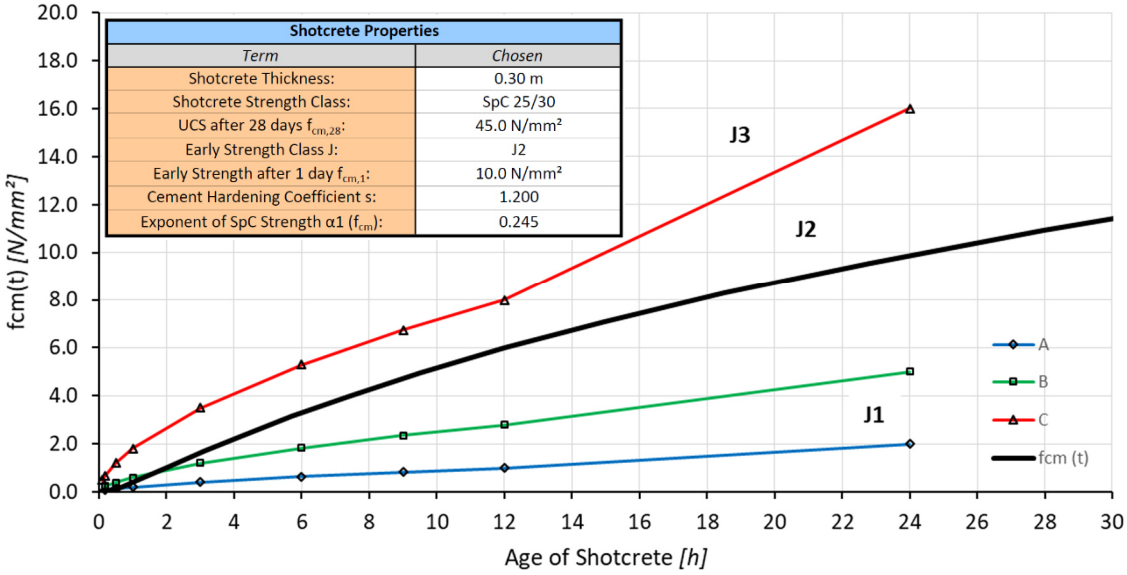

Fig. 24: Example of an early strength development of a shotcrete SpC 25/30 J2. Limit curves A, B, C and early strength classes J1, J2, J3 in-between are defined in [60].

The temporal development of modulus of elasticity $E_{cm}(t)$ is defined in Eq. 6:

$$E_{cm}(t) = \left(\frac{f_{cm}(t)}{f_{cm}}\right)^{\alpha 2} * E_{cm} \qquad \text{Eq. 6}$$

with: $E_{cm}(t)$ … mean shotcrete elastic modulus at an age of t days *[N/mm²]*
E_{cm} … mean shotcrete elastic modulus at 28 days *[N/mm²]*
$f_{cm}(t)$ … mean shotcrete compressive strength at an age of t days *[N/mm²]*
f_{cm} … mean cylinder compressive strength at 28 days *[N/mm²]*
α2 … exponent of shotcrete E-modulus *[-]*
(0.3 for standard concrete; substituted for shotcrete by author)

For detailed information regarding shotcrete materials, spraying- and testing procedures, early strength classes (J1 / J2 / J3) etc., it is referred to the *Guideline Sprayed Concrete* [60]. To verify the equations, data of early strengths have been kindly provided by ÖBB-Infrastruktur AG and BASF Performance Products GmbH.

4.8.2 Rheological Behaviour of Shotcrete

Besides the temporal development of shotcrete strength and stiffness, also the rheological behaviour must be considered, for which various methods are available [30–32, 61]. In this thesis a combination of the ansatz of Schubert P. [30] and Aldrian [31] is used (both based on the Rate-of-Flow Method).
To calculate stresses based on pre-determined strains, Eq. 7 (acc. to [30]) is used:

$$\sigma_2 = \frac{\varepsilon_2 - \varepsilon_1 + \frac{\sigma_1}{E_{cm}(t)} + \varepsilon_{d,2} * \left(1 - e^{-\frac{\Delta C(t)}{Q}}\right) - \Delta\varepsilon_{sh} - \Delta\varepsilon_t}{\frac{1}{E_{cm}(t)} + \Delta C(t) + C_{d\infty} * \left(1 - e^{-\frac{\Delta C(t)}{Q}}\right)} \qquad \text{Eq. 7}$$

with: σ_i … total stress in the liner at end of timespan Δt_i *[N/mm²]* (Eq. 7)
ε_i … total strain in the liner at end of timespan Δt_i *[-]* (section 4.7)
$E_{cm}(t)$ … age-dependent elastic modulus of shotcrete *[N/mm²]* (Eq. 6)
$\Delta C(t)$ … age-dependent change of viscous strain (Eq. 8)
$\varepsilon_{d,i}$ … viscoelastic strain at end of timespan Δt_i *[-]* (Eq. 11)
$\Delta\varepsilon_{sh}$ … change of shrinkage strain *[-]* (Eq. 9)
$\Delta\varepsilon_t$ … change of temperature strain *[-]* (Eq. 10)
$C_{d\infty}$ … limit value of reversible creep deformation
Q … creep-constant

The coefficients of Eq. 7 are calculated with Eq. 8 to Eq. 11:

$$C(t) = A * (t - t_1)^{0.25} \quad \text{Eq. 8}$$

with: C(t) … age-dependent trend of irreversible viscous strain (acc. to [31])
A … flow-parameter (constant)
t … age of shotcrete in hours *[h]*
t_1 … age of shotcrete at beginning of loading *[h]*
(here: assuming, load starts with excavation of next round)

$$\varepsilon_{sh} = \varepsilon_{sh\infty} * \frac{t}{(B + t)} \quad \text{Eq. 9}$$

with: ε_{sh} … shrinkage strain *[-]* (acc. to [30, 31])
$\varepsilon_{sh\infty}$ … limit value of shrinkage strain *[-]*
B … shrinkage-constant
t … age of shotcrete in days *[d]*

$$\varepsilon_t = [-\cos(t^{0.25} * 113) + 1] * 30 * 10^{-6} \quad \text{Eq. 10}$$

with: ε_t … temperature strain *[-]* (acc. to [31])
t … age of shotcrete in hours *[h]*

- temparature strain ε_t is just applied in the first four days after shotcreting
- the term $-cos(t^{0.25} * 113)$ must be calculated in radians *[rad]*

$$\varepsilon_{d,2} = (\sigma_1 * C_{d\infty} - \varepsilon_{d,1}) * \left[1 - \exp\left(\frac{-\Delta C(t)}{Q}\right)\right] + \varepsilon_{d,1} \quad \text{Eq. 11}$$

with: $\varepsilon_{d,i}$ … viscoelastic strain at end of timespan Δt_i *[-]* (based on [30])
σ_i … total stress in the liner at end of timespan Δt_i *[N/mm²]*
$C_{d\infty}$ … limit value of reversible creep deformation
$\Delta C(t)$ … age-dependent change of viscous strain
Q … creep-constant

The last long-term tests on shotcrete in Austria have been performed at the beginning of the 1990's, about 25 years ago [14]. Ever since the constituents, mix composition and production of the shotcrete significantly changed. Hence, an adjustment of the flow-rate parameters (A, B, Q, $C_{d\infty}$, $\varepsilon_{sh\infty}$) is necessary. For the thesis, this was done for a shotcrete SpC 25/30 J2, based on a detailed displacement monitoring and visual observation of the support at a specific monitoring section at the Semmering Base Tunnel. Since the moment when first cracks in the lining occurred (≙ μ = 100 % utilization) and strains at that time are known, these parameters could be roughly back-calculated. For an accurate determination, further laboratory tests are necessary.

4.9 Calculation of predicted Shotcrete Lining Utilization

The final step of the presented method is the calculation of shotcrete lining utilization by comparing actual stresses (Eq. 7) with the current shotcrete strength (Eq. 4):

$$\mu(t) = \frac{\sigma(t)}{f_{cm}(t)} * 100 \qquad \text{Eq. 12}$$

with: $\mu(t)$ … time-dependent degree of utilization of shotcrete lining *[%]*
$\sigma(t)$ … age-dependent stress in the liner *[N/mm²]* (Eq. 7)
$f_{cm}(t)$ … age-dependent mean shotcrete strength *[N/mm²]* (Eq. 4)

The most critical time regarding the shotcrete lining utilization are typically the first few days, when the displacement rate is highest and the shotcrete strength lowest [56]. Investigations have shown, that a utilization $\mu \geq 100$ % at an early stage does not necessarily trigger stability problems since the young shotcrete has a low initial stiffness and deformation potential, depending on the early strength class.

Due to increasing strength and relaxation of the shotcrete with time (rheological behaviour), a stress relief takes place, reducing the final degree of utilization. Fig. 25 shows a typical result for the temporal development of degree of utilization in a shotcrete lining.

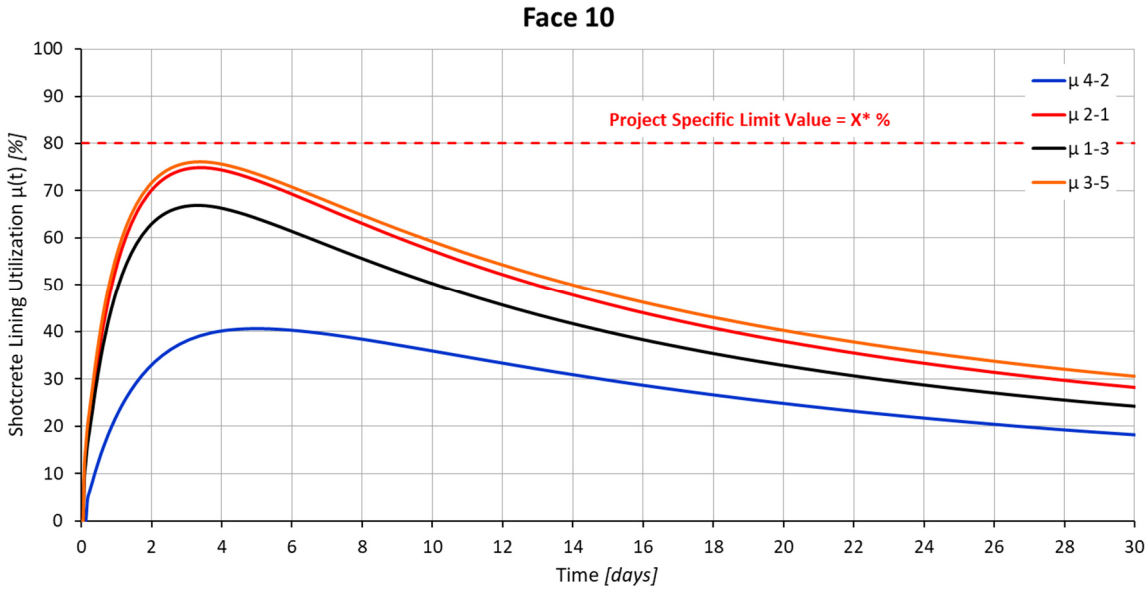

Fig. 25: Predicted temporal development of degree of utilization of a shotcrete lining based on Rate-of-Flow-Method. The curves (4-2, 2-1, 1-3, 3-5) are related to the segments between the corresponding virtual monitoring targets.
The limit value X* as specified in Fig. 5 should be defined project specific.

Since with the presented method the shotcrete lining utilization can be predicted at the current tunnel excavation area, a timely decision about the support concept is possible. In combination with a geotechnical safety management – as proposed by ÖGG [20] and Lenz et al. [18] – limit values for using a ductile support system instead of a closed lining should be defined.

If the shotcrete lining utilization stays below the project specific limit value, a closed lining with equal dimensioning as at the previous rounds is sufficient (see Fig. 5).
If the project specific limit value is exceeded, additional investigations and analyses (section 4.2.4) are necessary in order to determine whether a further increase of the utilization is expected or not. Based on these findings the support concept – closed lining or ductile support – is determined.
It is recommended to immediately apply a ductile support system if the predicted shotcrete lining utilization exceeds the ultimate limit state of 100 %.

Furthermore, by analysing results of the shotcrete lining utilization, conclusions regarding stress redistribution and system behaviour are possible [33].

5 Case Studies

To verify the proposed method, two sections at current tunnel projects are analysed. Both construction sites belong to the 27.3 km long *Semmering Base Tunnel* (SBT) in Austria. All data are kindly provided by the Austrian Federal Railways (ÖBB) and the geotechnical engineers and geologists on-site.

5.1 SBT1.1 – Tunnel Gloggnitz

Construction works at the eastern lot SBT1.1-*Tunnel Gloggnitz* started in July 2015. The lot includes two single-track tunnels each with a length of 7.4 km, 16 cross-passages and the intermediate construction access at *Göstritz* [62]. Tunnels are excavated conventionally according to NATM. The investigated section with an overburden of approximately 140 m is situated in the so-called *Haltestelle Eichberg* fault, which is part of the tectonic *Greywacke* unit. Lithology is dominated by tectonically intense sheared Schists and Phyllites with extreme heterogeneous characteristics.

5.1.1 Geotechnical Interpretation and Short-Term Prediction

In a first step, a systematic interpretation and short-term prediction of the geotechnical situation is done. An overview of the geological conditions is given in Fig. 26. The current tunnel face is located at chainage 1450.2 m, the vertical, red dot and dashed line represents the last monitoring section (MS) with at least two follow-up measurements. Ahead, just geological-geotechnical information is available.

Analysis: UCS of the intact rock is generally on a low level, following an almost constant trend for the last 20 m of tunnelling. The last three mapped tunnel faces indicate a decreasing foliation spacing and a slightly increasing joint- and slickenside spacing. Since the critical overburden is directly linked to rock mass properties (Eq. 1), an increasing ratio can be observed at the current excavation area. Hemispherical plots (lower hemisphere) of face mappings show a rotation of the spatial structure orientation from almost perpendicular (face 1439.2) to parallel (current face 1450.2) to the tunnel axis, leading to a more unfavourable spatial structure orientation regarding the deformation development. The interlocking strength along the investigated section is compact to moderately disintegrated.

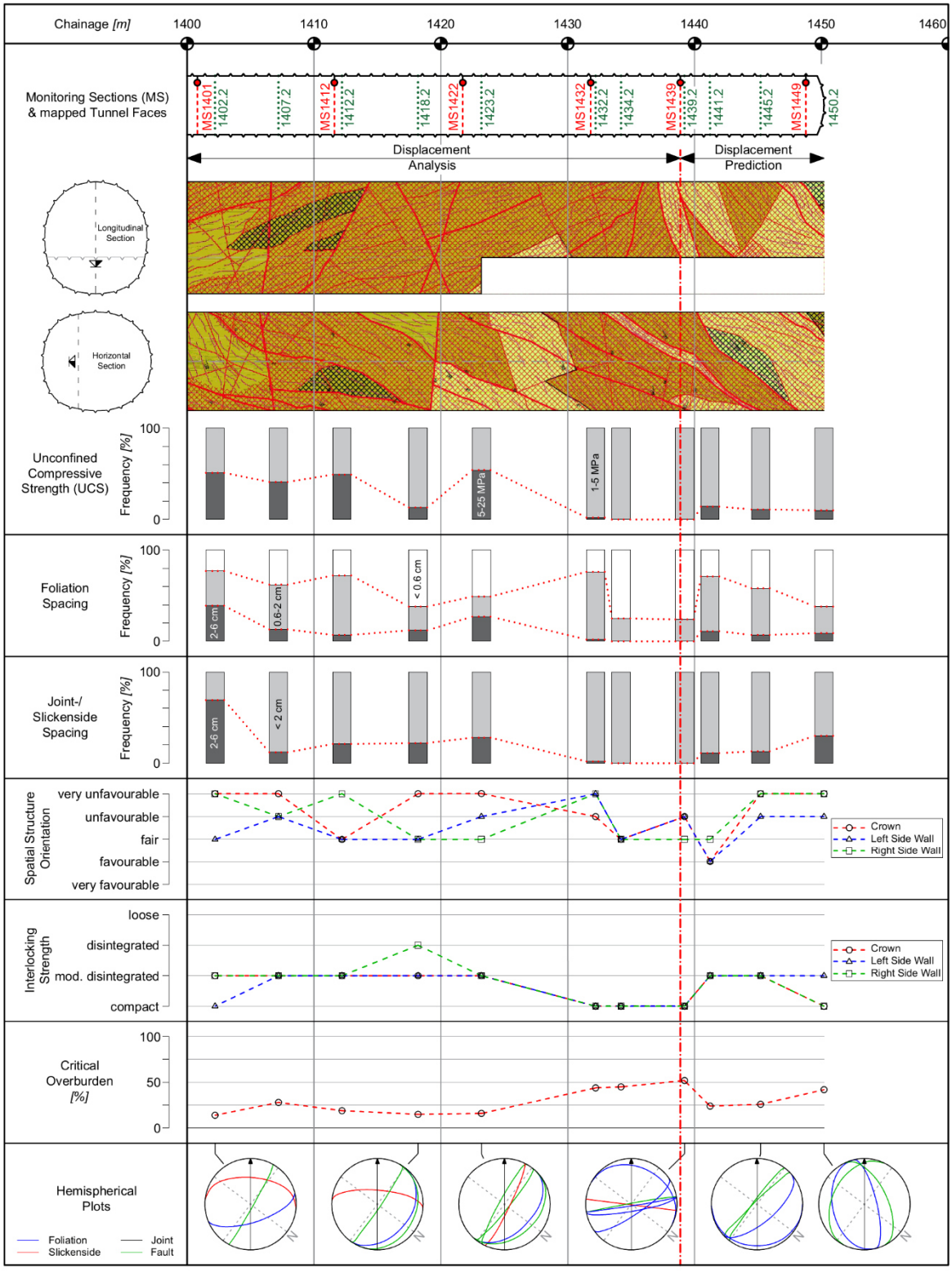

Fig. 26: Geological-geotechnical conditions, SBT1.1, Track 1, Chainage 1400 – 1450 m.

With the obtained geological-geotechnical observations (Fig. 26 & Fig. 29, left) and analyses, descriptive ratings (linked to the previous rounds) are performed (see Tab. 7).

Tab. 7: Assessment of geological-geotechnical parameters, SBT1.1, Track 1, Chainage 1450.2 m.

Face 1450.2				
	Term	**Left Side Wall** *[Target 4 & 2]*	**Crown** *[Target 1]*	**Right Side Wall** *[Target 3 & 5]*
Geological-Geotechnical Parameters	UCS	o	-	o
	Degree of Fragmentation	- -	- -	- -
	Spatial Structure Orientation	- -	- - -	- -
	Interlocking Strength	o	+	+
	Critical Overburden	- -	- -	- -

Interpretation: Based on geological-geotechnical parameters, a more unfavourable ground- and system behaviour is expected at the current face 1450.2 than at the last few rounds. Change of the degree of fragmentation and structure orientation might cause increasing displacements and increasing values for the parameter *X* (compare with Fig. 8).

5.1.2 Curve-Fitting of Displacements at Monitoring Sections

Fig. 27 shows the chosen Convergence-Law parameters (Eq. 2) for the top-heading advance. Displacements are fitted in cross-section (V-H). Behind the current tunnel face, MS 1449 is installed and the zero-reading taken. At MS 1439, three follow-up measurements are available, so a curve-fitting procedure is possible. To predict the displacement development ahead of MS 1439, four virtual monitoring sections at chainage 1440.2 m, 1441.2 m, 1442.2 m and 1443.2 m are analysed (for details see section 4.5.3.3).

Analysis: The largest displacements are constantly observed at the left- and right side wall of the tunnel (target 4 & 5). Displacements generally slightly increase over the last 40 m. Starting from MS 1432, the parameter *X* of all five targets increases. Analyses of virtual monitoring sections indicate an increase of displacements and of the curve-fitting parameter *X*. The time-dependent parameter *m* is almost constant along the investigated section. Due to a quick ring closure and stiff support, stable displacement developments are reached at an early stage and hence the exact determination of the parameter *m* is difficult. The displacement vector orientations in cross-section at the last five monitoring sections do not significantly change.

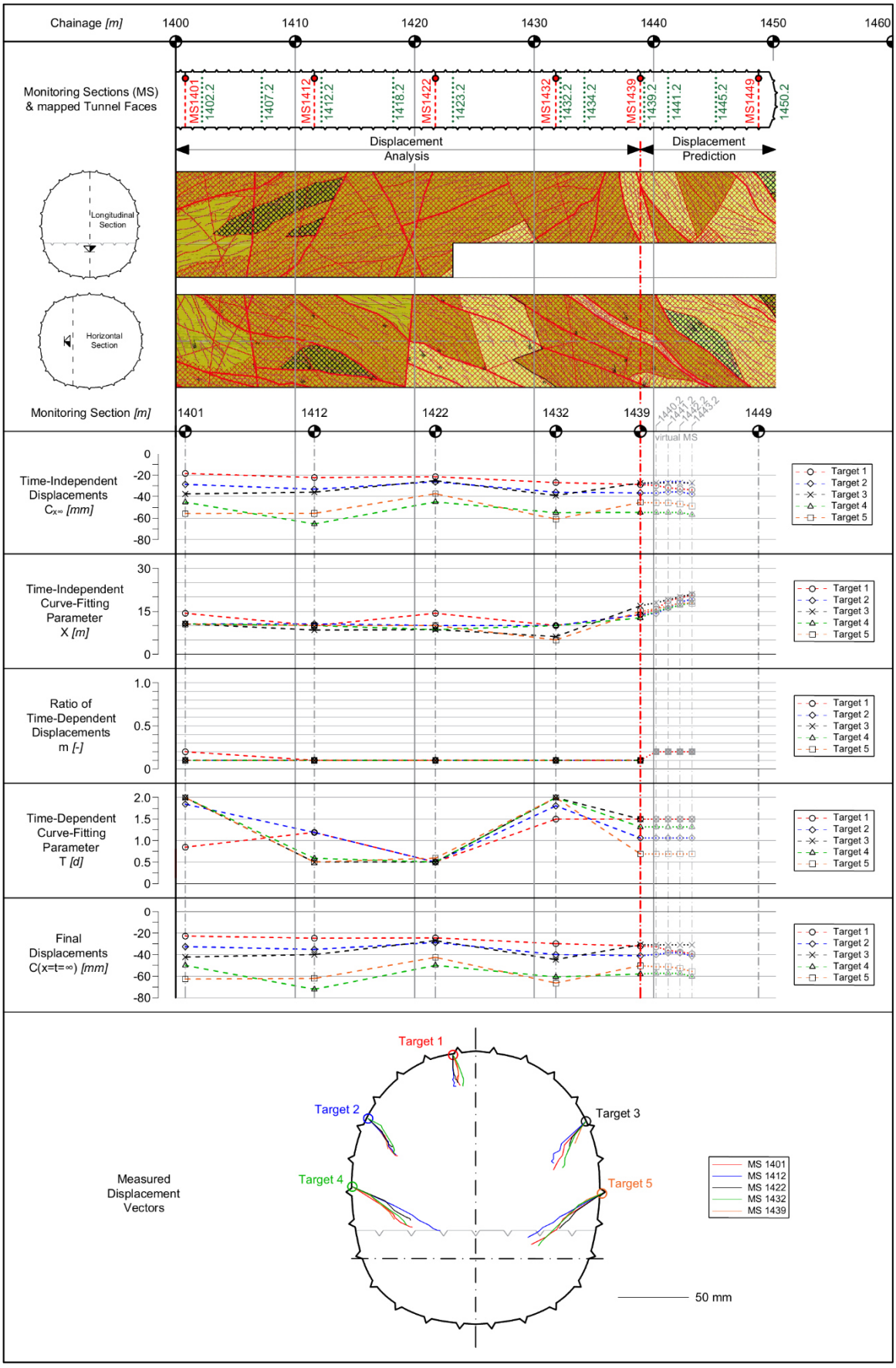

Fig. 27: Fitted function parameters and displacement vector orientations in cross-section, SBT1.1, Track 1, Chainage 1400 – 1450 m.

The function parameters $C_{x\infty}$, X, m and T at the last MS 1439 are shown in Tab. 8. The descriptive ratings are linked to the previous MS 1432.

Tab. 8: Determination of the fitted Convergence-Law parameters, SBT1.1, Track 1, MS 1439.

Convergence-Parameters at MS 1439									
		Trend Left Side Wall	*Target 4*	*Target 2*	*Trend Crown*	*Target 1*	*Trend Right Side Wall*	*Target 3*	*Target 5*
Fitted Parameters	$C_{x\infty}$	o	-54	-37	o	-29	+	-28	-46
	X	-	13	14	-	14	- -	16	15
	m	o	0.1	0.1	o	0.1	o	0.1	0.1
	T	- -	1.3	1.1	o	1.5	- -	1.5	0.7

Interpretation: Since the last monitoring section is 11 m behind the current face and geological conditions changed, no reliable short-term prediction of the Convergence-Law parameters based on these information is possible. Hence, information of the virtual monitoring sections are used to identify a trend of the function parameters at the current face, which indicate an increase of displacements and of the parameter X. Note that the results are based on two, respectively three virtual follow-up measurements and should therefore be seen as a trend and not as fixed values. Using the same support concept, the low strength and increasing degree of fragmentation of the rock mass probably cause a more pronounced time-dependent behaviour, which justifies the assumption of m = 0.2 ahead of MS 1439.

5.1.3 Short-Term Prediction based on State- and Trend Lines

To predict the system behaviour ahead of the last monitoring section, state- and trend lines are analysed. Fig. 28 summarises selected state- and trend lines for target 1 at the crown. However, for an appropriate prediction all targets and different types of trend lines (e.g. horizontal displacements) are evaluated.

Analysis: Trends of absolute V-H displacements at the crown and left side wall (not shown) – taken 5 m and 10 m behind the face – are slightly decreasing ahead of MS 1432 and both trend lines run almost parallel. On the right side wall (not shown), the displacement trend decreases and the distance between the trend lines is decreasing as well. The vector orientation L/S does not significantly change, hence similar stiffness conditions ahead of the face can be assumed. The area under the state lines increases over the investigated section and remains almost constant at the current excavation area. The deflection lengths show an increasing trend over the last ten meters. Trends of horizontal displacements at the side walls (not shown here) are slightly decreasing. Generally, the left side wall (target 4 & 2) behaves more unfavourable than the right side wall (target 3 & 5).

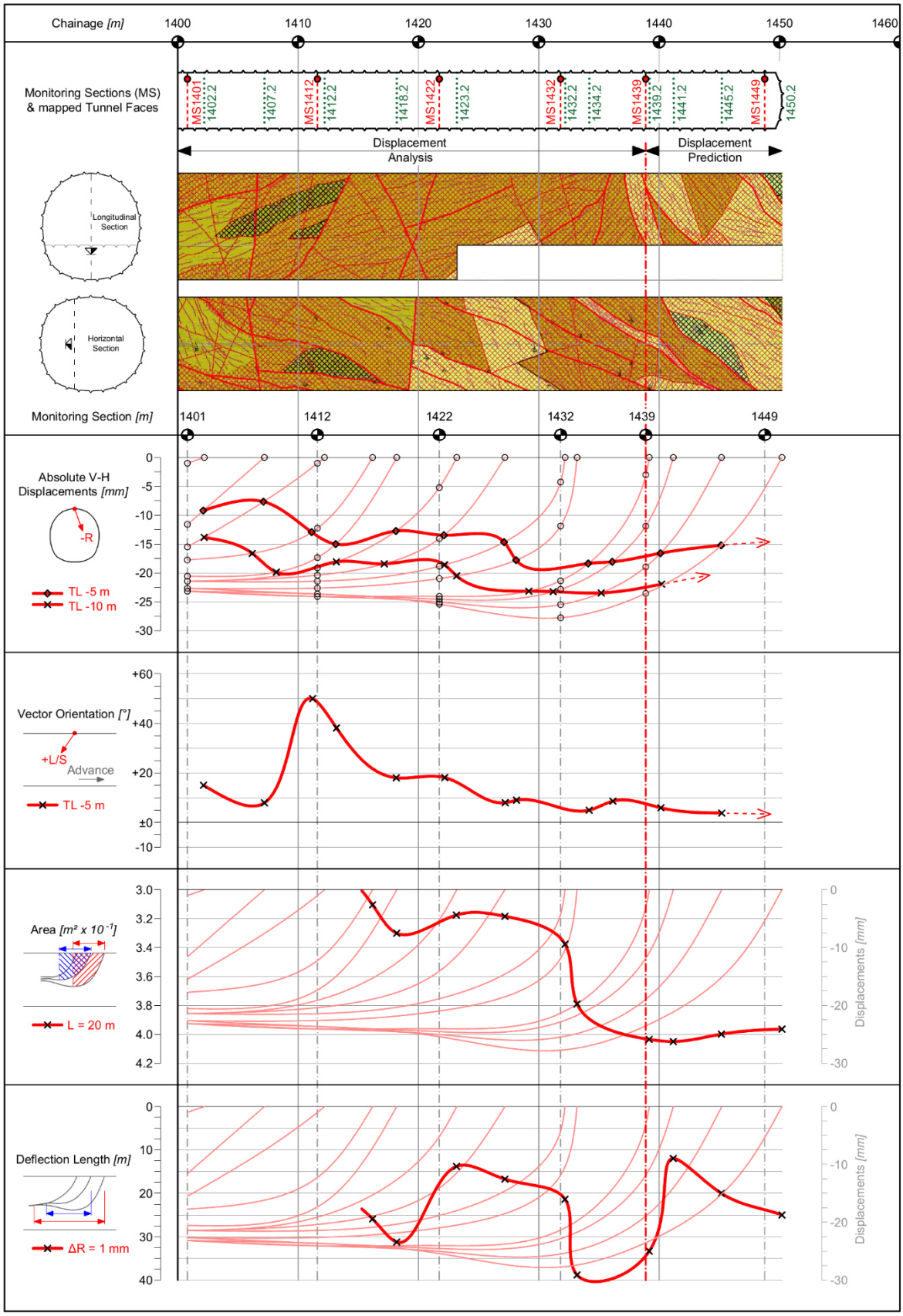

Fig. 28: Short-term prediction of the system behaviour with state- and trend lines of Target 1, SBT1.1, Track 1, Chainage 1400 – 1450 m.

The descriptive ratings of state- and trend lines in Tab. 9 are linked to the previous rounds.

Tab. 9: Assessment of state- and trend lines, SBT1.1, Track 1, Chainage 1450.2 m.

Face 1450.2				
	Term	Left Side Wall	Crown	Right Side Wall
		[Target 4 & 2]	*[Target 1]*	*[Target 3 & 5]*
State- & Trend Lines	Absolute Displacements	+	+	+ +
	Horizontal Displacements	+	n/s	+ +
	Vector Orientation L/S	o	o	-
	Area under State Lines	o	o	o
	Deflection Length	- -	- -	- -

Interpretation: The constant distance between absolute displacement trend lines (5 m and 10 behind the face) at the crown and left side wall is an indication for a constant value of the parameter *X* (see section 4.5.1). At the right side wall, the parameter *X* tends to decrease. The continuously increasing deflection length over the last ten meters and the increasing area under the state lines indicate a stress redistribution towards the supported (stiff) sections (against direction of drive), possibly caused by weaker ground ahead.

5.1.4 Prediction of Displacements in Excavation Area

Considering the evaluation and short-term prediction of geological-geotechnical parameters (section 5.1.1) and of the system behaviour (section 5.1.3), and utilizing the function parameters ($C_{x\infty}$, *X*, *m*, *T*) from the last MS 1439 (section 5.1.2) as a starting point, the displacement development of each virtual target at the current tunnel face is predicted.

Interpretation: Since the geological properties are similar to the ones at the previous virtual monitoring sections, time-dependent parameters *m* and *T* are kept constant. Analysing the spatial structure orientation, virtual monitoring sections and the distance between displacement trend lines, for the parameter *X* – a slightly increase at the crown and left side wall and a moderately decrease at the right side wall is expected. Due to a more unfavourable structure orientation, results of virtual monitoring sections, a constantly increasing area under the state lines and increasing deflection lengths, larger displacements ($C_{x\infty}$) are expected at the current tunnel face. The displacement vectors at the right side wall are expected to be dominated by the foliation and joints, and at the crown and left side wall to slightly rotate towards the centric located fault (see Fig. 29, left).

With these interpretations, the function parameters at chainage 1450.2 m are predicted. The descriptive ratings in Tab. 10 are linked to the previous MS 1439.

Tab. 10: Prediction of the Convergence-Law parameters, SBT1.1, Track 1, Chainage 1450.2 m.

Prediction at Face 1450.2									
		Trend Left Side Wall	*Target 4*	*Target 2*	*Trend Crown*	*Target 1*	*Trend Right Side Wall*	*Target 3*	*Target 5*
Prediction at current Face	$C_{x\infty}$	- -	-80	-55	- -	-45	- -	-45	-70
	X	-	15	15	-	15	+	12	10
	m	o	0.2	0.2	o	0.2	o	0.2	0.2
	T	o	1.3	1.1	o	1.5	o	1.5	0.7
	δ		-5°	-5°		±0°		+10°	+10°

The ground behaviour is dominated by small over-breaks and shear-failure at unfavourable intersections of discontinuities and the tunnel boundary (see Fig. 29).

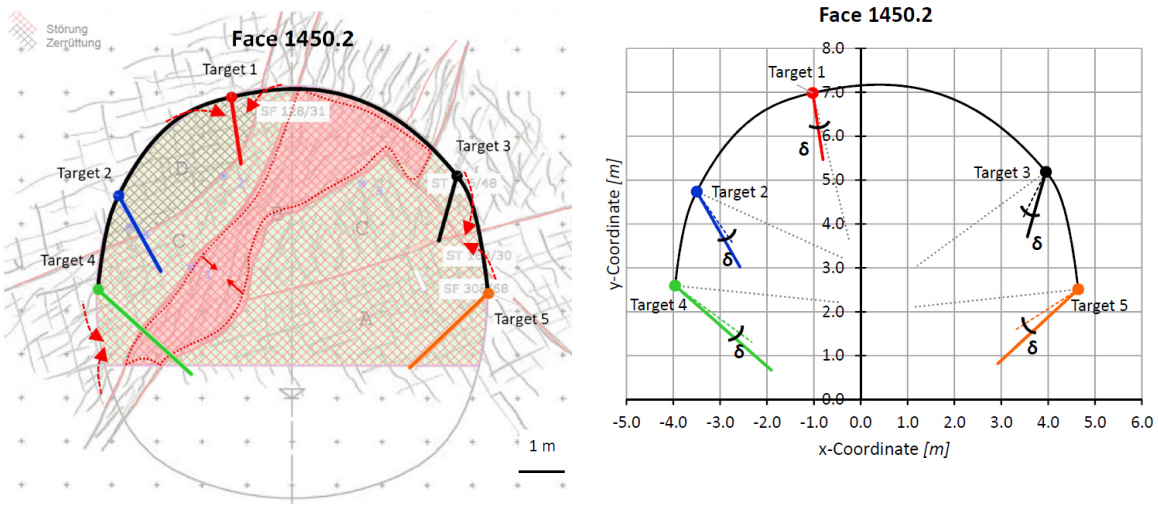

Fig. 29: Left: expected ground behaviour (red arrows) and possible development of displacement vectors (coloured solid lines) at the current tunnel face; Right: model for calculation process with predicted displacements (coloured solid lines), vector trends of the previous MS 1439 (coloured dashed lines and angle of deviation δ) and vectors for a radial deformation pattern (grey-dotted lines); displacements are scaled-up by a factor of 30; SBT1.1, Track 1, Chainage 1450.2 m.

With the function parameters in Tab. 10 and an expected advance rate of 3.2 m/day, the timely development of displacements at chainage 1450.2 m is calculated (Fig. 30). The largest displacements are expected to develop at the side walls (target 4 & 5), as they also have at the previous MS 1439.

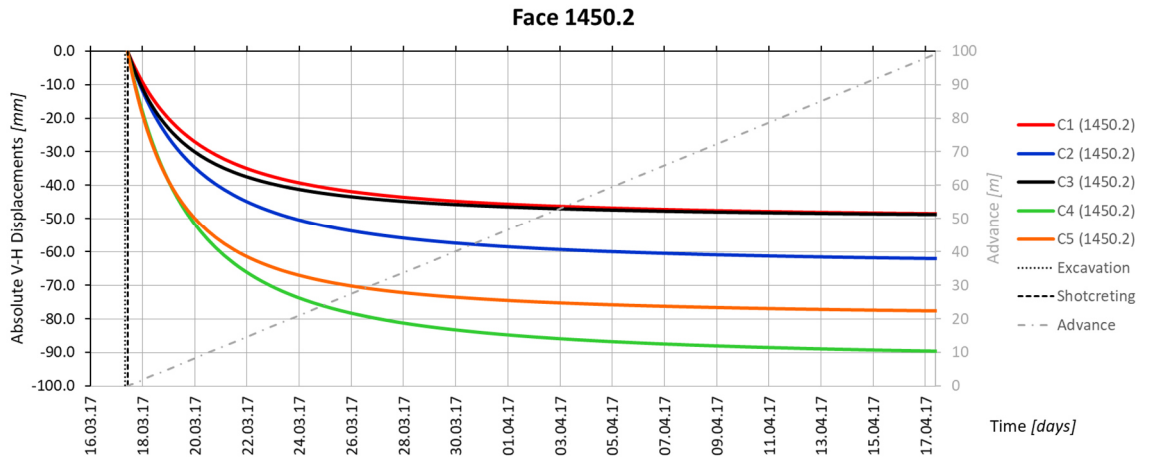

Fig. 30: Time-displacement graph of predicted displacement developments for five targets with expected advance rate of 3.2 m/day at SBT1.1, Track 1, Chainage 1450.2 m.

5.1.5 Calculation of predicted Shotcrete Lining Utilization

Tangential strains in-between the predicted displacement vectors (Fig. 29) are calculated using the cubic spline-interpolation method (section 4.7). The development of the strains between the virtual targets 4-2, 2-1, 1-3 and 3-5 are shown in Fig. 31. The largest strains are predicted to develop at the segment 3-5 due to the unfavourable orientation δ of the concerning displacement vectors. Although the predicted displacements at target 4 are the largest, the strains at segment 4-2 are the lowest due to the similar behaviour of the displacement vectors 4 and 2.

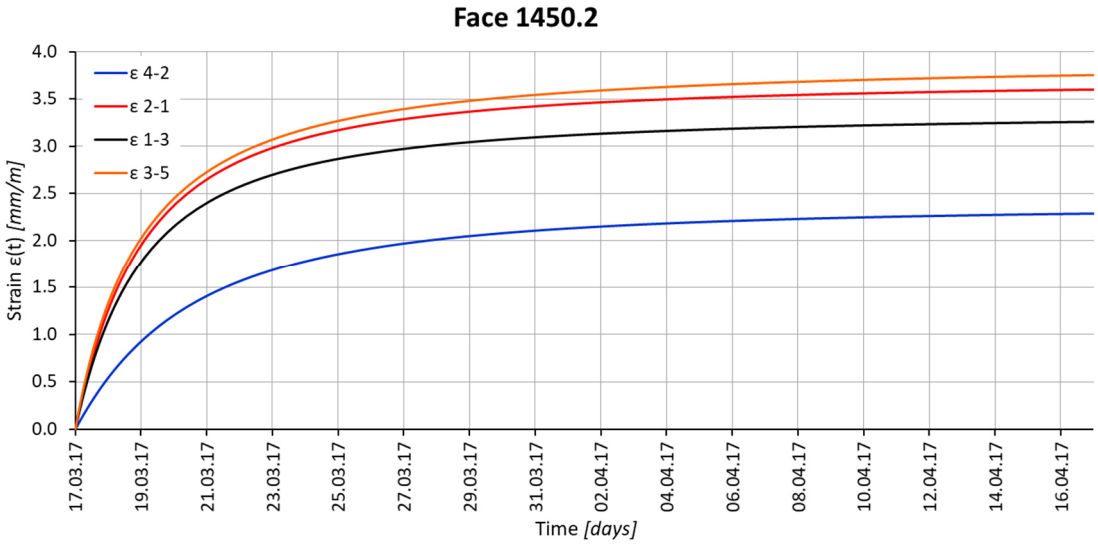

Fig. 31: Time-strain graph of SBT1.1, Track 1, Chainage 1450.2 m; based on predicted displacements shown in Fig. 30.

For the calculation of the lining utilization, shotcrete strength- and stiffness parameters (see section 4.8.1) – shown in Tab. 11 – are used.

Tab. 11: Shotcrete strength- and stiffness properties for the calculation of the lining utilization at SBT1.1, Track 1, Chainage 1450.2 m.

Shotcrete Properties	
Term	*Chosen*
Shotcrete Thickness:	0.25 m
Shotcrete Strength Class:	SpC 20/25
UCS after 28 days $f_{cm,28}$:	40.0 N/mm²
Early Strength Class J:	J2
Early Strength after 1 day $f_{cm,1}$:	10.0 N/mm²
E-Modulus after 28 days $E_{cm,28}$:	20,000 N/mm²
Cement Hardening Coefficient s:	1.150
Exponent of SpC Strength α1 (f_{cm}):	0.240
Exponent of SpC E-Modulus α2 (E_{cm}):	0.700

With the Rate-of-Flow-Method (section 4.8.2), the segmental lining utilization is calculated between the virtual targets 4-2, 2-1, 1-3 and 3-5 (see Fig. 32).

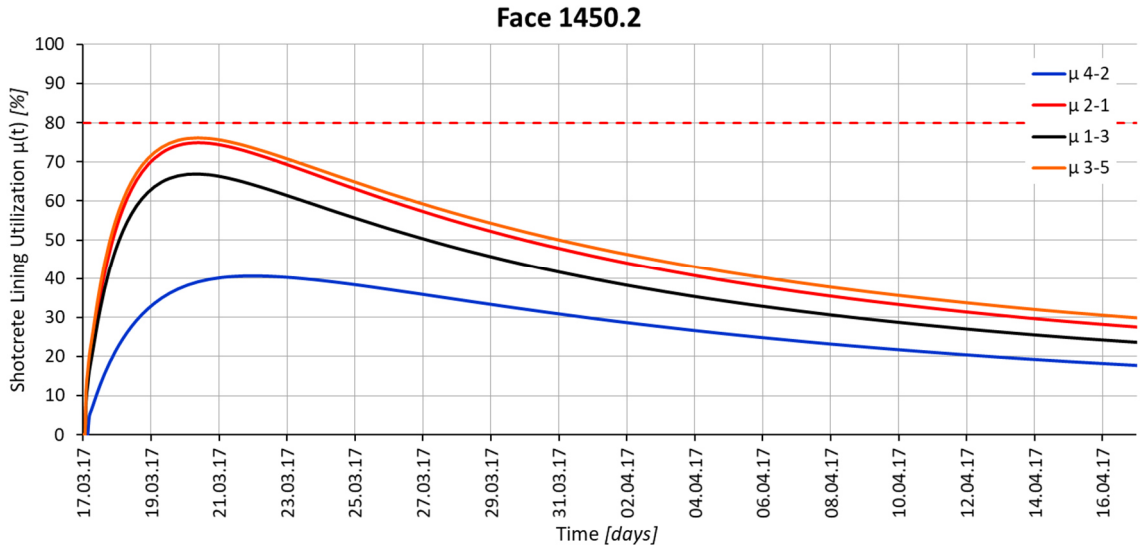

Fig. 32: Predicted shotcrete lining utilization at SBT1.1, Track 1, Chainage 1450.2 m.

Interpretation: With the predicted displacements and vector orientations, a maximum shotcrete lining utilization of approximately 75 % is expected to occur at the segment 3-5 (right side wall) and segment 2-1 (left shoulder). As the project specific limit value of 80 % (assumed by author as specified in Fig. 5, normally defined in the geotechnical safety management plan) will not be exceeded and the maximum value is reached at an early stage (see section 4.9), no additional analyses and/or investigations are required. Based on this information a closed shotcrete lining with the same dimension is recommended to be maintained at the next rounds.

5.1.6 Comparison of Predictions and Measurements

The predictions made with the presented method at chainage 1450.2 m are compared with measurements at MS 1449.

Predicted displacement developments at the crown, shoulders and right side wall (targets 1, 2, 3 and 5) fit well with the measurements as shown in Fig. 33. Displacements at the left side wall (targets 4) have been slightly underestimated. The initial displacements developed faster than expected, hence the parameters *X* have been overestimated for the prediction.

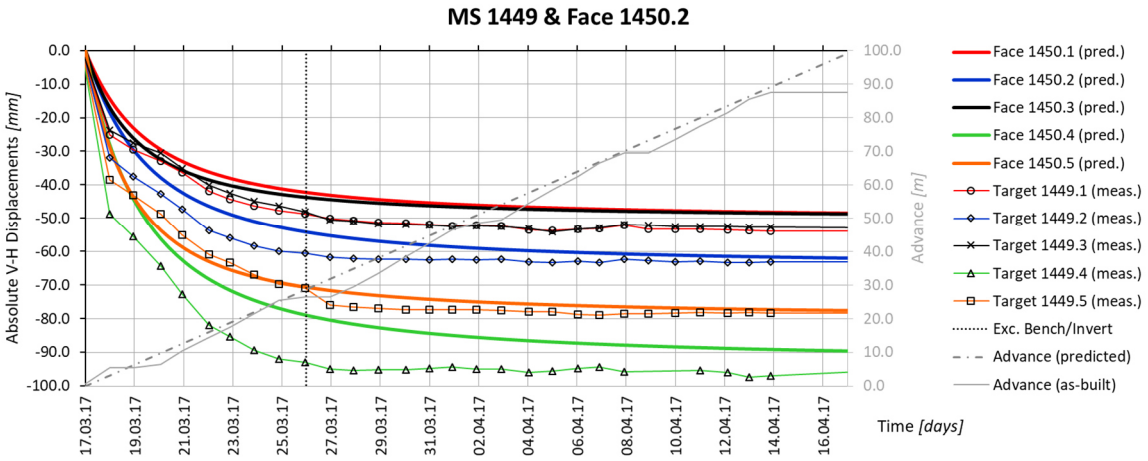

Fig. 33: Comparison of predicted displacement developments at face 1450.2 (coloured solid lines) and measured displacement developments at MS 1449 (coloured lines with markers) for targets 1-5 at SBT1.1, Track 1; predicted advance and advance as-built is scaled at the right ordinate; the dotted vertical line represents the time of bench/invert excavation at chainage 1450.2 m.

The predicted displacement vectors – shown in Fig. 34 – differ quite strongly from the measured displacements. Target 1 and target 2 display an untypical behaviour, which could not be foreseen at the time of prediction. The rotation of these two vectors might be triggered by the concave-shaped slickenside below the left shoulder and other geological features outside of the excavated profile. At the right side wall, displacements did not rotate as much downwards as expected.

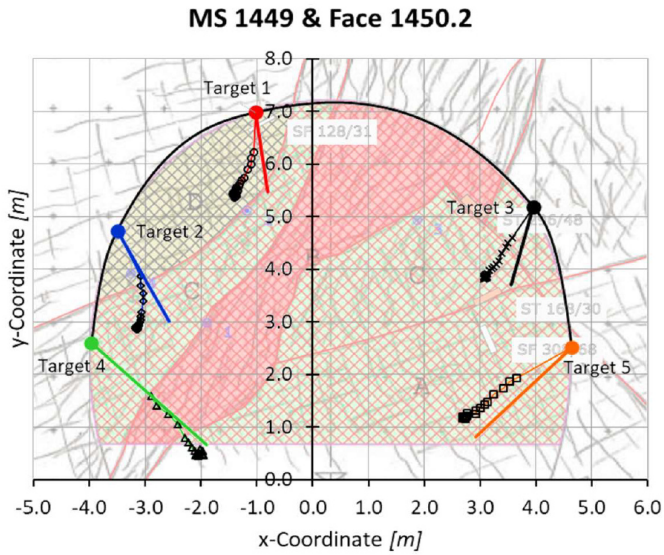

Fig. 34: Comparison of predicted displacements at face 1450.2 (coloured solid lines) and measured displacements at MS 1449 (coloured lines with markers) at SBT1.1, Track 1.

Although the predicted displacement vector orientations differ from the measured ones, the predicted shotcrete lining utilization fits well with the back-calculated utilization (Fig. 35) since all targets deform simultaneously in a more or less similar pattern (clockwise rotation). As the initial displacements developed faster than predicted, the back-calculated utilization ratios from measurements are higher at the early stages. Calculations with the software *Tunnel:Suite* [34] (based on Hybrid-Method and measured displacements) result in a maximum shotcrete lining utilization of 87 % on March 18th at target 1 and target 3 (not shown here). At the analysed section, no cracks are observed at the shotcrete lining, which confirms a utilization lower than 100 %.

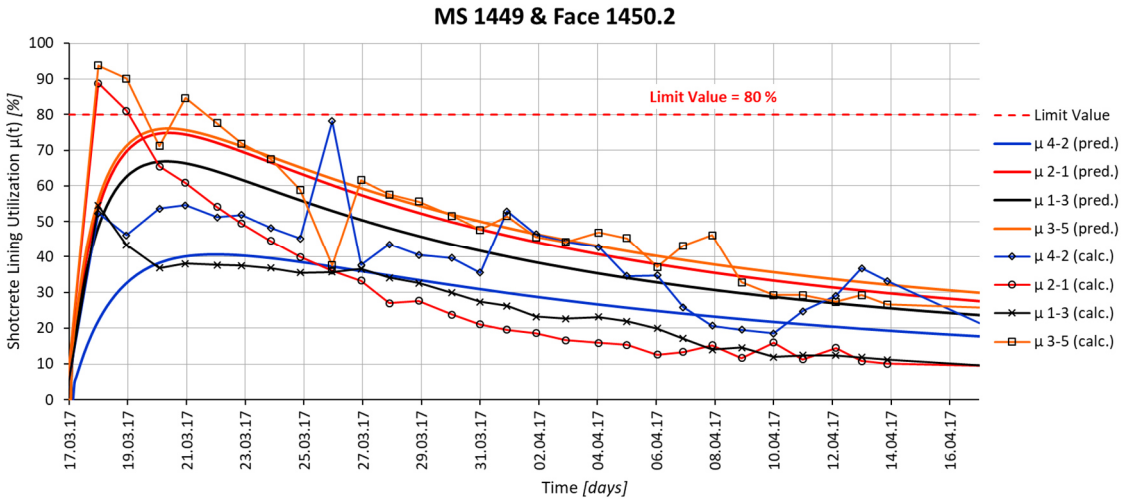

Fig. 35: Comparison of the predicted shotcrete lining utilization at face 1450.2 (coloured solid lines) and back-calculated shotcrete lining utilization from measured displacements at MS 1449 (coloured lines with markers) at SBT1.1, Track 1.

5.2 SBT2.1 – Emergency Stop Fröschnitzgraben

In January 2014, construction works at the lot SBT2.1-*Tunnel Fröschnitzgraben* started. For this intermediate construction access two 400 m deep shafts with diameters of 12 m and 10 m are sunk. At the bottom of the shafts, about 26 km of running tunnels will be excavated by two mechanised- and two conventional headings in the next years [63]. Due to constructional requirements a start-cavern for the TBM's with a face area of 285 m² is excavated in-between the running tunnels. The top-heading and first bench advance of the eastern section of this cavern is analysed here. Lithology is dominated by tectonically sheared Albite Gneisses, Albite Schists and intersecting fault zones with Cataclasite, all belonging to the tectonic *Wechsel-Gneiss* unit.

5.2.1 Geotechnical Interpretation and Short-Term Prediction

The current face of the investigated tunnel section – shown in Fig. 36 – is located at chainage 114.0 m. For the geotechnical interpretation, mappings of 14 faces are available. The last monitoring section with follow-up measurements – denoted with a red dot-dashed line (Fig. 36) – is MS 105.

Analysis: The initial high UCS of the intact rock at the investigated section severely drops at chainage 72.4 m, where a 10 m thick fault zone intersects the cavern at a perpendicular angle. Shortly thereafter, at chainage 81.5 m, the strength starts to increase again. The foliation- and discontinuity spacing decreases for the last 30 m of tunnelling. The increasing ratio of the critical overburden from chainage 81.5 m to 114.0 m is caused by the increasing degree of fragmentation and decreasing shear strength of discontinuities (slickensides with Sericite), both reducing the rock mass strength and stiffness. Since the tunnel is driven against the dip of the foliation as shown in the hemispherical plots (lower hemisphere), the spatial structure orientation is mostly rated as unfavourable along the entire section. The interlocking strength is observed to be more unfavourable at the last 12 m of tunnelling. For the next rounds, a ground type similar to the one at the current face at chainage 114.0 m with tectonically sheared and moderately fragmented rock masses is predicted.

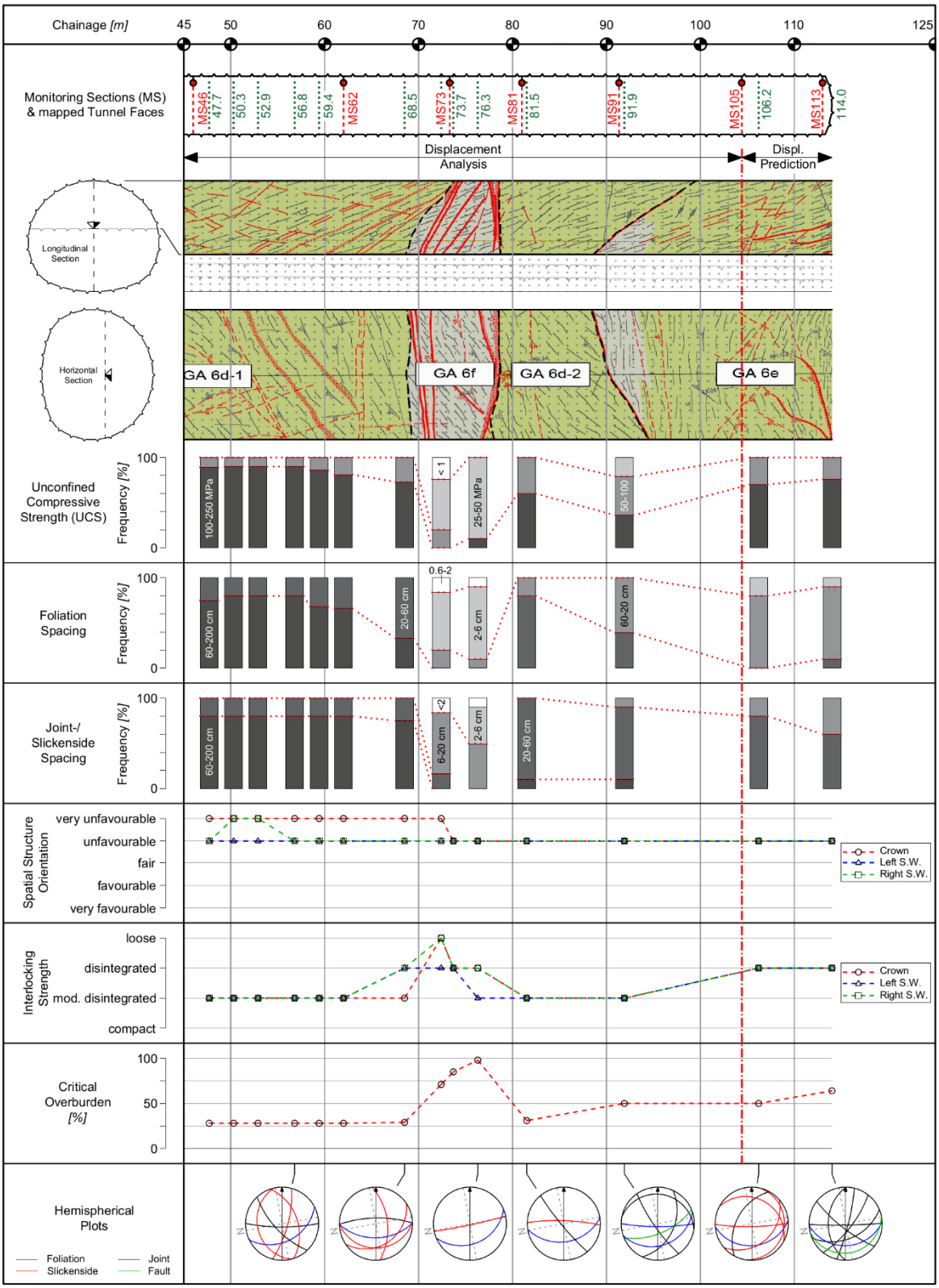

Fig. 36: Geological-geotechnical conditions, SBT2.1, Cavern East, Chainage 45 – 114 m.

The descriptive ratings of the geological-geotechnical parameters (linked to the previous rounds) are shown in Tab. 12.

Tab. 12: Assessment of geological-geotechnical parameters, SBT2.1, Cavern East, Chainage 114.0 m.

Face 114.0				
	Term	**Left Side Wall** *[Target 5 & 3]*	**Crown** *[Target 1]*	**Right Side Wall** *[Target 2 & 4]*
Geological-Geotechnical Parameters	UCS	+	+	+
	Degree of Fragmentation	- -	- -	- -
	Spatial Structure Orientation	o	o	o
	Interlocking Strength	-	-	-
	Critical Overburden	- -	- -	- -

Interpretation: Based on a continuously increasing degree of fragmentation between chainage 81.5 m and the current excavation area, an increasing occurrence of slickensides with Sericite, an ongoing unfavourable structure orientation and poor interlocking, larger displacements are expected in the next rounds.

5.2.2 Curve-Fitting of Displacements at Monitoring Sections

In Fig. 37 the fitted function parameters of the Convergence-Law and displacement vector orientations of six monitoring sections are shown. Displacements are fitted in cross-section (V-H). To gain information ahead of the last MS 105, virtual monitoring sections at chainage 106.2 m, 107.3 m, 108.3 m and 109.6 m are analysed. The numbering of the targets is chosen as applied on-site (target 5 & 3 - left side wall, target 2 & 4 - right side wall).

Analysis: Fitted absolute displacements of all targets increase along the investigated tunnel section. Displacements at the crown and left side wall show a significant increase between MS 91 and MS 105, and analyses of virtual monitoring sections indicate a further rise ahead of MS 105. The curve-fitting parameter *X* mostly stays within a range of 20 to 30 m at the last 23 m of tunnelling. A high ratio of time-dependent displacements is observed at MS 73. The displacement vector orientations in cross-section, especially at the right side wall, show a significant variance.

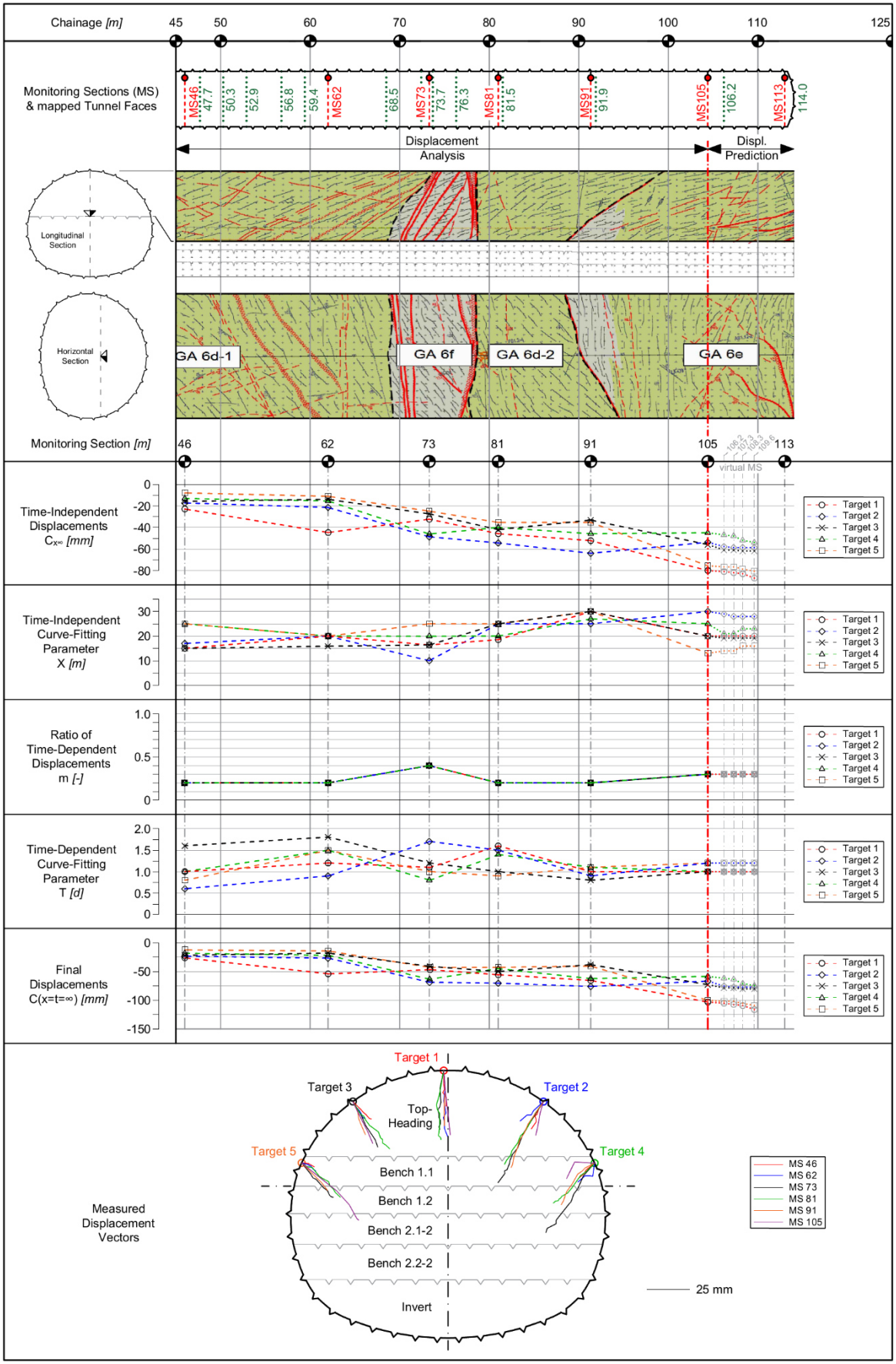

Fig. 37: Fitted function parameters and displacement vector orientations in cross-section, SBT2.1, Cavern East, Chainage 45 – 114 m.

Fitted function parameters $C_{x\infty}$, X, m and T at the last MS 105 are shown in Tab. 13. The descriptive ratings are linked to the previous MS 91.

Tab. 13: Determination of the fitted Convergence-Law parameters, SBT2.1, Cavern East, MS 105.

Convergence-Parameters at MS 105									
		Trend Left Side Wall	*Target 5*	*Target 3*	*Trend Crown*	*Target 1*	*Trend Right Side Wall*	*Target 2*	*Target 4*
Fitted Parameters	$C_{x\infty}$	- - -	-77	-57	- - -	-80	+	-53	-45
	X	+ +	14	20	+ +	20	o	30	25
	m	-	0.3	0.3	-	0.3	-	0.3	0.3
	T	+	1.2	1.0	o	1.0	+	1.2	1.0

Interpretation: Although the geological conditions improved after the fault zone (beginning approximately at chainage 79 m), the predicted magnitude of final displacements C(x=t=∞) for the targets 1, 2 and 5 increases. This is traced back to the decreasing surface quality of the discontinuities and an arching-effect, transferring stresses from the fault zone towards the adjacent stiffer rock masses. Based on analyses of virtual monitoring sections, a further increase of the displacements and an almost constant development of the parameter X is expected at the current excavation area. The highly time-dependent behaviour ($m \geq 0.2$) probably results from a combination of the geometry of the emergency stop cavern and of geological conditions. The high grade of excavation (cavern, running tunnels and cross-passages) can be compared to mining underground structures, where remaining pillars are highly utilized and extremely sensitive to additional stresses. Ongoing displacements without advance at the Cavern East can be linked to tunnelling works at other locations of this underground system. The multiple headings contribute to this long-term displacements.

5.2.3 Short-Term Prediction based on State- and Trend Lines

The system behaviour ahead of the last MS 105 is predicted with analyses of state- and trend lines. A selection of such lines for target 1 at the crown is shown in Fig. 38. However, for an appropriate prediction all targets and different types of trend lines are evaluated. The descriptive ratings of state- and trend lines in Tab. 14 are linked to the previous rounds.

Analysis: Trends of absolute V-H displacements and horizontal displacements of all targets (not shown) – taken 8 m and 15 m behind the face – are significantly increasing ahead of MS 91. Here, also the distance between the absolute displacement trend lines increases. At the same section, the vector orientation L/S remains almost constant. The area under the state lines shows a distinctive increase ahead of chainage 106.0 m. The general trend of the deflection length shows an increasing development. Trends of horizontal displacements at the side walls (not shown here) highly increase as well.

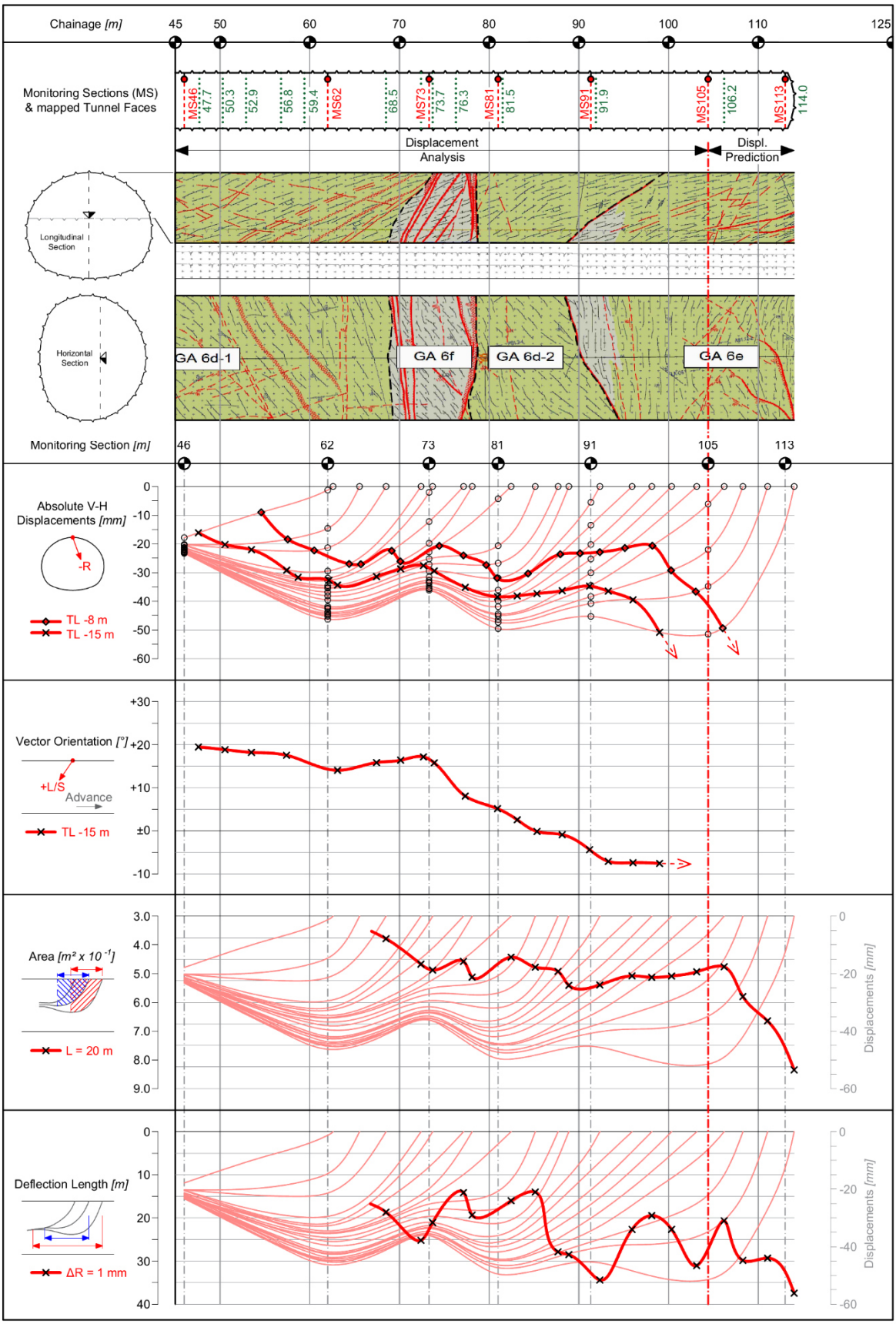

Fig. 38: Short-term prediction of the system behaviour with state- and trend lines of Target 1, SBT2.1, Cavern East, Chainage 45 – 114 m.

Tab. 14: Assessment of state- and trend lines, SBT2.1, Cavern East, Chainage 114.0 m.

Face 114.0				
	Term	Left Side Wall *[Target 5 & 3]*	Crown *[Target 1]*	Right Side Wall *[Target 2 & 4]*
State- & Trend Lines	Absolute Displacements	- - -	- - -	- -
	Horizontal Displacements	- - -	n/s	- -
	Vector Orientation L/S	o	o	o
	Area under State Lines	- - -	- - -	- -
	Deflection Length	- -	- -	- -

During visual observations of the installed support, transversal and longitudinal cracks in the shotcrete lining ahead of chainage 93.0 m – starting from the left side wall and propagating to the right side wall – are recorded.

Interpretation: Absolute- and horizontal displacement trend lines at the current excavation area indicate a distinct increase of the displacement magnitude. The increasing distance between trend lines, established for different locations behind the face, is an indication for changing stress redistribution. Based on analyses of the area under state lines and of deflection lengths, stress redistribution towards the supported (stiff) sections (against direction of drive) are expected, indicating weaker ground conditions ahead. On the other hand, the vector orientation L/S shows no significant change at the current excavation area.

5.2.4 Prediction of Displacements in Excavation Area

Considering information on the geological-geotechnical conditions (section 5.2.1) in combination with short-term predictions of the system behaviour (section 5.2.3) and the utilization of function parameters from the last MS 105 (section 5.2.2) as a starting point, the displacement development at the current tunnel face is predicted.

Interpretation: The geological conditions are similar to the ones at the previous MS 105, therefore the time-dependent parameters *m* and *T* are kept constant. For the prediction of the curve-fitting parameter *X*, the spatial structure orientation, virtual monitoring sections and the distance between displacement trend lines are evaluated. The parameter *X* is expected to increase at the virtual target 5, decrease at the virtual target 4 and remain constant at the virtual targets 1, 2 and 3. Due to results of the virtual monitoring sections (Fig. 37), significantly increasing displacement trends, an increasing area under the state lines and increasing deflection lengths, larger displacements are expected to develop at the current face 114.0 than at the previous rounds. The displacement vectors at the left shoulder (target 3) and crown (target 1) are expected to rotate towards the left side wall due to the influence of joints and the foliation, and displacement vectors at the targets 4 & 5 may rotate downwards due to the ground behaviour dominated by the foliation (see Fig. 39).

Based on these interpretations and utilizing the fitted parameters in Tab. 13 as start values, the function parameters at chainage 114.0 m are predicted. The descriptive ratings in Tab. 15 are linked to the previous MS 105 (see Tab. 13).

Tab. 15: Prediction of the Convergence-Law parameters, SBT2.1, Cavern East, Chainage 114.0 m.

Prediction at Face 114.0									
		Trend Left Side Wall	*Target 5*	*Target 3*	*Trend Crown*	*Target 1*	*Trend Right Side Wall*	*Target 2*	*Target 4*
Prediction at current Face	$C_{x\infty}$	- -	-90	-70	- -	-95	- -	-65	-60
	X	-	20	20	o	20	+	30	20
	m	o	0.3	0.3	o	0.3	o	0.3	0.3
	T	o	1.2	1.0	o	1.0	o	1.2	1.0
	δ		-10°	-5°		-10°		-5°	+15°

Fig. 39 shows the expected ground behaviour at the current face at chainage 114.0 m. Due to unfavourable intersections of foliation planes (dip against direction of drive) and faults with the excavation boundary, over-breaks with a depth up to 1 m occurred.

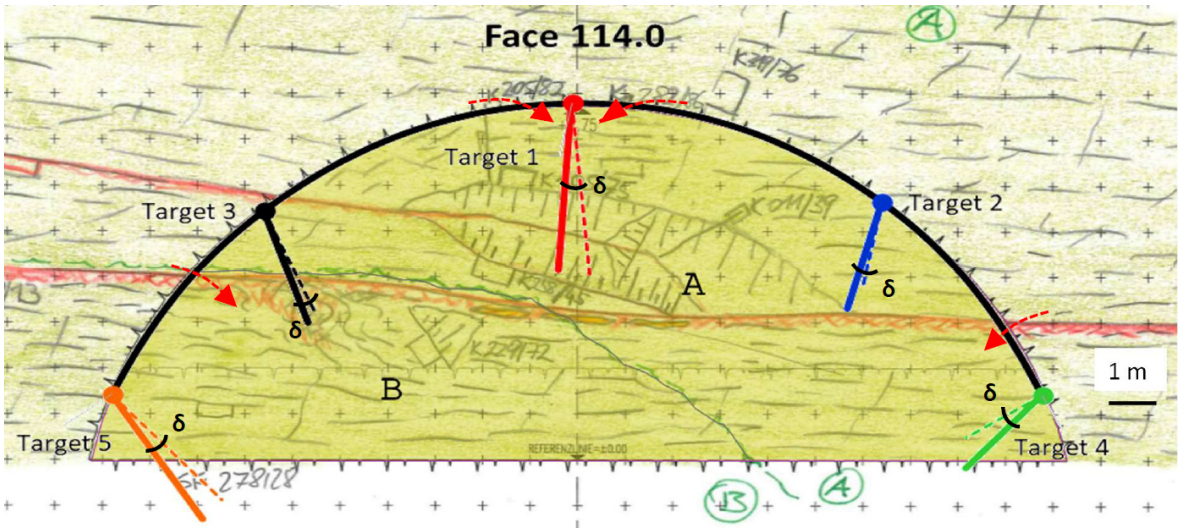

Fig. 39: Expected ground behaviour (red arrows) and possible development of displacement vectors (coloured solid lines), scaled-up by a factor of 30; deviation of vector orientation δ in relation to the previous MS highlighted for each target; SBT2.1, Cavern East, Chainage 114.0 m.

The temporal development of the predicted displacements, determined with the parameters defined in Tab. 15, is shown in Fig. 40. The calculation is based on an expected average advance rate of 1.8 m/day, starting one day after excavation due to an advance stop (assuming no displacements during that time). Largest displacements are expected to develop at the crown (target 1) as at the last monitoring section.

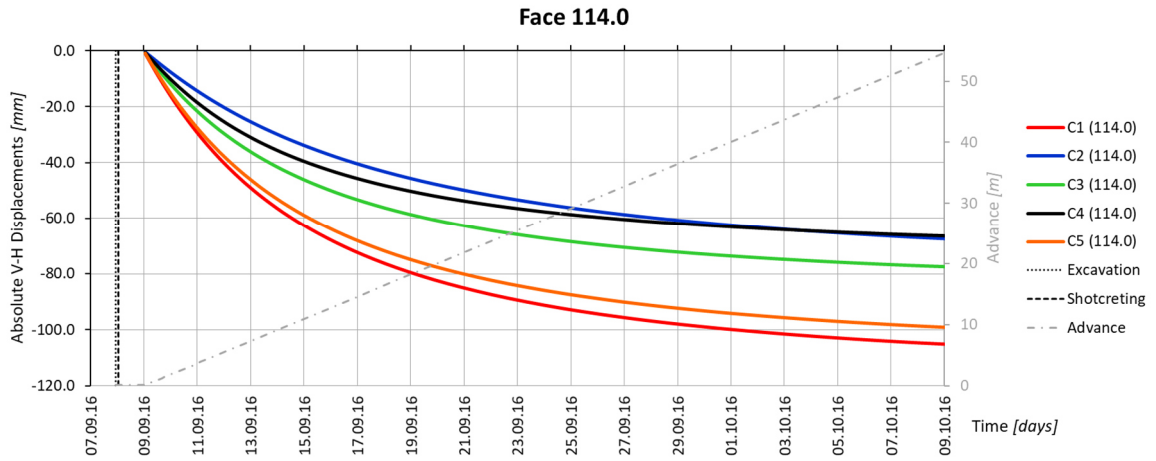

Fig. 40: Time-displacement graph of predicted displacement developments for five targets with expected advance rate of 1.8 m/day at SBT2.1, Cavern East, Chainage 114.0 m.

5.2.5 Calculation of predicted Shotcrete Lining Utilization

With the cubic spline-interpolation, tangential strains in-between the predicted displacement vectors are calculated. The development of the strains between the virtual targets 5-3, 3-1, 1-2 and 2-4 are shown in Fig. 41. The largest strains are expected to develop at the left shoulder (segment 3-1) due to the contra-rotating orientation of the concerning displacement vectors.

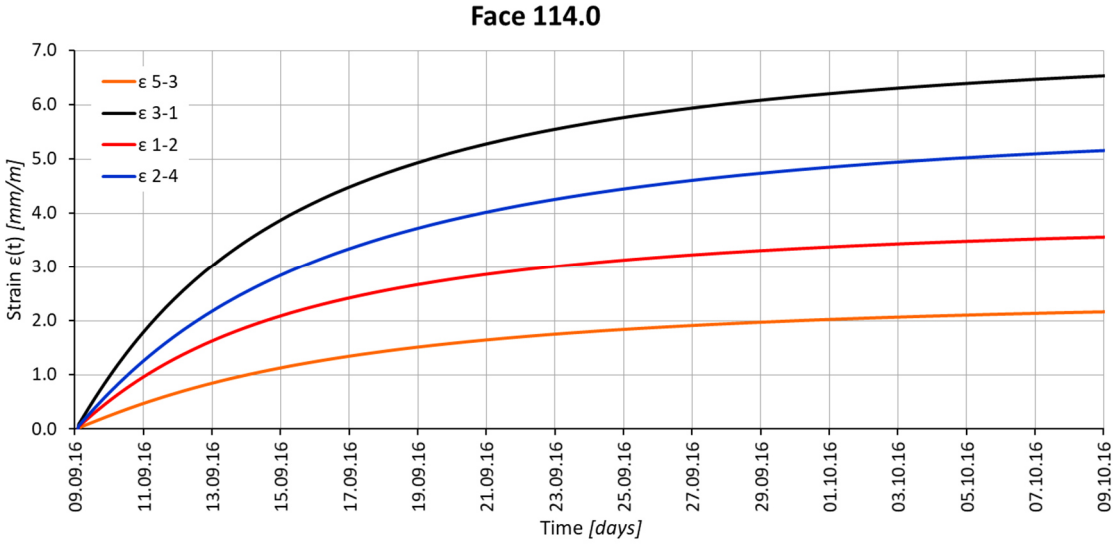

Fig. 41: Time-strain graph of SBT2.1, Cavern East, Chainage 114.0 m; based on predicted displacements shown in Fig. 40.

For the calculation of the lining utilization, shotcrete strength- and stiffness parameters in Tab. 16 are used.

Tab. 16: Shotcrete strength- and stiffness properties for the calculation of the lining utilization at SBT2.1, Cavern East, Chainage 114.0 m.

Shotcrete Properties	
Term	*Chosen*
Shotcrete Thickness:	0.30 m
Shotcrete Strength Class:	SpC 25/30
UCS after 28 days $f_{cm,28}$:	45.0 N/mm²
Early Strength Class J:	J2
Early Strength after 1 day $f_{cm,1}$:	10.0 N/mm²
E-Modulus after 28 days $E_{cm,28}$:	20,000 N/mm²
Cement Hardening Coefficient s:	1.200
Exponent of SpC Strength α1 (f_{cm}):	0.245
Exponent of SpC E-Modulus α2 (E_{cm}):	0.700

Based on the Rate-of-Flow-Method (section 4.8.2), the segmental lining utilization is calculated between the virtual targets 5-3, 3-1, 1-2 and 2-4 (see Fig. 42).

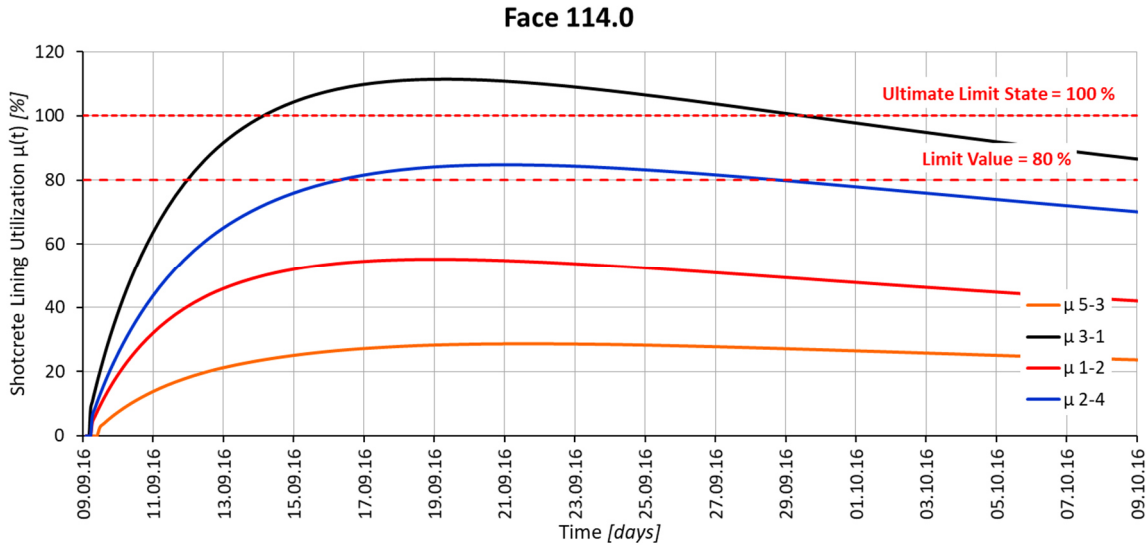

Fig. 42: Predicted shotcrete lining utilization at SBT2.1, Cavern East, Chainage 114.0 m.

Interpretation: Based on the predicted displacements and vector orientations, a maximum long-lasting shotcrete lining utilization of approximately 115 % is expected to occur at the left shoulder (segment 3-1). Since the ultimate limit state will be exceeded, an immediate application of a ductile support system is recommended. Furthermore, additional support measures (e.g. densification of rock bolt pattern) might be applied at the relevant locations.

For the presented case, it must be mentioned that when the tunnel drive was at chainage 114.0 m, the situation could not be observed as critical, considering the information available and the state-of-the-art data evaluation methods. At the measuring sections behind the current face (MS 91 & MS 105), the back-calculated shotcrete lining utilization from measurements was for all lining segments less than 63 % and decreased with further progress (not shown here). Even though the absolute displacements increased (Fig. 38), neither the vector orientation gave a clear hint for the situation to worsen drastically (Fig. 38) nor did the geological observations (Fig. 36).

Only when using the novel approach presented in this thesis – quantitative prediction of displacements at the current excavation area considering both, geotechnical and geological observations – the situation appears to be more critical.

Another aspect which could not be foreseen at the time of construction is, that the unknown presence of a fault zone at the end of the cavern led to stress concentrations in the area of the already constructed openings due to multiple simultaneous excavations, causing long-term displacements. A discussion of these large area stress redistribution processes can be found in [64].

It is explicitly mentioned that for the case studies in this thesis neither contractual- or design aspects, nor on-site restrictions regarding construction sequence and logistics are considered. The general applicability of the novel approach presented requires validation on other cases, implying that at the current time it cannot be considered to be a proven technique.

5.2.6 Comparison of Predictions and Measurements

The predictions made with the presented method at chainage 114.0 m are compared with measurements at MS 113.

Fig. 43 shows the comparison of predicted displacement developments and measured displacement developments at the investigated section. Displacements at the right side wall (target 4) have been slightly underestimated (~ 10 mm), whereas displacements at the left side wall (target 5) have been slightly overestimated. However, all predictions are within a reasonable range. Note that the prediction was done assuming a constant average advance rate of 1.8 m/day, but the advance of the top-heading stopped on September 28th.

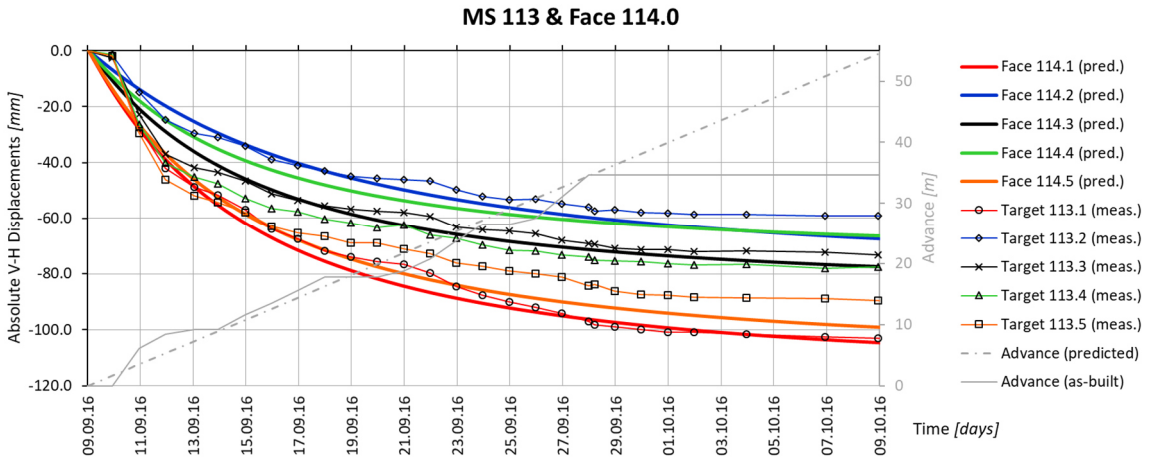

Fig. 43: Comparison of predicted displacement developments at face 114.0 (coloured solid lines) and measured displacement developments at MS 113 (coloured lines with markers) for targets 1-5 at SBT2.1, Cavern East; predicted advance and advance as-built is scaled at the right ordinate; note the advance stop on September 28th.

The predicted displacement vector orientations δ fit well with the monitored displacements in cross-section, as one can observe in Fig. 44. All vectors develop according to the expected ground behaviour (section 5.2.4).

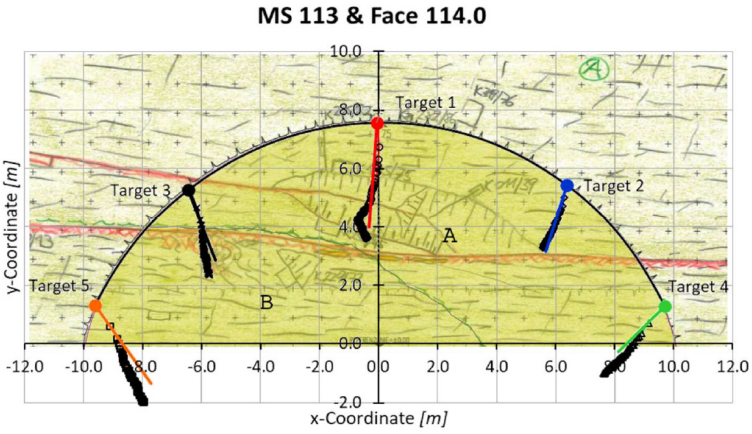

Fig. 44: Comparison of predicted displacement vectors at face 114.0 (coloured solid lines) and measured displacement vectors at MS 113 (lines with markers) in cross-section at SBT2.1, Cavern East.

The predicted shotcrete lining utilizations are in good conformity with the shotcrete lining utilizations back-calculated from measured displacements (see Fig. 45). On September 23rd cracks occurred in the lining at the crown at MS 113, so at that time the load-bearing capacity has been reached, which can also be observed in Fig. 45. This highlights the practicability of the presented method to identify potential stability problems of the support and to predict the moment for a timely application of ductile support systems to avoid such problems. Calculations with the software *Tunnel:Suite* [34] (based on Hybrid-Method and measured displacements) yield a maximum shotcrete lining utilization of 91 % on September 28th at target 1 (not shown here).

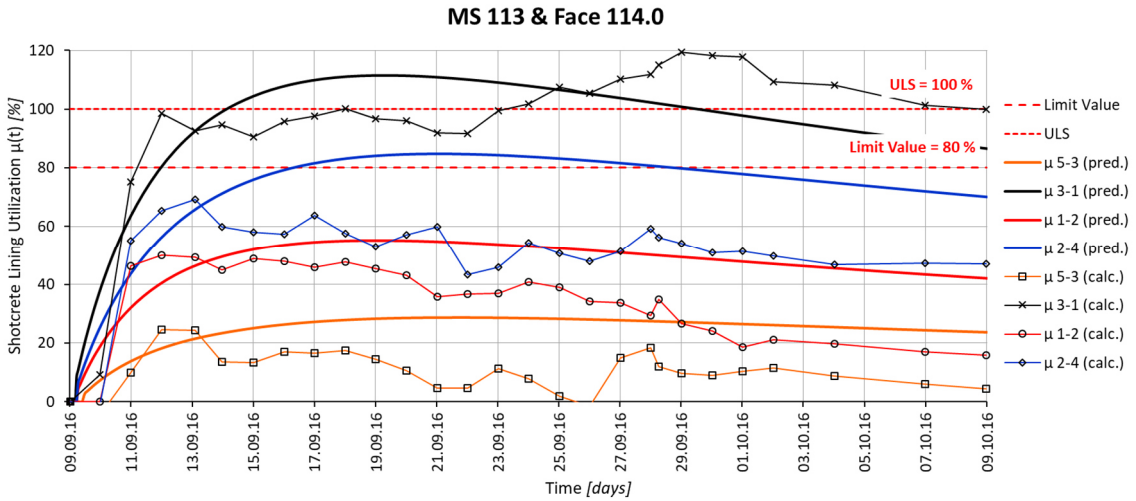

Fig. 45: Comparison of the predicted shotcrete lining utilization at face 114.0 (coloured solid lines) and back-calculated shotcrete lining utilization from measured displacements at MS 113 (coloured lines with markers) at SBT2.1, Cavern East.

6 Conclusion

The aim of this thesis was to develop a consistent method for the prediction of displacements and shotcrete lining utilization at the current excavation area in order to identify the optimal moment for the initial application of ductile support systems. In combination with geological-geotechnical interpretations, short-term predictions with existing and new developed approaches for the analyses of state- and trend lines and with mathematical curve-fitting procedures, an increase of the accuracy of the displacement prediction can be achieved. Using spline interpolations to calculate strains in-between the virtual monitoring targets and applying an adapted constitutive material model for shotcrete, enables the calculation of the shotcrete lining utilization based on predicted displacements.

A reliable 3D displacement monitoring with sufficient small distances between the monitoring sections – depending on the current geological situation – and a detailed knowledge of the construction sequences, are the basis for all further predictions. Under heterogeneous ground conditions a prediction of displacements based on monitoring data interpretations only, is hardly feasible. Hence, an interpretation in combination with geological-geotechnical parameters is recommended. The evaluation of spatial structure orientation, unconfined compressive strength of the intact rock, degree of fragmentation and interlocking strength are found to be suitable for this purpose. Depending on the geological situation, other parameters (e.g. seepage, etc.) should be evaluated as necessary. A graphical illustration of the development of these parameters facilitates the evaluation process.

Semi-automatic curve-fitting procedures based on the Convergence-Law are useful for a timely prediction of the displacement development. Especially at small displacement levels, the influence of the accuracy of measurements has to be considered for the evaluation. State lines provide useful information about the system behaviour behind the face, whereas trend lines can be used for short-term predictions ahead of the face. Trend lines of displacements often give indications to changing ground conditions too late. The vector orientation, the distance between two displacement trend lines and the new introduced evaluations of the area under the state lines and of the deflection lengths seem to be more suitable to predict changing ground conditions ahead. Further investigations are necessary to confirm the general applicability of these new evaluation techniques. In critical situations, the evaluation of virtual monitoring sections can help to estimate function parameters of the Convergence-Law.

For a comprehensible prediction of displacements ahead of the last monitoring section, a systematic assessment of all information available is necessary. Using descriptive ratings facilitates this task to include qualitatively assessed parameters. Based on displacement predictions of all targets at a specific chainage, strains in-between the displacement vectors – highly depending on the displacement vector orientation in cross-section – can be back-calculated. Due to the high variability of spline functions, the mathematical definition of a stable curve is necessary in order to calculate the strains properly. Shotcrete properties significantly changed in the last decades, whereas in Austria almost no tests regarding the rheological behaviour have been performed in this time. The existing constitutive material models are practicable, only their input parameters have to be determined accordingly. The adapted equations for the temporal development of shotcrete strength and stiffness allow an individual adjustment to different kinds of shotcretes.

The prediction of shotcrete lining utilization is a sufficient tool for a timely identification of the need for a ductile support systems as demonstrated in the case studies. With a consistent implementation of the presented method in a software, a quick evaluation of the lining utilization at the current excavation area should be possible at least on a daily basis.

7 References

[1] H. Pöchhacker, “Moderner Tunnelvortrieb in sehr stark druckhaftem Gebirge”, *Porr Nachrichten Heft 57/58*, 1974.

[2] B. Moritz, “Ductile Support System for Tunnels in Squeezing Rock”, PhD Thesis, Institute of Rock Mechanics and Tunnelling, Graz University of Technology, Graz/Austria, 1999.

[3] M. Brandtner, B. Moritz and P. Schubert, “On the Challenge of Evaluating Stresses in a Shotcrete Lining”, *Felsbau*, vol. 25, no. 5, pp. 93–98, 2007.

[4] W. Schubert, M. Blümel, R. Staudacher and S. Brunnegger, “Support aspects of tunnels in fault zones”, *Geomechanics and Tunnelling*, vol. 10, no. 4, pp. 342–352, 2017.

[5] *ÖNORM EN 1997-1: Geotechnical design | Part 1: General rules*, 2014.

[6] United States Department of Homeland Security, *Critical Infrastructure*. Electronic Publication. [Online] Available: https://www.dhs.gov/science-and-technology/critical-infrastructure. Accessed on: Feb. 18 2017.

[7] Austrian Society for Geomechanics, *Guideline for the Geotechnical Design of Underground Structures with Conventional Excavation: Version 2.1*. Salzburg/Austria: Austrian Society for Geomechanics (ÖGG), 2010.

[8] W. Schubert, J. Golser and P. Schwab, “Weiterentwicklung des Ausbaus für stark druckhaftes Gebirge”, *Felsbau*, vol. 14, no. 1, pp. 36–40, 1996.

[9] K. Lenk, *Der Ausgleich des Gebirgsdruckes in großen Teufen beim Berg- und Tunnelbau*. Berlin/Germany: Julius Springer Verlag, 1930.

[10] L. v. Rabcewicz, *Gebirgsdruck und Tunnelbau*: Springer Verlag, 1944.

[11] ITA - Austria, *50 Years of NATM: Experience Reports*. Vienna/Austria: ITA - Austrian National Commitee of ITA, 2012.

[12] W. Schubert and G. Riedmüller, “Geotechnische Nachlese eines Verbruches - Erkenntnisse und Impulse”, *Semprich, S. (eds.), Innovationen in der Geotechnik; Proc. 10. Christian-Veder-Kolloquium*, April 20-21, 1995 Graz/Austria, pp. 59–68, 1995.

[13] G. Anagnostou and L. Cantieni, “Design and analysis of yielding support in squeezing ground”, *In: Proceedings of the ISRM 11th International Congress on Rock Mechanics*, July 9-13, 2007 in Lisbon/Portugal, 2007.

[14] W. Schubert, Personal communication with author, 2017.

[15] M. Sitzwohl, “Optimierung der Lining Stress Controller durch zementgebundene poröse Füllung”, Master's Thesis, Institute of Rock Mechanics and Tunnelling, Graz University of Technology, Graz/Austria, 2011.

[16] M. Verient, “Investigations on telescope yielding elements with porous filling”, Master's Thesis, Institute of Rock Mechanics and Tunnelling, Graz University of Technology, Graz/Austria, 2014.

[17] S. Brunnegger, “Optimization of Yielding Elements”, Master's Thesis (in progress), Institute of Rock Mechanics and Tunnelling, Graz University of Technology, Graz/Austria.

[18] G. Lenz, G. Gschwandtner and P. Schubert, “Geotechnical Safety Management in Underground Structures - On the Challenge of Determining Appropriate Trigger Levels”, *In: Proceedings of the ITA-AITES World Tunnel Congress 2017 in Bergen/Norway*, 2017.

[19] F. Weidinger, “Tauerntunnel 1. und 2. Röhre: Markante Entwicklungsschritte der NATM”, *Berg- und Hüttenmännische Monatshefte (BHM)*, vol. 157, pp. 444–447, 2012.

[20] Austrian Society for Geomechanics, *Geotechnical Monitoring in Conventional Tunnelling*. Salzburg/Austria: Austrian Society for Geomechanics (ÖGG), 2014.

[21] W. Schubert, A. F. Steindorfer and E. Button, “Displacement Monitoring in Tunnels - an Overview”, *Felsbau*, vol. 20, no. 2, pp. 7–15, 2002.

[22] W. Schubert and G. M. Vavrovsky, “Interpretation of monitoring results”, *In: World Tunnelling*, vol. 11, pp. 351–356, 1994.

[23] A. F. Steindorfer, “Short Term Prediction of Rock Mass Behaviour in Tunnelling by Advanced Analysis of Displacement Monitoring Data”, PhD Thesis, Institute of Rock Mechanics and Tunnelling, Graz University of Technology, Graz/Austria, 1997.

[24] A. Budil, “Längsverschiebungen beim Tunnelvortrieb”, PhD Thesis, Institute of Rock Mechanics and Tunnelling, Graz University of Technology, Graz/Austria, 1996.

[25] K. Großauer and W. Schubert, “Analysis of Tunnel Displacements for the Geotechnical Short Term Prediction”, *Geomechanics and Tunnelling*, vol. 1, no. 5, pp. 477–485, 2008.

[26] W. Schubert, K. Großauer and E. Button, “Interpretation of displacement monitoring data for tunnels in heterogeneous rock masses”, *International Journal of Rock Mechanics and Mining Sciences*, vol. 41, no. 1, pp. 882–887, 2004.

[27] J. S. Jeon, C. D. Martin, D. H. Chan and J. S. Kim, “Influence of changing ground conditions on deformations near the tunnel face”, *Tunnelling and Underground Space Technology*, vol. 20, pp. 344–355, 2004.

[28] M. Egger and B. Schukoff, “Kontinuierliche reflektorlose Ortsbrustdeformationsmessung”, *Felsbau*, vol. 25, no. 5, pp. 80–85, 2007.

[29] L. Cantieni, “Spatial Effects in Tunnelling through Squeezing Ground”, PhD Thesis, ETH Zurich, Zurich/Switzerland, 2011.

[30] P. Schubert, “Beitrag zum rheologischen Verhalten von Spritzbeton”, *Felsbau*, vol. 6, no. 3, pp. 150–153, 1988.

[31] W. Aldrian, “Beitrag zum Materialverhalten von früh belastetem Spritzbeton”, PhD Thesis, Montanuniversität Leoben, Leoben/Austria, 1991.

[32] C. Hellmich, “Shotcrete as part of the new Austrian tunneling method: from thermochemomechanical material modeling to structural analysis and safety assessment of tunnels”, PhD Thesis, Vienna University of Technology, Vienna/Austria, 1999.

[33] R. B. Rokahr and R. Zachow, “Ein neues Verfahren zur täglichen Kontrolle der Auslastung einer Spritzbetonschale”, *Felsbau*, vol. 15, no. 6, pp. 430–434, 1997.

[34] IGT ZT GmbH, iC consulenten ZT GmbH and 3G ZT GmbH, *Tunnel:Suite* [Software]: Gruppe Tunnel:Monitor, 2017.

[35] J. Sulem, M. Panet and A. Guenot, “Closure Analysis in Deep Tunnels”, *Int. J. Rock Mech. Min. Sci. & Geomech.*, vol. 24, no. 3, pp. 145–154, 1987.

[36] *ÖNORM EN ISO 14689-1: Geotechnical investigation and testing - Identification and classification of rock* | *Part 1: Identification and description*, 2016.

[37] T. E. Francis, “Determination of the influence of joint orientation on rock mass classification for tunnelling using a stereographic overlay”, *Quaterly Journal of Engineering Geology*, no. 24, pp. 267–273, 1991.

[38] G. Lenz *et al.,* “Prediction of fault zones based on geological and geotechnical observations during tunnel construction”, *Geomechanics and Tunnelling*, vol. 10, no. 4, 366-379, 2017.

[39] M. Lengauer, “Case study on the crack development in a shotcrete lining at the Semmering Base Tunnel, Construction Lot SBT1.1”, Master's Thesis (in progress), Institute of Rock Mechanics and Tunnelling, Graz University of Technology, Graz/Austria.

[40] ÖBB-Infrastruktur AG and PGGT, *Tunnelkette Granitztal: Stellungnahme Planer/GTU/GEO Stauchelemente Permomesozoikum*. Kriterien zum Einsatz von Stauchelementen, 2016.

[41] M. Schmidt, T. Richter and P. Lehmann, “Innovative geophysical technologies for the exploration of faults, karst structures and cavities in tunnelling”, *Geomechanics and Tunnelling*, vol. 10, no. 4, pp. 380–394, 2017.

[42] T. Yamamoto, S. Shirasagi, M. Inou and K. Aoki, “Correlation with various systems for foward prediction of geological condition ahead of the tunnel face”, *In: Proceedings of the ISRM regional symposium EUROCK 2001*, June 3-7, 2001 in Espoo/Finland, 2001.

[43] A. Goricki, E. Button, W. Schubert, M. Pötsch and R. Leitner, “The influence of Discontinuity Orientation on the Behaviour of Tunnels”, *Felsbau*, vol. 23, no. 5, 2005.

[44] F. Tonon and B. Amadei, “Effect of Elastic Anisotropy on Tunnel Wall Displacements Behind a Tunnel Face”, *Rock Mechanics and Rock Engineering*, vol. 35, no. 3, pp. 141–160, 2002.

[45] J. Klopčič, “Analyses and prediction of displacements for tunnels in foliated rock mass of Perm-Carboniferous age”, PhD Thesis, University of Ljubljana, Ljubljana/Slovenia, 2009.

[46] International Society for Rock Mechanics (ISRM), “Suggested Methods for the Quantitative Description of Discontinuities in Rock Masses”, *International Journal of Rock Mechanics and Mining Sciences*, vol. 15, no. 6, pp. 319–368, 1978.

[47] E. Hoek, P. K. Kaiser and W. F. Bawden, *Support of underground excavations in hard rock*. Rotterdam: Balkema, 1995.

[48] H. Prinz and R. Strauß, *Ingenieurgeologie,* 5th ed. Heidelberg: Spektrum Akademischer Verlag, 2011.

[49] N. Radončić, “Tunnel design and prediction of system behaviour in weak ground”, PhD Thesis, Institute of Rock Mechanics and Tunnelling, Graz University of Technology, Graz/Austria, 2011.

[50] G. Feder and M. Arwanitakis, “Zur Gebirgsmechanik ausbruchnaher Bereiche tiefliegender Hohlraumbauten”, *Berg- und Hüttenmännische Monatshefte (BHM)*, vol. 121, no. 4, pp. 103–117, 1976.

[51] C. Carranza-Torres, “Elasto-plastic solution of tunnel problems using the generalized form of the Hoek-Brown failure criterion”, *International Journal of Rock Mechanics and Mining Sciences*, vol. 41, no. 1, pp. 629–639, 2004.

[52] J. Sulem, M. Panet and A. Guenot, “An Analytical Solution for Time-dependent Displacements in a Circular Tunnel”, *Int. J. Rock Mech. Min. Sci. & Geomech.*, vol. 24, no. 3, pp. 155–164, 1987.

[53] E. Hoek, C. Carranza-Torres and B. Corkum, “Hoek-Brown failure criterion - 2002 Edition”, *Proceedings of NARMS-Tac*, vol. 1, pp. 267–273, 2002.

[54] M. Panet and A. Guenot, “Analysis of convergence behind the face of a tunnel”, *In: Tunnelling, The Institution of Mining and Metallurgy*, vol. 82, pp. 197–204, 1982.

[55] P. Sellner, “Prediction of Displacements in Tunnelling”, PhD Thesis, Institute of Rock Mechanics and Tunnelling, Graz University of Technology, Graz/Austria, 2000.

[56] W. Schubert, “Design of Ductile Tunnel Linings”, *In: Proceedings of the 42nd US Rock Mechanics Symposium and 2nd US-Canada Rock Mechanics Symposium*, June 29-July 2, 2008 in San Francisco/U.S., 2008.

[57] R. W. Freund and R. Hoppe, *Stoer/Bulirsch: Numerische Mathematik 1,* 10th ed. Berlin/Germany: Springer Verlag, 2007.

[58] L. Wagner, “Concept and realisation of a distributed fibre-optic sensing system for direct and continuous strain measurement in a shotcrete lining”, Master's Thesis, Institute of Rock Mechanics and Tunnelling, Graz University of Technology, Graz/Austria, 2017.

[59] *ÖNORM EN 1992-1-1: Design of concrete structures | Part 1-1: General rules and rules for buildings*, 2015.

[60] Austrian Society for Construction Technology, *Guideline Sprayed Concrete: Edition 2013*. Vienna/Austria: Austrian Society for Construction Technology, 2013.

[61] R. B. Rokahr and K. H. Lux, “Einfluß des rheologischen Verhaltens des Spritzbetons auf den Ausbauwiderstand”, *Felsbau*, vol. 5, no. 1, pp. 11–18, 1987.

[62] O. K. Wagner, D. Haas, H. Druckfeuchter and T. Schachinger, “The challenges of contract SBT1.1 "Tunnel Gloggnitz"”, *Geomechanics and Tunnelling*, vol. 8, no. 6, pp. 554–567, 2015.

[63] W. Pacher and G. C. Putz, “Semmering Base Tunnel Contract SBT2.1 Tunnel Fröschnitzgraben - Creative solutions for complex shafts”, *Geomechanics and Tunnelling*, vol. 9, no. 5, pp. 391–404, 2016.

[64] A. Poisel, J. Weigl, T. Schachinger, R. Vanek, and G. Nipitsch, “Semmering base tunnel - excavation of the emergency station in complex ground conditions”, *Geomechanics and Tunnelling*, vol. 10, no. 5, (not published yet), 2017.